Doctoral Dissertation

Development of Novel Doubly Labelled Peptide Probes with Identical Fluorophores for Protease Activity Measurement

Daisuke Sato

Graduate School of Life Science and Systems Engineering

Kyushu Institute of Technology

Contents

2

Chapter 3

Novel bispyrenyl substrates for detection of thrombin and trypsin

Chapter4

Chapter 1

General introduction

1.1. Preface

Almost all chemical reactions including post-translational modification of proteins in living organisms are catalyzed by enzymes, and enzymes play a significant role in many physiological processes such as signaling, metabolism, and gene regulation. There are thousands of enzymes in living body, and enzymes are known to play a fundamental role in the pathology of several major human diseases. Therefore, the detection of disease-related enzymes in living samples is essential for research in biology and medicine, and many techniques for enzyme assay have been intensely developed. Herein, we focus on proteases defined as hydrolase, and provide a concise but general background of proteases and protease assays.

1.2. Protease

Proteases, which are some of the most vital physiological enzymes, have been targeted for the development of simple and sensitive assays for disease diagnosis, therapy, and biological research. Proteases hydrolyze the amide bond at specific sites of the polypeptide chain, and play key roles in the regulation of a large number of physiological processes such as cell proliferation and differentiation, apoptosis, DNA replication, hemostasis (coagulation), and immune responses.[1,2]

5

For instance, caspases, which are one of cysteine proteases, play a critical role in cell regulation such as controlling inflammation and cell death, and dysregulation of caspases is involved in human diseases such as cancer, degenerative disease, and inflammatory disorders.[3−5] Cathepsins, digestive and regulatory proteases, also participate in many physiological processes such as antigen presentation in immune system, collagen turnover in bone and cartilage, and neuropeptide and hormone processing.[6] Cathepsins are associated with various human diseases including cancer, arthritis, and osteoporosis.[7−10] Human immunodeficiency virus (HIV)-1 protease is essential for the maturation of HIV, and the detection and inhibition of HIV-1 protease in the HIV life cycle are required for diagnosis and therapy of acquired immunodeficiency syndrome (AIDS).[11−13]

As stated above, proteases have key roles in multiple physiological and pathological processes, and have potential for promising drug targets or diagnostic and prognostic biomarkers.[14] Therefore, various approaches for protease assay have been enthusiastically studied and developed due to the significance of protease detection.

1.3. Immunology-based method

Immunological detection methods for protease, which utilize antigen-antibody reaction, can quantify a desired protease in even complicated samples derived from living body because the antigen-antibody reaction is specific and sensitive. Western blot and enzyme-

linked immuno-sorbent assay (ELISA) methods are widely used for qualification of proteins including protease.[15]

Western blotting, which was reported by Burnette in 1981, is a method that sodium dodecyl sulfate-polyacrylamide gel electrophoresis (SDS-PAGE) technique is combined with antigen-antibody reaction.[16] After completion of the electrophoresis, a replica of the separated proteins can be made onto an adsorbent such as polyvinylidenefluoride (PVDF) or nitrocellulose (Fig. 1).[17] Subsequently, primary antibody is bound to a specific band on the blot, and secondary antibody conjugated to an enzyme such as alkaline phosphatase or horse radish peroxidase is bound to the primary antibody. Finally, color of specific band is developed and measured to detect target protease.
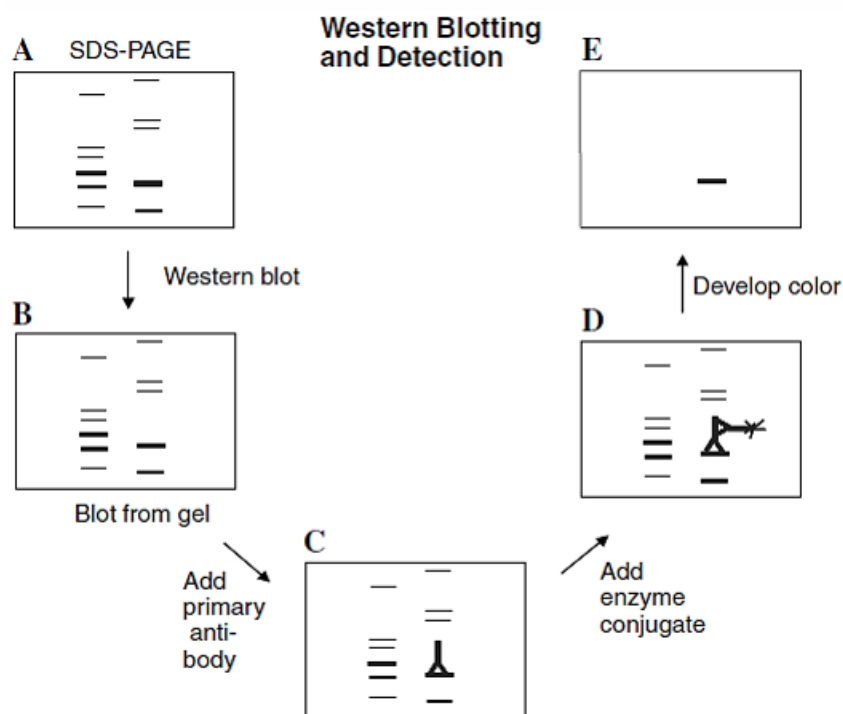
Fig. 1 Schematic representation of western blotting and detection procedure.[18]

ELISA, which was reported by Engvall and Perlmann in 1971, is a technique that the specificity of antibodies is combined with the sensitivity of simple enzyme assays by using antibodies or antigens coupled to an enzyme which can be readily assayed.[19] Although many variants of ELISA test procedures have been developed to date, sandwich-ELISA is the most common kind.[20,21] In sandwich-ELISA, the amount of target protease (antigen) between two layers of antibodies which are consisted of immobilized or labelled antibodies respectively is measured (Fig. 2). Antigen-specific antibody is immobilized on the well of microplate. Antigen binds to immobilized antibody when adding antigen. Next, enzyme-labelled antibody is added, and bound to antigen-conjugated immobilized antibody. Finally, the chromogenic or fluorogenic substrates for the detection of labelled enzyme are added, and the colored product is measured to detect the target protease.

1. Immobilization of the antigen-specific antibody on the well.
2. Addition of the antigen.
3. Addition of the enzyme-labelled antibody.
4. Introduction of the enzyme's substrate and apparition of the colored product.

Y : Antigen specific antibody.

◆ : Antigen (bacteria).

⅄ : Enzyme labelled antibody.

△ : Enzymatic substrate.

✷ : Coloured product.

Fig. 2 Schematic representation of sandwich-ELISA protocol.[21]

However, immunological methods cannot be used for the detection of protease activity because these methods are focused on quantitating the amount of protease.[22] Measurement of the protease activity is significant because the disease states are directly related to protease activity rather than protease quantity. For example, prion disease is relevant to several protease activities. Prion disease is a group of human and animal neurodegenerative disorders, and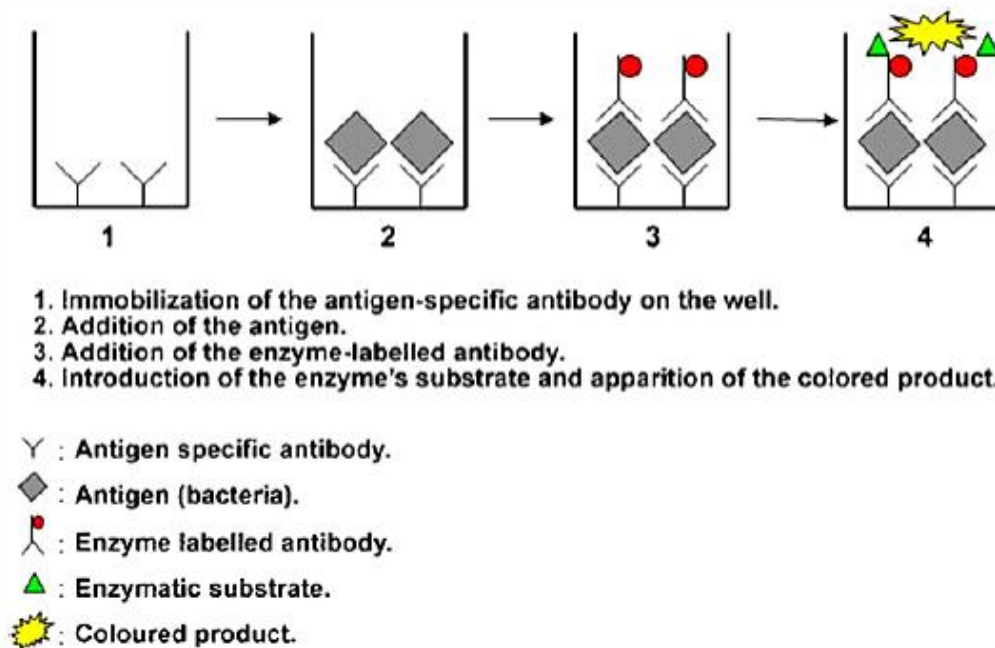 results from the conversion of a normal cell-surface glycoprotein (PrP^C) with a primarily α-helical structure into conformationally altered pathogenic isoform (PrP^{Sc}) which is β-sheet rich.[23,24] PrP^{Sc} has partial resistance to proteolysis,[25] and is an essential component of proteinaceous infectious particles (prions).[26] PrP^C is shed at plasma membrane by metalloprotease ADAM10, and the shed PrP^C may impact on prion disease.[27] The prion-related proteins are subject to proteolytic processing, and these cleavages are potentially involved in progression of prion disease.[28] *Porphyromonas gingivalis*, which is one of the major pathogens of periodontitis, secretes cysteine proteases gingipains.[29,30] Gingipain activities are implicated in infection, acquisition of nutrients, evasion of antibacterial defenses, and tissue invasion and dissemination.[31] Therefore, gingipain activities are directly involved in pathological events during development and progression of periodontitis.[32] According to these findings, protease activity is intimately correlated to progression and state of diseases, and measuring protease activity is meaningful in terms of disease diagnosis, pathophysiological research, and drug discovery. Moreover, evaluation of protease inhibitors cannot be performed by the immunological techniques. Inhibitor evaluation is considered as a valuable work by medicinal chemists and pharmacologists because it is necessary in drug discovery. Besides, the immnological assays are time consuming, and required expensive reagents and specific instruments.[33,34] To overcome the limitations in

these immunological assays, optical methods using chromogenic or fluorogenic substrates are commonly used for protease assay.[35]

1.4. Colorimetric method

Chromogenic substrates for protease assay are comprised of a substrate peptide and a dye, and its absorbance at particular wavelength is changed before and after enzymatic degradation. In detection of protease activity, Peptide-p-nitroanilide (pNA) is commonly used as the chromogenic substrate.[26] When colorless Peptide-pNA is cleaved by protease, yellow p-nitroaniline is liberated (Fig. 3). Hence, protease activity can be detected by measurement of the absorbance of free p-nitroaniline at 405 nm.
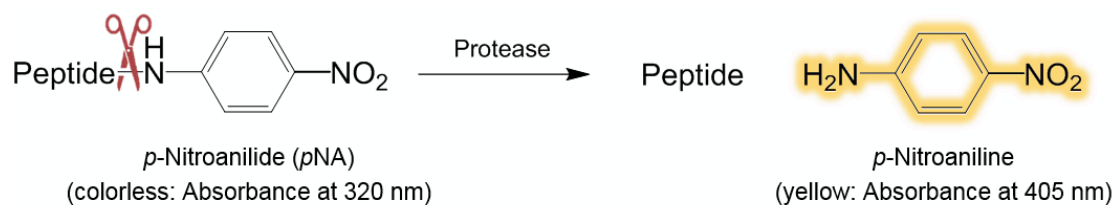

Fig. 3 Schematic representation of the detection of protease activity using Peptide-pNA.

A number of protease activities such as trypsin, subtilisin, and chymotrypsin could be successfully detected using specific Peptide-pNA.[37−39] However, in protease assay, fluorometric method is preferable to colorimetric method in terms of its sensitivity.

1.5. Fluorometric method

Fluorogenic substrates have been more eagerly developed as the sensitivity of fluorometric method is generally three orders of magnitude higher than colorimetric method.[40,41] Fluorogenic substrates change its fluorescent property after hydrolyzation by a specific protease. Measurement of the degree of this alteration allows for the detection of the activity of target protease. Until now, a variety of fluorogenic substrates for protease assay have been developed.

1.5.1. Peptide-MCA

Peptide-4-methylcoumarin amide (MCA) is one of commonly used fluorogenic substrates for protease assay. Zimmerman *et al.* was the first to report that Peptide-MCA was successfully applied to the detection of protease activity as a substrate in 1976.[42] Since then, Peptide-MCA was applied to the detection of many proteases.[43−48] Peptide-MCA emits the fluorescence at 400 nm upon excitation at 330 nm. 7-Amino-4-methylcoumarin (AMC) is released when Peptide-MCA is hydrolyzed by protease (Fig. 4). AMC emits the fluorescence at 460 nm upon excitation at 380 nm. Therefore, measuring the degree of the change in fluorescence intensity at 460 nm allows for the detection of protease activity. The fluorescence of AMC can be measured upon the light which is selectively excited not MCA group but AMC, resulting the detection with high signal-to-noise (S/N) ratio.

4-Methylcoumarin amide (MCA)
(λex = 330 nm, λem = 400 nm)

7-Amino-4-methylcoumarin (AMC)
(λex = 380 nm, λem = 460 nm)
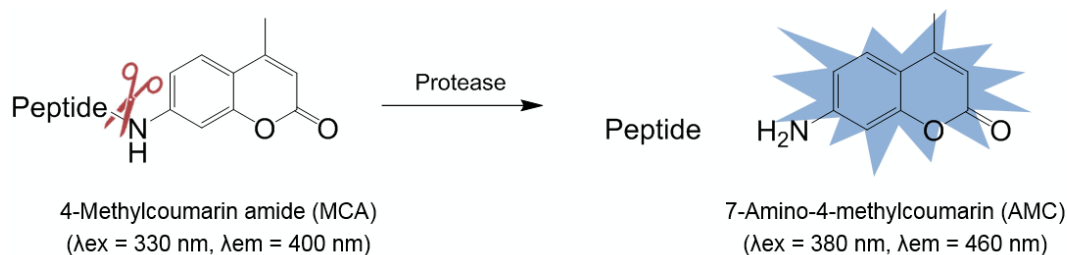
Fig. 4 Schematic representation of the detection of protease activity using Peptide-MCA.

However, in the case of an AMC-based assay, the specificity for the P1′ amino acid residue (counterpart of the S1′ subsite of the protease), which is important for substrate recognition and catalytic efficiency, is not reflected in the artificial substrate (Fig. 5).[49]
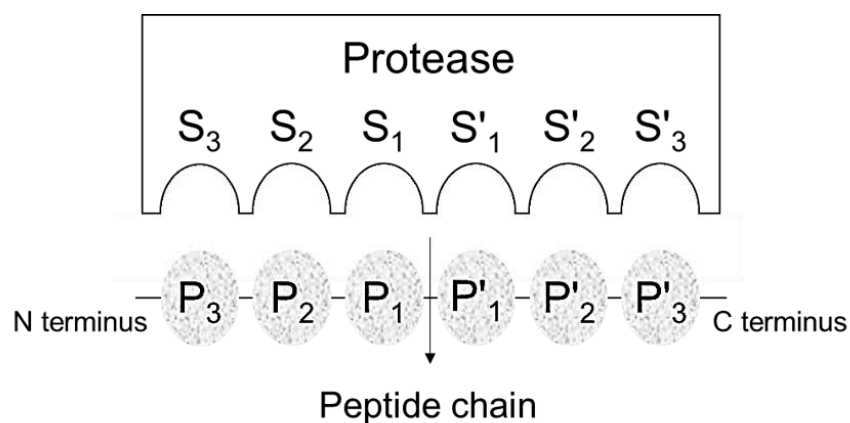
Fig. 5 The subsites of proteases.

Additionally, AMC-based assay requires ultraviolet (UV) light irradiation for the excitation of AMC, which may cause unexpected autofluorescence and photodamage to some biological species.[50]

1.5.2. Rhodamine substrate

Rhodamine-based substrate for protease assay was reported by Leytus *et al.* in 1983.[51] Rhodamine dyes are fluorophores which belong to the family of xanthenes along with fluorescein and eosin dyes. Rhodamines are used for fluorogenic substrates owing to their excellent photostability and photophysical properties such as high quantum yield, and a variety of derivatives of rhodamine have been developed (Table 1). For protease assay, rhodamine 110 is the most used.[52]

Table 1 Commercially available rhodamines.[53]
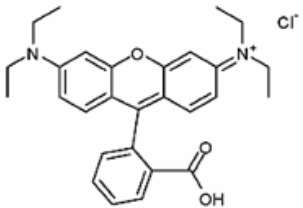
	Structure	€/g[a]
Rho B		0.45
Rho 6G		1.60
Rho 19		156
Rho 101		80
Rho 110		128
Rho 116		205
Rho 123		1650
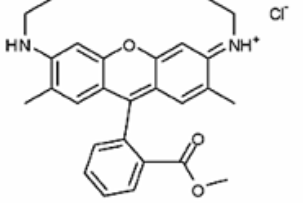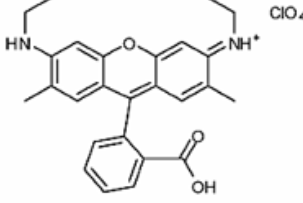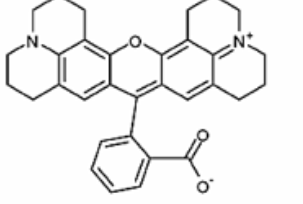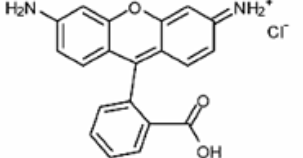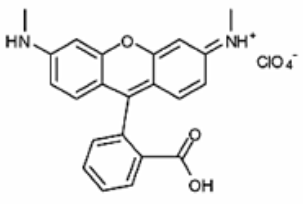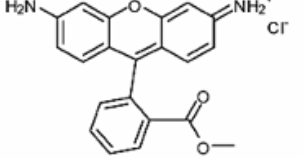
[a] An average for common suppliers: Acros Organics, Aldrich, Alfa Aesar, Fluka, Radiant dyes laser, Sigma.

Double-substitution of rhodamine 110 yields a non-fluorescent lactone, and the hydrolyzation of the substrate at two cleavage sites by protease is ascribed to the fluorescence emission of rhodamine 110 (Fig. 6).
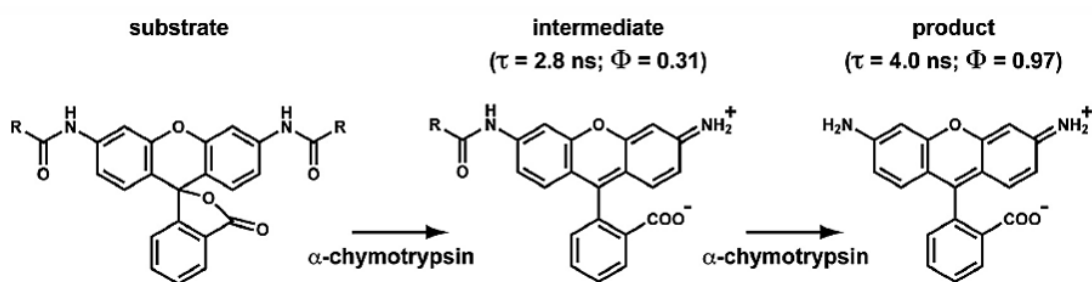
Fig. 6   Fluorescent reporter system for measuring the activity of α-chymotrypsin at the single-molecule level.[54]

Although rhodamine 110-based substrates have been adopted as fluorogenic substrates for many proteases,[55−59] these two step enzymatic reactions cause not only a reduction in the speed and efficiency of fluorescence activation but also complicated kinetic analysis.[60] In addition, as with Peptide-MCA, the specificity of the P′ site is not reflected in the synthesized substrate.

1.5.3. FRET-based substrate

Intramolecularly quenched fluorescent substrates (IQFS), one of Förster resonance energy transfer (FRET)-based substrates, have been used for the detection of various protease activities.[61−67] FRET is that the transfer of fluorescence energy from a donor dye to an acceptor dye whenever the distance between both dyes is smaller than a critical

15

radius known as the Förster radius (typically 3–6 nm).[68,69] Latt. *et al.* was the first to report that FRET-based fluorescent substrate for protease assay was successfully developed in 1972.[70] Proximate fluorophore and quencher in the substrate occur FRET, and fluorescence of the substrate is quenched (Fig. 7). Degradation of the substrate peptide by protease leads to the separation of the intramolecular fluorophore-quencher pair, allowing the increase of the fluorescence of the fluorophore.
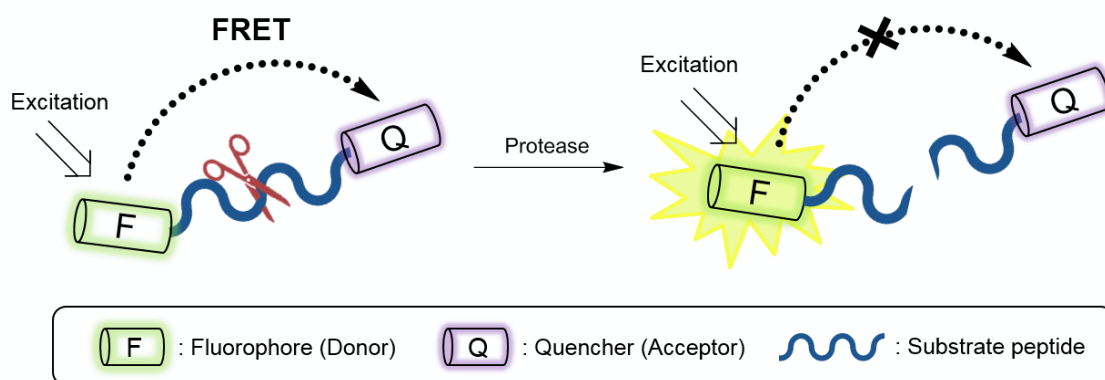
Fig. 7   Schematic representation of the detection of protease activity using IQFS.

Recently, quantum dots (QDs) have been reported as attractable inorganic fluorophores in FRET technologies for protease assay.[71−73] Luminescent semiconductor QDs have unique optical properties for bioanalytical applications. QDs have broad absorption and narrow emission spectra, which enable the excitation by a wide range of wavelength and multi-color sensing.[74] In addition, the emission profile can be precisely controlled through the variation of core size, composition, and surface coatings (Fig. 8).[75]
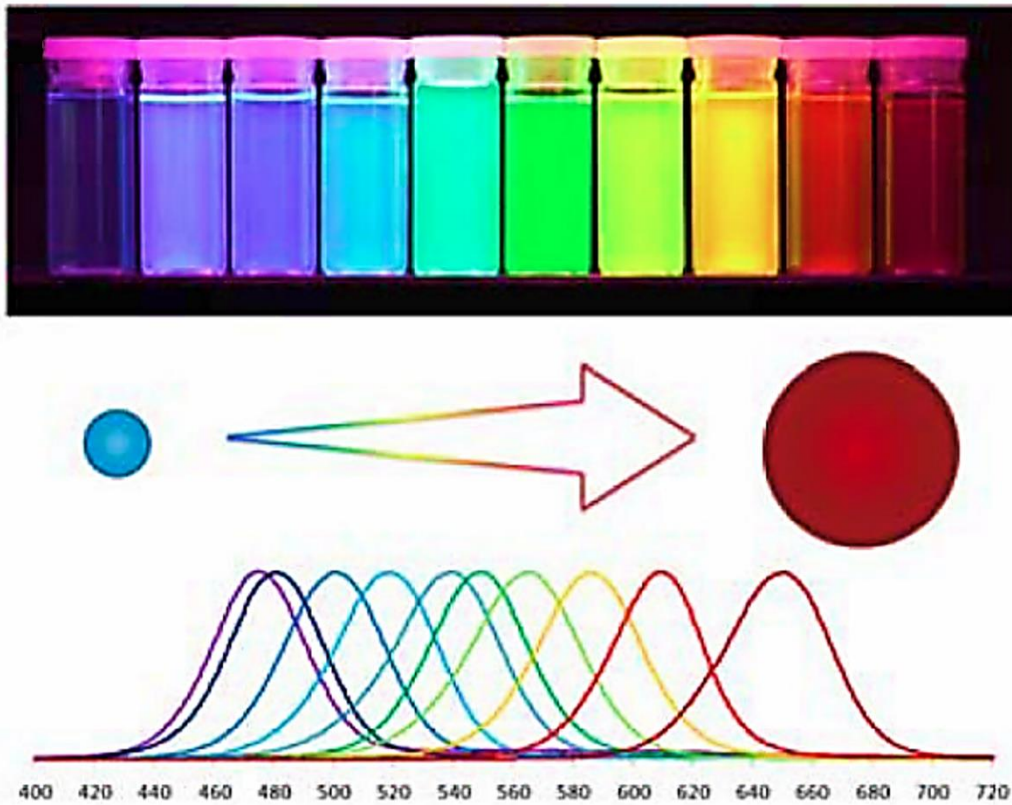
Fig. 8 Narrow size-tunable light emission profile enables precise control over the probe color via varying the nanoparticle size.[76]

In protease assay, QD-peptide conjugate, which has substrate peptide for target protease with fluorophore or quencher, has been used. The fluorescence of the QD-peptide conjugate is quenched by FRET (Fig. 9). The substrate peptide is specifically cleaved by protease, followed by the release of the acceptor fluorophore from the QD-peptide conjugate, leading to the recovery of QD fluorescence.[77]
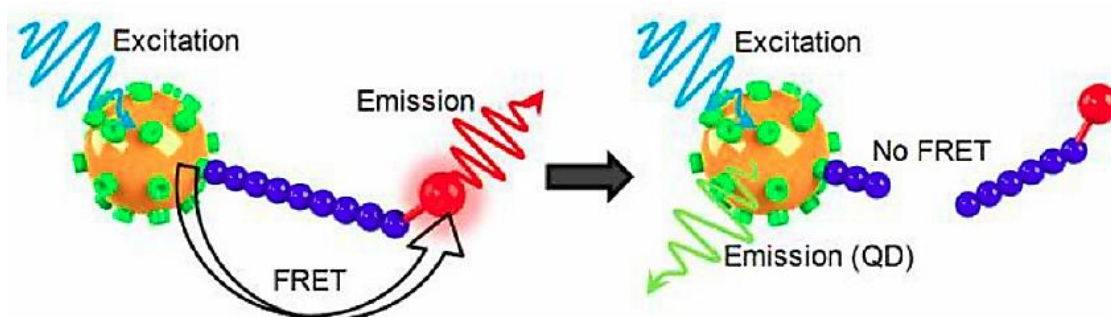
Fig. 9 QD-FRET sensor for the study of protease.[78]

However, in a FRET-based assay, the combination of fluorophores and quenchers can be limiting, and expensive fluorophores or quenchers are often required. Furthermore, the synthesis of FRET-based substrate is usually complicated because at least one pair of orthogonal protecting groups is needed so that the two different dyes required for the FRET are coupled.

1.7. Aim of this study

Proteases are significant physiological enzymes, and a variety of methodologies have been keenly studied. Especially, the fluorescent peptide probe is considered as a strong tool for biochemical research and clinical diagnostic application because fluorometric method using the fluorogenic peptide substrate enables facile and sensitive detection of protease activity and evaluation of protease inhibitor. Although currently Peptide-MCA and FRET-based substrates for many kinds of proteases are commercially available, meaning these fluorogenic peptide substrates are considered as standard fluorescent peptide probes for protease assay, these substrates are not necessarily versatile. In the case of Peptide-MCA, MCA group next to the proteolytic cleavage site prohibits the reflection

18

and characterization of prime subsites in the substrate peptide. As for FRET-based substrate, relatively complicated synthesis is inevitable due to the incorporation of two different dyes. In addition, the limitation of the combination of fluorophore and quencher may demand the use of expensive dyes.

To overcome above defects, in this study, we developed novel doubly labelled fluorescent peptide probes for protease assays exploiting the intramolecular interaction between identical fluorophores such as internal self-quenching or excimer formation.

1.8. References

1. Turk, B. Targeting proteases: successes, failures and future prospects. *Nat. Rev. Drug Discov.* 2006, **5**(9), 785−799.

2. Rakashanda, S.; Rana, F.; Rafiq, S.; Masood, A.; Amin, S. Role of proteases in cancer: a review. *Biotechnol. Mol. Biol. Rev.* 2012, **7**(4), 90−101.

3. McIlwain, D. R.; Berger, T.; Mak, T. W. Caspase functions in cell death and disease. *Cold Spring Harb. Perspect Biol.* 2013, **5**(4), a008656.

4. Bantel, H.; Ruck, P.; Gregor, M.; Schulze-Osthoff, K. Detection of elevated caspase activation and early apoptosis in liver diseases. *Eur. J. Cell Biol.* 2001, **80**(3), 230−239.

5. Bredesen, D. E. Neurodegeneration in Alzheimer's disease: caspases and synaptic element interdependence. *Mol. Neurodegener.* 2009, **4**, 27.

6. Reiser, J.; Adair, B.; Reinheckel, T. Specialized roles for cysteine cathepsins in health and disease. *J. Clin. Invest.* 2010, **120**(10), 3421−3431.

7. Olson, O. C.; Joyce, J. A. Cysteine cathepsin proteases: regulators of cancer progression and therapeutic response. *Nat. Rev. Cancer* 2015, **15**(12), 712−729.

8. Lutgens, S. P. M.; Cleutjens, K. B. J. M.; Daemen, M. J. A. P.; Heeneman, S. Cathepsin cysteine proteases in cardiovascular disease. *FASEB J.* 2017, **21**(12), 3029−3041.

9. Brix, K.; Dunkhorst, A.; Mayer, K.; Jordans, S. Cysteine cathepsins: cellular roadmap to different functions. *Biochimie* 2008, **90**(2), 194−207.

10. Cheng, X. W.; Shi, G. P.; Kuzuya, M.; Sasaki, T.; Okumura, K.; Murohara, T. Role for cysteine protease cathepsins in heart disease: focus on biology and mechanisms with clinical implication. *Circulation* 2012, **125**(12), 1551−1562.

11. Esseghaier, C.; Ng, A.; Zourob, M. A novel and rapid assay for HIV-1 protease detection using magnetic bead mediation. *Biosens. Bioelectron.* 2013, **41**, 335−341.

12. Lv, Z.; Chu, Y.; Wang, Y. HIV protease inhibitors: a review of molecular selectivity and toxicity. *HIV AIDS (Auckl)* 2015, **7**, 95−104.

13. Ghosh, A. K.; Osswald, H. L.; Prato, G. Recent progress in the development of HIV-1 protease inhibitors for the treatment of HIV/AIDS. *J. Med. Chem.* 2016, **59**(11), 5172−5208.

14. López-Otín, C.; Bond, J. S. Proteases: multifunctional enzymes in life and disease. *J. Biol. Chem.* 2008, **283**(45), 30433−30437.

15. Jiang, Z.; Jiang, X.; Li, C.; Xue, H.; Zhang, X. Development of an IgY antibody-based immunoassay for the screening of the CYP2E1 inhibitor/enhancer from herbal medicines. *Front. Pharmacol.* 2016, **7**, 502.

16. Burnette, W. N. "Western blotting": electrophoretic transfer of proteins from sodium dodecyl sulfate-polyacrylamide gels to unmodified nitrocellulose and radiographic detection with antibody and radioiodinated protein A. *Anal. Biochem.* 1981, **112**(2), 195−203.

17. MacPhee, D. J. Methodological considerations for improving western blot analysis. *J. Pharmacol. Toxicol. Methods* 2010, **61**(2), 171−177.

18. Kurien, B. T.; Scofield, R. H. Western blotting. *Methods* 2006, **38**(4), 283−293.

19. Engvall, E.; Perlmann, P. Enzyme-linked immunosorbent assay (ELISA): quantitative assay of immunoglobulin G. *Immunochemistry* 1971, **8**(9), 871−874.

20. Lequin, R. M. Enzyme immunoassay (EIA)/enzyme-linked immunosorbent assay (ELISA). *Clin. Chem.* 2005, **51**(12), 2415−2418.

21. Lazcka, O.; Campo, F. J. D.; Muñoz, F. X. Pathogen detection: a perspective of traditional methods and biosensors. *Biosens. Bioelectron.* 2007, **22**(7), 1205−1217.

22. Creasy, B. M.; Hartmann, C. B.; White, F. K. H.; McCoy, K. L. New assay using fluorogenic substrates and immunofluorescence staining to measure cysteine cathepsin activity in live cell subpopulations. *Cytometry A* 2007, **71**(2), 114−123.

23. Geschwind, M. D. Prion diseases. *Continuum (Minneap Minn)* 2015, **21**(6, Neuroinfectious Disease), 1612−1638.

24. Prusiner, S. B. Molecular biology and pathogenesis of prion diseases. *Trends Biochem. Sci.* 1996, **21**(12), 482−487.

25. Cronier, S.; Gros, N.; Tattum, M. H.; Jackson, G. S.; Clarke, A. R.; Collinge, J.; Wadsworth, J. D. F. Detection and characterization of proteinase K-sensitive disease-related prion protein with thermolysin. *Biochem. J.* 2008, **416**(2), 297−305.

26. Altmeppen, H. C.; Prox, J.; Puig, B.; Dohler, F.; Falker, C.; Krasemann, S.; Glatzel, M. Roles of endoproteolytic α-cleavage and shedding of the prion protein in neurodegeneration. *FEBS J.* 2013, **280**(18), 4338−4347.

27. Altmeppen, H. C.; Prox, J.; Krasemann, S.; Puig, B.; Kruszewski, K.; Dohler, F.; Bernreuther, C.; Hoxha, A.; Linsenmeier, L.; Sikorska, B.; Liberski, P. P.; Bartsch, U.; Saftig, P.; Glatzel, M. The sheddase ADAM10 is a potent modulator of prion disease. *eLife* 2015, **4**, e04260.

28. Altmeppen, H. C.; Puig, B.; Dohler, F.; Thurm, D. K.; Falker, C.; Krasemann, S.; Glatzel, M. Proteolytic processing of the prion protein in health and disease. *Am. J. Neurodegener. Dis.* 2012, **1**(1), 15−31.

29. Kadowaki, T.; Takii, R.; Yamatake, K.; Kawakubo, T.; Tsukuba, T.; Yamamoto, K. A role for gingipains in cellular responses and bacterial survival in *Porphyromonas gingivalis*-infected cells. *Front. Biosci.* 2007, **12**, 4800−4809.

30. Mysak, J.; Podzimek, S.; Sommerova, P.; Lyuya-Mi, Y.; Bartova, J.; Janatova, T.; Prochazkova, J.; Duskova, J. *Porphyromonas gingivalis*: major periodontopathic pathogen overview. *J. Immunol. Res.* 2014, **2014**, 476068.

31. Olsen, I.; Potempa, J. Strategies for the inhibition of gingipains for the potential treatment of periodontitis and associated systemic diseases. *J. Oral Microbiol.* 2014, **6**, 24800.

32. Potempa, J.; Travis, J. Porphyromonas gingivalis proteinases in periodontitis, a review. *Acta Biochim. Pol.* 1996, **43**(3), 455−465.

33. Liu, Y. F.; Chen, J. X.; Xu, M. Q.; Zhao, G. C. A novel photoelectrochemical platform for detection of protease. *Int. J. Electrochem. Sci.* 2014, **9**, 4014−4023.

34. Wu, L.; Yang, S. H.; Xiong, H.; Yang, J. Q.; Guo, J.; Yang, W. C.; Yang, G. F. Nonpeptide-based small-molecule probe for fluorogenic and chromogenic detection of chymotrypsin. *Anal. Chem.* 2017, **89**(6), 3687−3693.

35. Ullmann, S. G. D.; Jakubke, H. D. Design and synthesis of fluorogenic trypsin peptide substrates based on resonance energy transfer. *Anal. Biochem.* 1998, **265**(2), 225−231.

36. Somorin, O.; Tokura, S.; Nishi, N.; Noguchi, J. The action of trypsin on synthetic chromogenic arginine substrates. *J. Biochem.* 1978, **85**(1), 157−162.

37. Lesner, A.; Brzozowski, K.; Kupryszewski, G.; Rolka, K. Design, chemical synthesis and kinetic studies of trypsin chromogenic substrates based on the proteinase binding loop of *Cucurbita maxima* trypsin inhibitor (CMTI-III). *Biochem. Biophys. Res. Commun.* 2000, **269**(1), 81−84.

38. Pozsgay, M.; Gáspár, R; Elödi, P. Investigations on new tripeptidyl-*p*-nitroanilide substrates for subtilisins. *FEBS Lett.* 1977, **74**(1), 67−70.

39. Stepanov, V. M.; Terent'eva, E. Y.; Voyushina, T. L.; Gololobov, M. Y. Subtilisin and α-chymotrypsin catalyzed synthesis of peptides containing arginine and lysine *p*-nitroanilides as C-terminal moieties. *Bioorg. Med. Chem.* 1995, **3**(5), 479−485.

40. Liao, D.; Li, Y.; Chen, J.; Yu, C. A fluorescence turn-on method for real-time monitoring of protease activity based on the electron transfer between a fluorophore labeled oligonucleotide and cytochrome *c*. *Anal. Chim. Acta* 2013, **784**, 72−76.

41. Bisswanger, H. Enzyme assays. *Perspectives in Science* 2014, **1**(1-6), 41−55.

42. Zimmerman, M.; Yurewicz, E.; Patel, G. A new fluorogenic substrate for chymotrypsin. *Anal. Biochem.* 1976, **70**, 258−262.

43. Morita, T.; Kato, H.; Iwanaga, S.; Takada, K.; Kimura, T; Sakakibara, S. New fluorogenic substrates for α-thrombin, factor Xa, kallikreins, and urokinase. *J. Biochem.* 1977, **82**(5), 1495−1498.

44. Kawabata, S.; Miura, T.; Morita, T.; Kato, H.; Fujikawa, K.; Iwanaga, S.; Takada, K.; Kimura, T.; Sakakibara, S. Highly sensitive peptide-4-methylcoumaryl-7-amide substrates for blood-clotting proteases and trypsin. *Eur. J. Biochem.* 1988, **172**(1), 17−25.

45. Azaryan, A. V.; Hook, V. Y. H. Unique cleavage specificity of 'prohormone thiol protease' related to proenkephalin processing. *FEBS Lett.* 1994, **341**(2-3), 197−202.

46. Ranol, T. A.; Timkey, T.; Peterson, E. P.; Rotonda, J.; Nicholson, D. W.; Becker, J. W.; Chapman, K. T.; Thornberry, N. A. A combinatorial approach for determining protease specificities: application to interleukin-1β converting enzyme (ICE). *Chem. Biol.* 1997, **4**(1), 149−155.

47. Lee, D.; Adams, J. L.; Brandt, M.; DeWolf, W. E.; Keller, P. M.; Levy, M. A. A substrate combinatorial array for caspases. *Bioorg. Med. Chem. Lett.* 1999, **9**(12), 1667−1672.

48. Harris, J. L.; Backes, B. J.; Leonetti, F.; Mahrus, S.; Ellman, J. A.; Craik, C. S. Rapid and general profiling of protease specificity by using combinatorial fluorogenic substrate libraries. *Proc. Natl. Acad. Sci. USA* 2000, **97**(14), 7754−7759.

49. Ahn, T.; Kim, J. S.; Choi, H. I.; Yun, C. H. Development of peptide substrates for trypsin based on monomer/excimer fluorescence of pyrene. *Anal. Biochem.* **2002**, 306(2), 247−251.

50. Sakabe, M.; Asanuma, D.; Kamiya, M.; Iwatate, R. J.; Hanaoka, K.; Terai, T.; Nagano, T.; Urano, Y. Rational design of highly sensitive fluorescence probes for protease and glycosidase based on precisely controlled spirocyclization. *J. Am. Chem. Soc.* 2013, **135**(1), 409−414.

51. Leytus, S. P.; Melhado, L. L.; Mangel, W. F. Rhodamine-based compounds as fluorogenic substrates for serine proteinases. *Biochem. J.* 1983, **209**(2), 299−307.

52. Gooch, J.; Abbate, V.; Daniel, B.; Frascione N. Solid-phase synthesis of Rhodamine-110 fluorogenic substrates and their application in forensic analysis. *Analyst* 2016, **141**(8), 2392−2395.

53. Beija, M.; Afonso, C. A. M.; Martinho, J. M. G. Synthesis and applications of Rhodamine derivatives as fluorescent probes. *Chem. Soc. Rev.* 2009, **38**(8), 2410−2433.

54. Turunen, P.; Rowan, A. E.; Blank, K. Single-enzyme kinetics with fluorogenic substrates: lessons learnt and future directions. *FEBS Lett.* 2014, **588**(19), 3553−3563.

55. Ganesh, S.; Klingel, S.; Kahle, H.; Valet, G. Flow cytometric determination of aminopeptidase activities in viable cells using fluorogenic rhodamine 110 substrates. *Cytometry* 1995, **20**(4), 334−340.

56. Hug, H.; Los, M.; Hirt, W.; Debatin, K. M. Rhodamine 110-linked amino acids and peptides as substrates to measure caspase activity upon apoptosis induction in intact cells. *Biochemistry* 1999, **38**(42), 13906−13911.

57. Grant, S. K.; Sklar, J. G.; Cummings, R. T. Development of novel assays for proteolytic enzymes using rhodamine-based fluorogenic substrates. *J. Biomol. Screen.* 2002, **7**(6), 531−540.

58. Pinto, M. R.; Schanze, K. S. Amplified fluorescence sensing of protease activity with conjugated polyelectrolytes. *Proc. Natl. Acad. Sci. USA* 2004, **101**(20), 7505−7510.

59. Sueyoshi, K.; Nogawa, Y.; Sugawara, K.; Endo, T.; Hisamoto, H. Highly sensitive and multiple enzyme activity assay using reagent-release capillary-isoelectric focusing with rhodamine 110-based substrates. *Anal. Sci.* 2015, **31**(11), 1155−1161.

60. Terentyeva, T. G.; Rossom, W. V.; Auweraer, M. V.; Blank, K.; Hofkens, J. Morpholinecarbonyl-rhodamine 110 based substrates for the determination of protease activity with accurate kinetic parameters. *Bioconjugate Chem.* 2011, **22**(10), 1932−1938.

61. Carmel, A.; Yaron, A. An intramolecularly quenched fluorescent tripeptide as a fluorogenic substrate of angiotensin-I-converting enzyme and of bacterial dipeptidyl carboxypeptidase. *Eur. J. Biochem.* **1978**, 87(2), 265−273.

62. Holskin, B. P.; Bukhtiyarova, M.; Dunn, B. M.; Baur, P.; Chastonay, J.; Pennington, M. V. A continuous fluorescence-based assay of human cytomegalovirus protease using a peptide substrate. *Anal. Biochem.* 1995, **227**(1), 148−155.

63. Taliani, M.; Bianchi, E.; Narjes, F.; Fossatelli, M.; Urbani, A.; Steinkühler, C.; Francesco, R. D.; Pessi, A. A continuous assay of hepatitis C virus protease based on resonance energy transfer depsipeptide substrates. *Anal. Biochem.* 1996, **240**(1), 60−67.

64. Sun, H.; Panicker, R. C.; Yao, S. Q. Activity based fingerprinting of proteases using FRET peptides. *Biopolymers* 2007, **88**(2), 141−149.

65. Linder, K. E.; Metcalfe, E.; Nanjappan, P.; Arunachalam, T.; Ramos, K.; Skedzielewski, T. M.; Marinelli, E. R.; Tweedle, M. F.; Nunn, A. D.; Swenson, R. E. Synthesis, in Vitro evaluation, and in vivo metabolism of fluor/quencher compounds containing IRDye 800CW and Black Hole Quencher-3 (BHQ-3). *Bioconjugate Chem.* 2011, **22**(7), 1287−1297.

66. Oliveira, L. C. G.; Silva, V. O.; Okamoto, D. N.; Kondo, M. Y.; Santos, S. M. B.; Hirata, I. Y.; Vallim, M. A.; Pascon, R. C.; Gouvea, I. E.; Juliano, M. A.; Juliano, L. Internally quenched fluorescent peptide libraries with randomized sequences designed to detect endopeptidases. *Anal. Biochem.* 2012, **421**(1), 299−307.

67. Poreba, M.; Szalek, A.; Rut, W.; Kasperkiewicz, P.; Rutkowska-Wlodarczyk, I.; Snipas, S. J.; Itoh, Y.; Turk, D.; Turk, B.; Overall, C. M.; Kaczmarek, L.; Salvesen, G. S.; Drag, M. Highly sensitive and adaptable fluorescence-quenched pair discloses the substrate specificity profiles in diverse protease families. *Sci. Rep.* 2017, **7**, 43135.

68. Sapsford, K. E.; Berti, L.; Medintz, I. L. Materials for fluorescence resonance energy transfer analysis: beyond traditional donor-acceptor combinations. *Angew. Chem. Int. Ed.* 2006, **45**(28), 4562−4589.

69. Sekar, R. B.; Periasamy, A. Fluorescence resonance energy transfer (FRET) microscopy imaging of live cell protein localizations. *J. Cell Biol.* 2003, **160**(5), 629−633.

70. Latt, S. A.; Auld, D. S.; Vallee, B. L. Fluorescence determination of carboxypeptidase A activity based on electronic energy transfer. *Anal. Biochem.* 1972, **50**(1), 56−62.

71. Medintz, I. L.; Clapp, A. R.; Brunel, F. M.; Tiefenbrunn, T.; Uyeda, H. T.; Chang, E. L.; Deschamps, J. R.; Dawson, P. E.; Mattoussi, H. Proteolytic activity monitored by fluorescence resonance energy transfer through quantum-dot-peptide conjugates. *Nat. Mater.* 2006, **5**(7), 581−589.

72. Chang, E.; Miller, J. S.; Sun, J.; Yu, W. W.; Colvin, V. L.; Drezek, R.; West, J. L. Protease-activated quantum dot probes. *Biochem. Biophys. Res. Commun.* 2005, **334**(4), 1317−1321.

73. Petryayeva, E.; Algar, W. R. Multiplexed homogeneous assays of proteolytic activity using a smartphone and quantum dots. *Anal. Chem.* 2014, **86**(6), 3195−3202.

74. Jamieson, T.; Bakhshi, R.; Petrova, D.; Pocock, R.; Imani, M.; Seifalian, A. M. Biological applications of quantum dots. *Biomaterials* 2007, **28**(31), 4717−4732.

75. Han, M.; Gao, X.; Su, J. Z.; Nie, S. Quantum-dot-tagged microbeads for multiplexed optical coding of biomolecules. *Nat. Biotechnol.* 2001, **19**(7), 631−635.

76. Zrazhevskiy, P.; Sena, M.; Gao, X. Designing multifunctional quantum dots for bioimaging, detection, and drug delivery. *Chem. Soc. Rev.* 2010, **39**(11), 4326−4354.

77. Kim, G. B.; Kim, Y. P. Analysis of protease activity using quantum dots and resonance energy transfer. *Theranostics* 2012, **2**(2), 127−138.

78. Zhang, Y.; Wang, T. H. Quantum dot enabled molecular sensing and diagnostics. *Theranostics* 2012, **2**(7), 631−654.

Chapter 2

Novel self-quenching-based substrates for measurement of thrombin, trypsin, and chymotrypsin activities

2.1. Introduction

As mentioned in preceding chapter, commercially available fluorescent peptide probes such as Peptide-MCA and FRET-based substrate have some problems which are the deficient reflection of the specificity in prime region, complicated synthesis, and the restriction attributed to fluorophore and quencher. To solve these challenging matters, we focused on self-quenching-based substrates.

Several self-quenching-based substrates, which are peptide substrates multiply labelled with the identical fluorophores, have been already reported. The fluorescence of these substrates is self-quenched owing to the highly assembled fluorophores on the substrates. The release of these concentrated fluorophores by a protease allows for fluorescence recovery. Packard *et al.* reported the design of profluorescent elastase substrates where an undecapeptide in the substrate is labelled with two xanthene dyes on each side of the cleavage site.[1] While these substrates showed high quenching efficiency, the synthesis of these substrates remain unsophisticated. The synthesis of the substrates requires the coupling of two tetramethylrhodamines to the substrate in liquid phase synthesis after the completion of the synthesis of the substrate peptide by solid-phase peptide synthesis

(SPPS) because their substrates do not have branched unit. Ternon *et al.*, Galande *et al.*, and Avlonitis *et al.* designed multi-branched fluorescent probes, which consisted of branched unit such as lysines or a 1,1,1-tris(hydroxymethyl)aminomethane derivative, substrate peptides, and several identical fluorophores.[2-4] However, in the case of these substrates, three or more fluorophores should be coupled to multi-branched compound on the resin, meaning this is directed against simple synthesis. In addition, these multi-labelled substrates tend to be poor solubility and sterically hindered, and have several proteolytic cleavage sites. These properties cause slow hydrolyzation and complication of the reaction system.

There is still room for improvement in design of self-quenching-based substrates for easier synthesis and kinetic analysis. Moreover, detailed kinetic assays and inhibitor evaluation using these substrates have not been described yet.

2.2. Design

In this study, we designed two simple and easily synthesizable self-quenching-based substrates **1** and **2** for the detection of thrombin and trypsin activities (Fig. 1). A kinetic assay and inhibitor evaluation were carried out using these substrates. Additionally, substrate **3** was designed for chymotrypsin (Fig. 2).

FITC-β-Ala-L-Val-L-Pro-L-Arg⌐
FITC-β-Ala-L-Val-L-Pro-L-Arg-L-Lys-NH₂ **(1)**

FITC-β-Ala-L-Val-L-Pro-L-Arg-Gly⌐
FITC-β-Ala-L-Val-L-Pro-L-Arg-Gly-L-Lys-NH₂ **(2)**
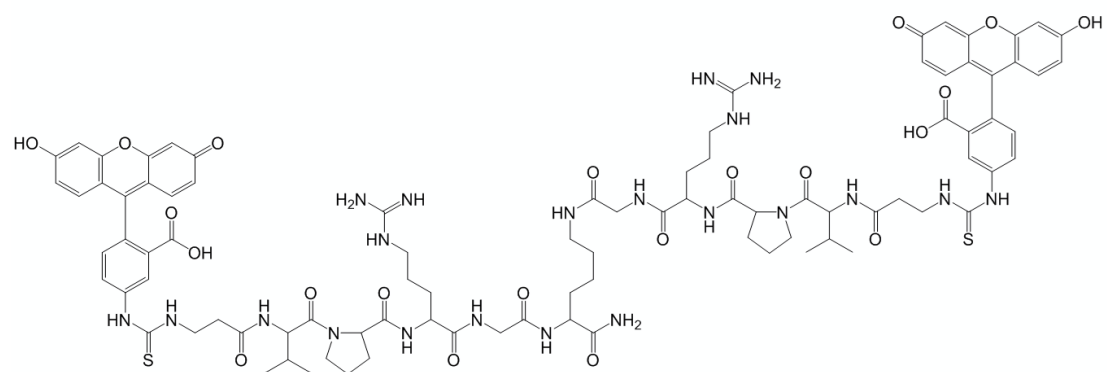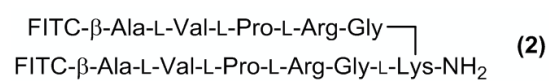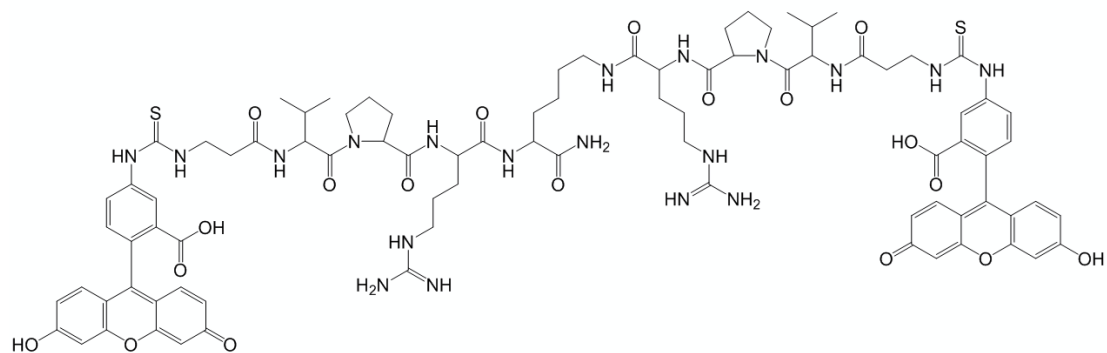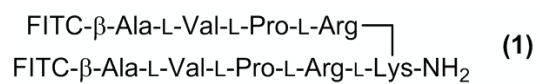
Fig. 1 Design of the self-quenching-based substrates for trypsin.

FITC-β-Ala-L-Ala-L-Ala-L-Phe⌐
FITC-β-Ala-L-Ala-L-Ala-L-Phe-L-Lys-NH₂ **(3)**
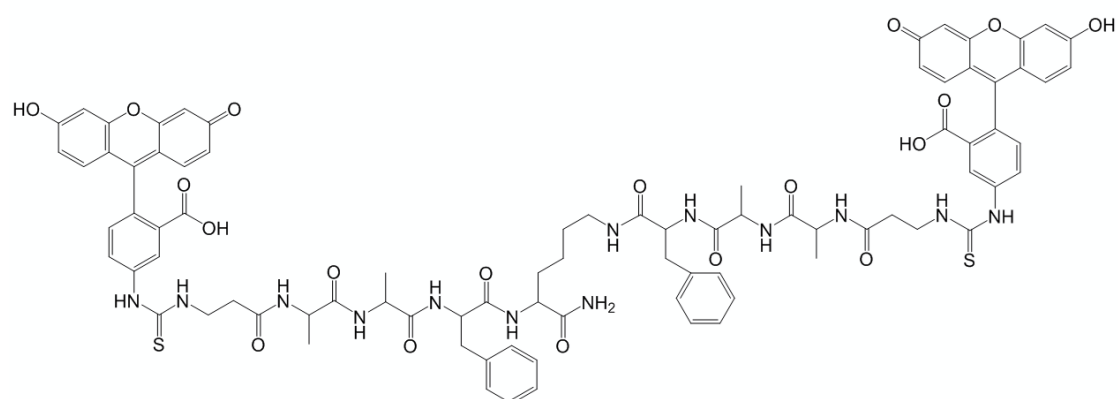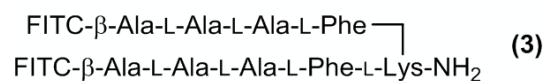
Fig. 2 Design of the self-quenching-based substrate for chymotrypsin.

32

The self-quenching-based substrates consist of two fluorescein isothiocyanates (FITCs) and the corresponding enzyme specific peptides. FITC has an excellent fluorescence quantum yield, good water solubility, and it readily reacts with amino groups. Therefore, it is commonly applied in a variety of assays. One extra amino acid was inserted between the arginine and lysine residues in **2** to demonstrate that the specificity of the P1′ amino acid residue can be reflected in the artificial substrate. These two FITC-binding substrate peptides are linked to two amino groups of lysine. Lysine was selected for the branched unit because of the convenient preparation of these substrates using only SPPS. Two FITCs were densely assembled on the substrates to quench the fluorescence via self-quenching. Before the proteolytic cleavage, the emission of FITC is quenched by intramolecular self-quenching (Fig. 3). After the cleavage, FITC is liberated, and its fluorescence is recovered.
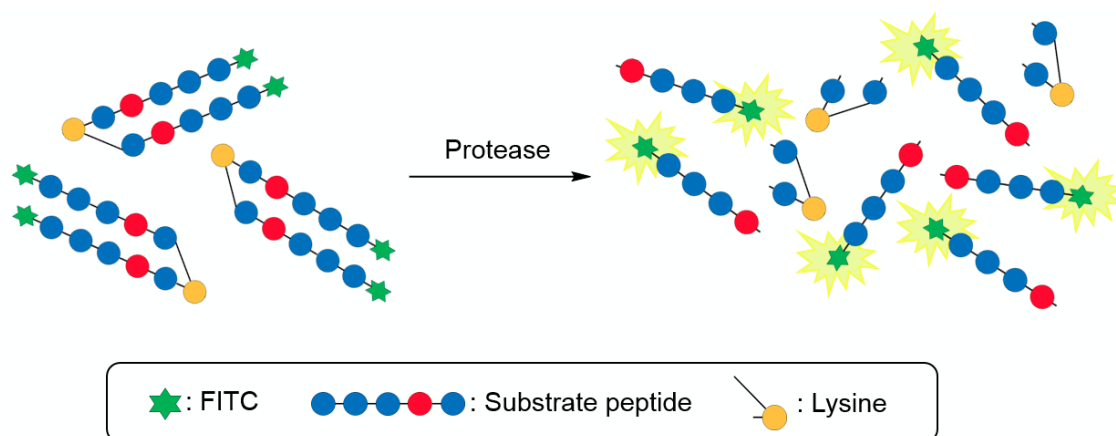
Fig. 3 Schematic representation of the detection system for **2**.

The syntheses of these substrates were very simple (Scheme 1 and 2). The corresponding FITC-peptide chains of the substrate peptides were elongated from the two amino groups

of lysine on the amide resin using standard Fmoc SPPS. After cleavage from the solid support, three self-quenching-based substrates **1**, **2**, and **3** were obtained.
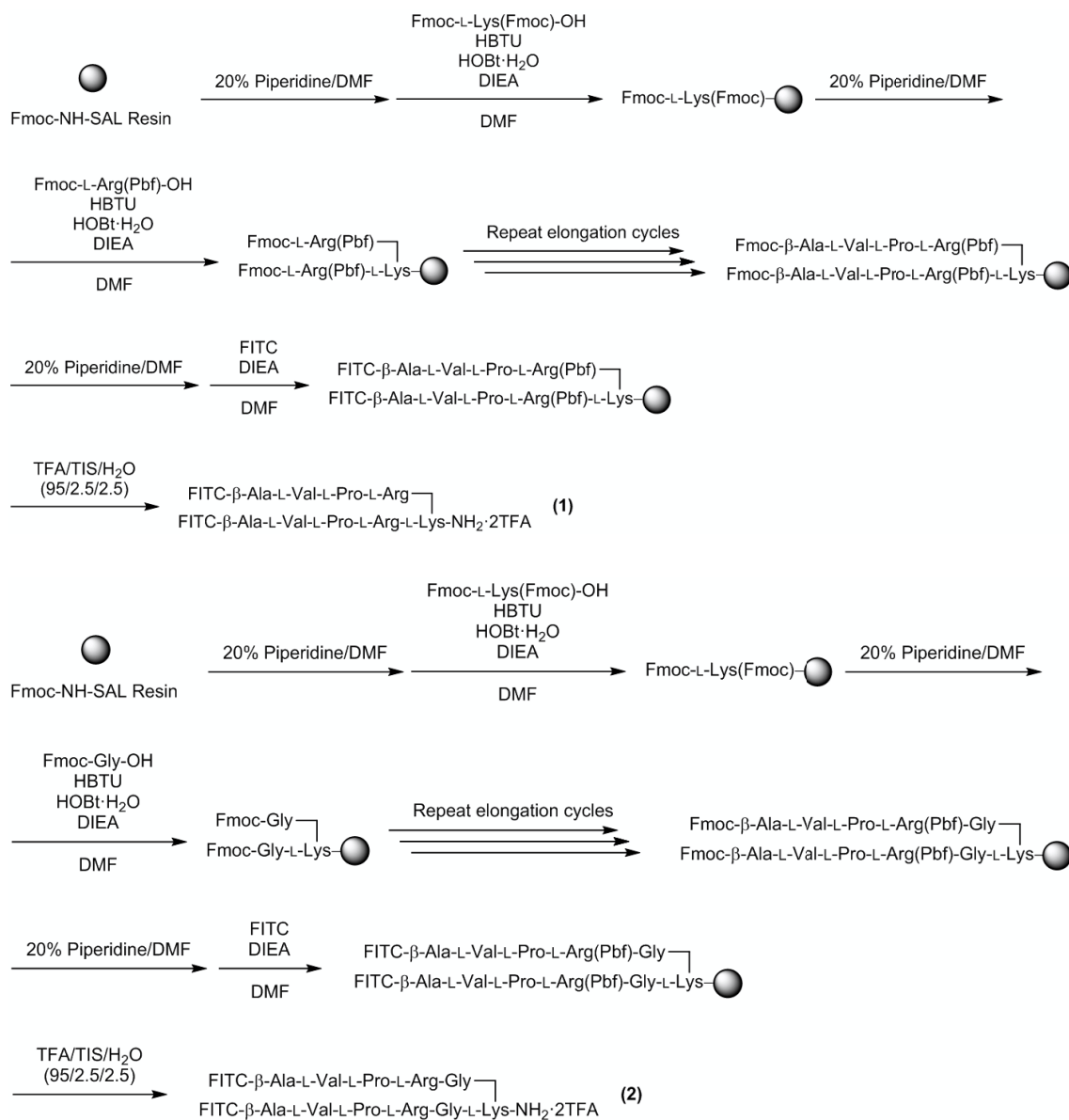
Scheme 1   Synthetic routes of **1** and **2**.
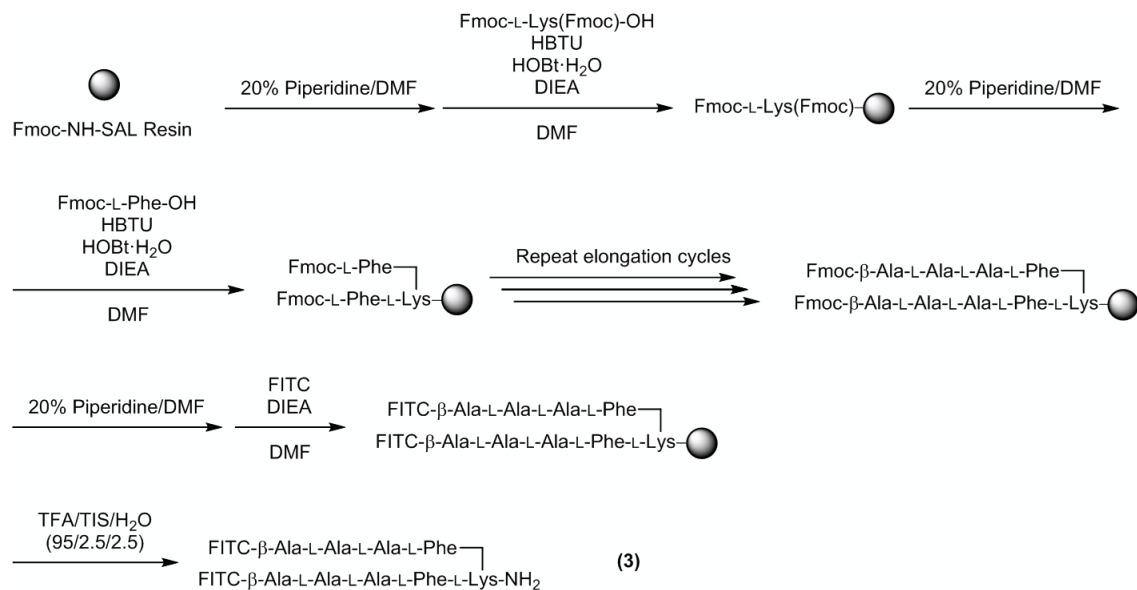
Scheme 2 Synthetic route of **3**.

2.3. Target proteases

2.3.1. Thrombin

Thrombin (EC 3.4.21.5) is a trypsin-like serine protease in blood, and can cleave polypeptide substrates at Arg/Lys-Xaa bonds (where Xaa is any amino acid). Thrombin serves as a regulator in the cascade of blood coagulation (Fig. 4).[5]

Fig. 4   Multifunctional roles of thrombin.[6]

Thrombin is originally secreted as its inactive precursor prothrombin from liver. Cleavage of prothrombin at R_{323} by factor Xa which is one of serine proteases results in the conversion of prothrombin into meizothrombin as an intermediate, followed by subsequent hydrolyzation at R_{274} to produce thrombin (Fig. 5). When these bond cleavages proceed in the opposite order (cleavage at R_{323}, followed by cleavage at R_{274}), prethrombin is yielded as an intermediate.[7,8]

Fig. 5   Pathways of prothrombin activation.[9]

Thrombin cleaves fibrinogen to form fibrin which is the scaffolding of thrombosis.[10,11] In addition, thrombin plays key roles in platelet receptor activation, endothelium activation, and activation of factors V, VIII, XI (coagulation factors), and XIII (fibrin stabilizing factor) (Fig. 6).[12−14]

Fig. 6 Antagonizing actions of thrombin in coagulation cascade.[15]

Therefore, thrombin may be associated with various diseases such as thrombosis, inflammation, Alzheimer's disease, and cancers.[16−19] Recently, it was reported that urinary thrombin activity could be used as a specific biomarker for crescentic glomerulonephritis (CresGN).[20,21] CresGN rapidly progresses to renal failure; however, the appropriate treatment at early stages may cure of this disease without impaired renal function. Hence, the detection of urinary thrombin activity is required for the noninvasive diagnosis of CresGN at early stages.

2.3.2. Trypsin

Trypsin (EC 3.4.21.4) can also cleave polypeptide substrates at Arg/Lys-Xaa bonds and is required for protein digestion.[22,23] Trypsin is primarily produced as its inactive precursor trypsinogen from pancreas, and trypsinogen is activated as trypsin by enterokinase (Fig. 7).[24,25] Moreover, trypsin can activate not only trypsinogen and many other digestive proenzymes (*e.g.* chymotrypsinogen, proelastase, kallikreinogen, procarboxypeptidase, and some prolipases) but also pancreatic and inflammatory cells.
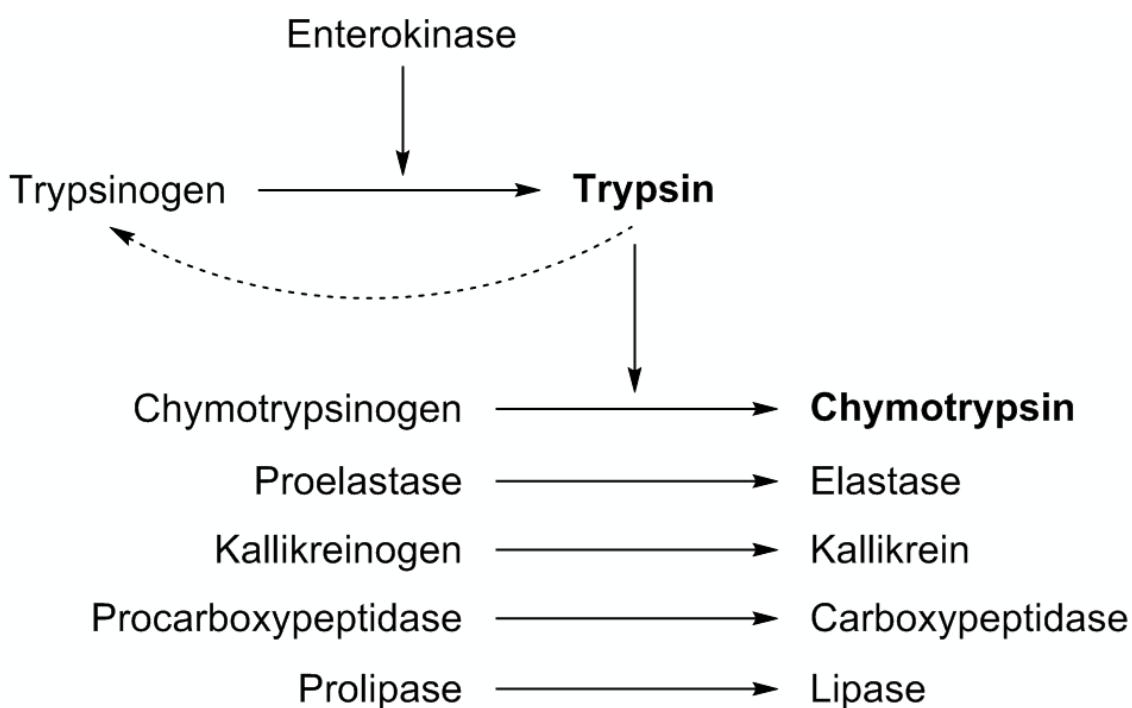
Fig. 7 Activation of trypsin, chymotrypsin, and other digestive proenzymes.

Therefore, trypsin plays an essential role in regulating pancreatic exocrine function. However, overexpression or deficiency of trypsin is directly associated with some types of pancreatic and other diseases.[26–30] Although trypsin is commonly used as a model

protease because it is inexpensive and readily available, trypsin can be considered as a promising biomarker for some pancreatic diseases.

2.3.3. Chymotrypsin

Chymotrypsin (EC 3.4.21.1) is also one of the most common serine proteases, and is relevant to many physiological processes such as digestion, hemostasis, apoptosis, signal transduction, reproduction, and the immune response.[4] Chymotrypsin is specifically hydrolyzed the peptide bond at Phe/Tyr/Trp-Xaa of polypeptide. Chymotrypsin is initially secreted as its inactive precursor chymotrypsinogen from pancreas, and chymotrypsinogen is activated as chymotrypsin by trypsin (Fig. 7).[26] Chymotrypsin is known as not only a model protease as well trypsin but also one of disease-related proteases. Chymotrypsin is associated with pancreatic fibrosis, maldigestion, diabetes mellitus, hypertension, inflammation, and many types of cancers, particularly pancreatic cancer.[31] Furthermore, elevated level of chymotrypsin in serum is involved in acute pancreatitis and renal failure.[32] Therefore, the detection of chymotrypsin activity is significant in drug discovery and clinical diagnosis.

2.4. Experimental section

2.4.1. Materials and instruments

All Fmoc-protected amino acids, Fmoc-NH-SAL resin, piperidine, *O*-(1H-benzotriazol-1-yl)-*N,N,N′,N′*-tetramethyluronium hexafluorophosphate (HBTU), 1-hydroxy-1H-benzotriazole hydrate (HOBt·H$_2$O), *N,N*-diisopropylethylamine (DIEA), and 2,2,2-trifluoroacetic acid (TFA) were purchased from Watanabe Chemical Industries, Ltd. FITC-I was supplied from Dojindo Molecular Technologies, Inc. α-Trypsin from bovine pancreas, α-chymotrypsin from bovine pancreas, thrombin from human plasma, and Bowman-Birk inhibitor from *Glycine max* (soybean) were obtained from Sigma-Aldrich Co. LLC. All solvents and other reagents were ordered from Wako Pure Chemical Industries, Ltd. The assay buffer solution was 50 mM Tris-HCl buffer (pH 8.0) containing 150 mM NaCl, 1 mM CaCl$_2$, and 0.1 mg/mL bovine serum albumin (BSA). Analytical high performance liquid chromatography (HPLC) was performed on a Hitachi L-7100 instrument equipped with a chromolith performance RP-18e column (4.6 x 100 mm; Merck). The mobile phases were 0.1% TFA in H$_2$O (solvent A) and 0.1% TFA in H$_2$O (solvent B) using a linear gradient of solvent B in solvent A (0–50% over 15 min) with a flow rate of 2.0 mL/min, and absorbance at 220 nm was used for the detection. Semi-preparative HPLC was performed on a Hitachi L-7100 instrument equipped with an XTerra Prep MS C18 OBD 10 μm (19 x 150 mm; Waters). The mobile phases were 0.1% TFA in H$_2$O (solvent A) and 0.1% TFA in H$_2$O (solvent B) using a linear gradient of solvent B in solvent A (25–35% or 40–50% over 30 min) with a flow rate of 5.0 mL/min, and absorbance at 220 nm or 290 nm was used for the detection. High resolution mass

spectrometry (HR-MS) (Electrospray ionization time-of-flight mass spectrometer (ESI-TOF-MS)) data were measured on a JEOL THE ACCUTOF LC-PLUS JMS-T100LP instrument. pH measurements were made with a D-71 LAQUA portable pH meter (Horiba). Lyophilization was carried out on a VD-800F freeze dryer (TAITEC). Absorbance was measured using a GE Healthcare Ultrospec 3300 pro UV/Vis spectrometer or a JASCO V-550 UV/VIS spectrophotometer. Fluorescence spectra were measured on a JASCO FP-6600 spectrofluorometer. The enzyme reaction was investigated using a Wallac ARVO SX 1420 Multilabel Counter on a 96-well black plate. Deionized water was obtained from a Milli-Q Plus system (Millipore).

2.4.2. Synthesis

2.4.2.1. Solid-phase synthesis of 1, 2, and 3

Fmoc-L-Lys(Fmoc)-OH was loaded onto Fmoc-NH-SAL resin (0.54 mmol/g resin) using Fmoc/piperidine strategies on a 0.432 mmol scale. HBTU and HOBt·H_2O were used as activating agents. After capping the *N*-terminal with acetic anhydride, the corresponding peptide chain was elongated. Subsequently, FITC-I was coupled to the elongated peptide in the presence of DIEA. The resin-supported peptide was cleaved from the resin in the cleavage cocktail (TFA/Triisopropylsilane/H_2O = 95:2.5:2.5). The peptide was precipitated by ether in an ice bath. The crude peptide was purified by HPLC. The purified substrate was analyzed by HR-MS (ESI-TOF-MS).

Substrate **1**; Overall yield: 17% (0.012 g, 0.006 mmol). *m/z* calcd. for $[(M+H)^+]$ $C_{86}H_{104}N_{19}O_{19}S_2$: 1770.71972; found: 1770.72794, Retention time: 8.51 min.

8.51 min

Fig. 8 HPLC profile of **1**. HPLC conditions: a linear gradient of solvent B in solvent A (0–50% over 15 min); Chromolith performance RP-18e column (4.6 x 100 mm; Merck); flow rate, 2 mL/min; solvent A: 0.1% TFA in H_2O; solvent B: 0.1% TFA in CH_3CN; detection at 220 nm.

Mass	Intensity	Calc. Mass	Mass Difference [mDa]	Mass Difference [ppm]	Possible Formula	Unsaturation Number
1770.72794	18560.62	1770.71972	8.21	4.64	$^{12}C_{86}{}^1H_{104}{}^{14}N_{19}{}^{16}O_{19}{}^{32}S_2$	46.5
1771.73159	20234.09	1771.72755	4.04	2.28	$^{12}C_{86}{}^1H_{105}{}^{14}N_{19}{}^{16}O_{19}{}^{32}S_2$	46.0

Fig. 9 MASS spectrum of **1**.

Substrate **2**; Overall yield: 24% (0.022 g, 0.010 mmol). *m/z* calcd. for $[(M+H)^+]$ $C_{90}H_{110}N_{21}O_{21}S_2$: 1884.76265; found: 1884.76489, Retention time: 7.86 min.

7.86 min

Fig. 10 HPLC profile of **2**. HPLC conditions: a linear gradient of solvent B in solvent A (0–50% over 15 min); Chromolith performance RP-18e column (4.6 x 100 mm; Merck); flow rate, 2 mL/min; solvent A: 0.1% TFA in H_2O; solvent B: 0.1% TFA in CH_3CN; detection at 220 nm.

Mass	Intensity	Calc. Mass	Mass Difference [mDa]	Mass Difference [ppm]	Possible Formula	Unsaturation Number
1884.76489	9801.09	1884.76265	2.23	1.19	$^{12}C_{90}{}^{1}H_{110}{}^{14}N_{21}{}^{16}O_{21}{}^{32}S_2$	48.5
1885.76739	12708.90	1885.77048	−3.09	−1.64	$^{12}C_{90}{}^{1}H_{111}{}^{14}N_{21}{}^{16}O_{21}{}^{32}S_2$	48.0

Fig. 11 MASS spectrum of **2**.

Substrate **3**; Overall yield: 7% (0.011 g, 0.007 mmol). m/z calcd. for $[(M+H)^+]$ $C_{84}H_{86}N_{13}O_{19}S_2$: 1644.56043; found: 1644.55988, Retention time: 8.42 min.
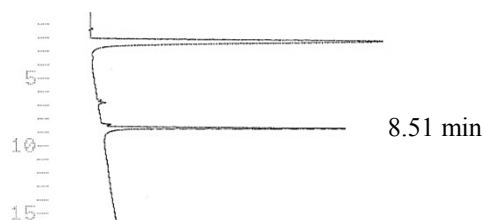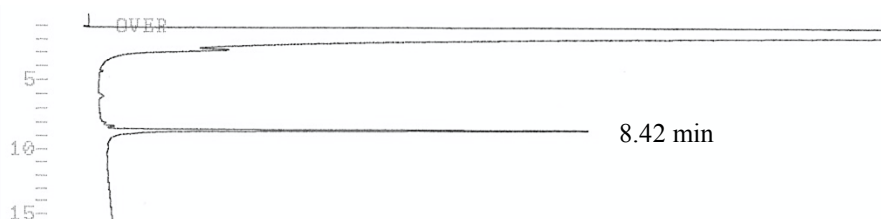

8.42 min

Fig. 12 HPLC profile of **3**. HPLC conditions: a linear gradient of solvent B in solvent A (0–50% over 15 min); Chromolith performance RP-18e column (4.6 x 100 mm; Merck); flow rate, 2 mL/min; solvent A: 0.1% TFA in H_2O; solvent B: 0.1% TFA in CH_3CN; detection at 220 nm.
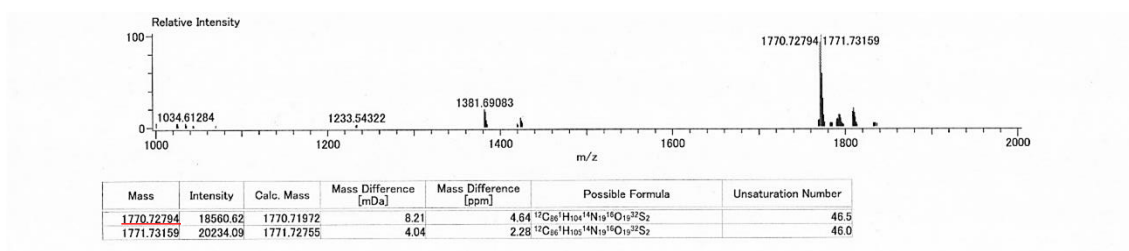
Relative Intensity

Mass	Intensity	Calc. Mass	Mass Difference [mDa]	Mass Difference [ppm]	Possible Formula	Unsaturation Number
1644.55988	3127.91	1644.56043	−0.55	−0.34	$^{12}C_{84}{}^{1}H_{86}{}^{14}N_{13}{}^{16}O_{19}{}^{32}S_2$	50.5
1666.54078	6822.35	1666.54238	−1.59	−0.96	$^{12}C_{84}{}^{1}H_{85}{}^{14}N_{13}{}^{23}Na_1{}^{16}O_{19}{}^{32}S_2$	50.5

Fig. 13 MASS spectrum of **3**.

2.4.2.2. Solid-phase synthesis of 4 and 5
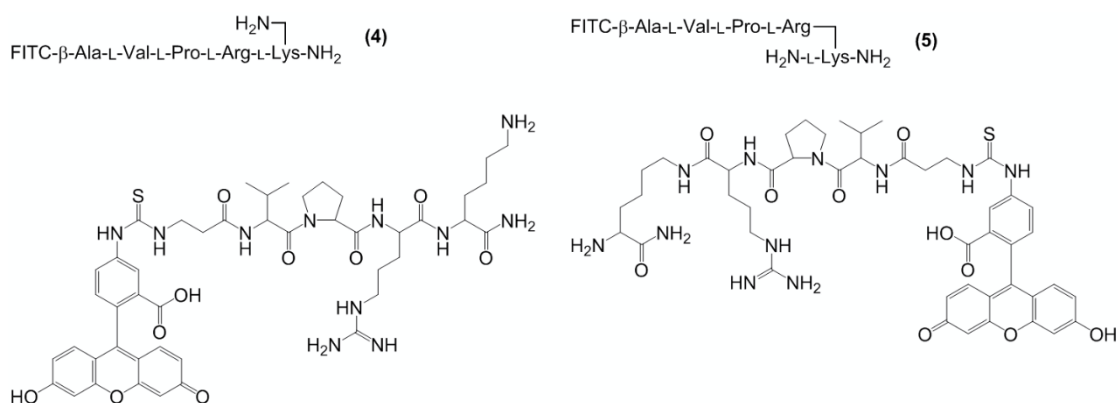
Fig. 14 Cleavable substrate residues **4** and **5**.

Fmoc-L-Lys(Boc)-OH or Boc-L-Lys(Fmoc)-OH was loaded onto Fmoc-NH-SAL resin (0.56 mmol/g resin) using Fmoc/piperidine strategies on a 0.448 mmol scale. HBTU and HOBt·H_2O were used as activating agents. After capping the *N*-terminal with acetic anhydride, the corresponding peptide chain was elongated. Subsequently, FITC-I was coupled to the elongated peptide in the presence of DIEA. The resin-supported peptide was cleaved from the resin in the cleavage cocktail (TFA/Triisopropylsilane/H_2O = 95:2.5:2.5). The peptide was precipitated by ether in an ice bath. The crude peptide was purified by HPLC. The purified substrate was analyzed by HR-MS (ESI-TOF-MS).

Substrate **4**; Overall yield: 24% (0.040 g, 0.034 mmol). *m/z* calcd. for $[(M+H)^+]$ $C_{46}H_{60}N_{11}O_{10}S$: 958.42453; found: 958.42301, Retention time: 5.32 min.
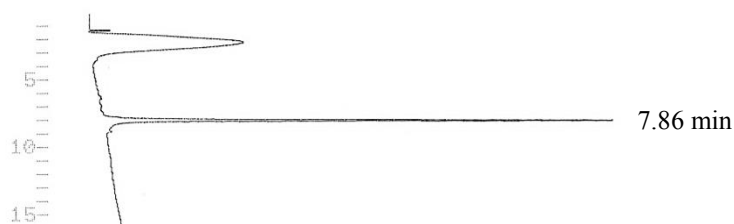

Fig. 15   HPLC profile of **4**. HPLC conditions: a linear gradient of solvent B in solvent A (0–50% over 15 min); Chromolith performance RP-18e column (4.6 x 100 mm; Merck); flow rate, 2 mL/min; solvent A: 0.1% TFA in H_2O; solvent B: 0.1% TFA in CH_3CN; detection at 220 nm.
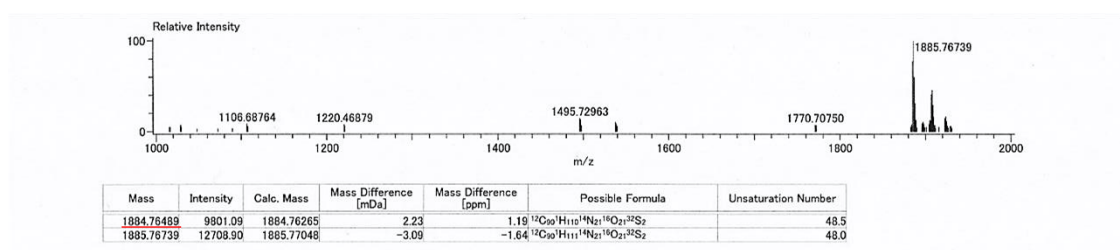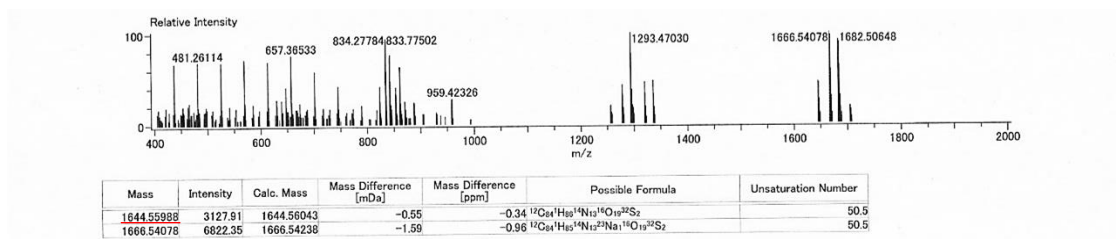

Mass	Intensity	Calc. Mass	Mass Difference [mDa]	Mass Difference [ppm]	Possible Formula	Unsaturation Number
958.42301	425566.10	958.42453	−1.52	−1.59	$^{12}C_{45}{}^{1}H_{60}{}^{14}N_{11}{}^{16}O_{10}{}^{32}S_1$	23.5

Fig. 16   MASS spectrum of **4**.

Substrate **5**; Overall yield: 24% (0.043 g, 0.036 mmol). *m/z* calcd. for $[(M+H)^+]$ $C_{46}H_{60}N_{11}O_{10}S$: 958.42453; found: 958.42737, Retention time: 5.30 min.
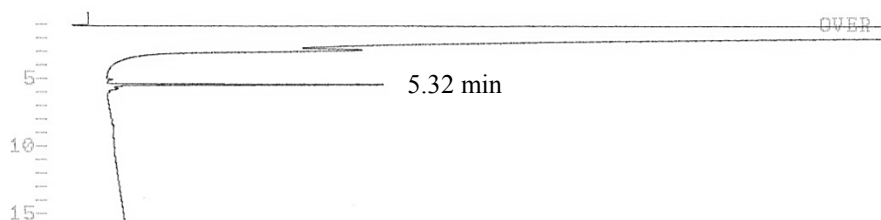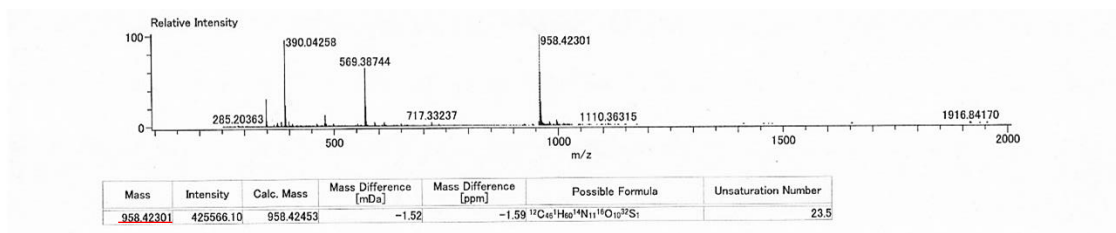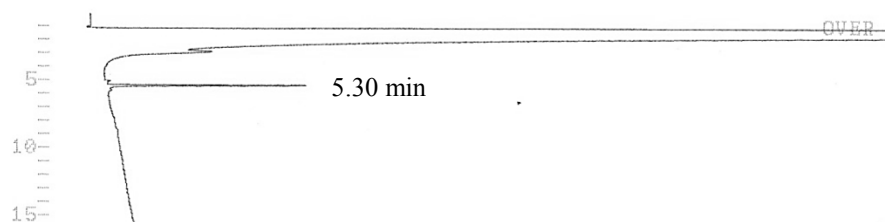
5.30 min

Fig. 17 HPLC profile of **5**. HPLC conditions: a linear gradient of solvent B in solvent A (0–50% over 15 min); Chromolith performance RP-18e column (4.6 x 100 mm; Merck); flow rate, 2 mL/min; solvent A: 0.1% TFA in H$_2$O; solvent B: 0.1% TFA in CH$_3$CN; detection at 220 nm.

Mass	Intensity	Calc. Mass	Mass Difference [mDa]	Mass Difference [ppm]	Possible Formula	Unsaturation Number
958.42737	1003432.37	958.42453	2.84	2.96	$^{12}C_{46}{}^{1}H_{60}{}^{14}N_{11}{}^{16}O_{10}{}^{32}S_1$	23.5
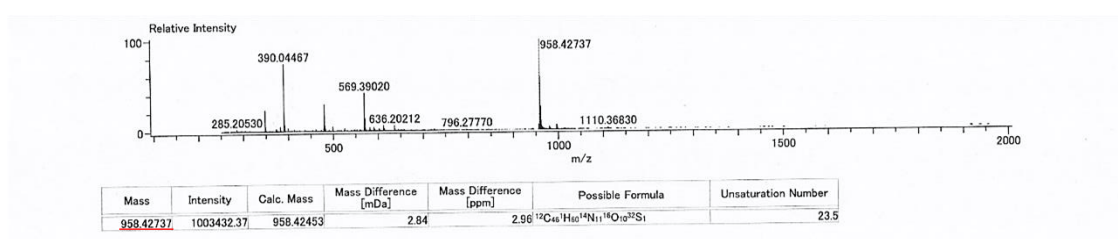
Fig. 18 MASS spectrum of **5**.

2.4.3. Analysis

2.4.3.1. Preparation of stock solutions

The stock solutions of **1**, **2**, **3**, **4**, **5**, ^{i}Boc-VPR-MCA (**6**), and FITC-β-Ala-OH were prepared in dimethylsulfoxide (DMSO) and stored in a refrigerator. The concentration of the FITC solutions was determined by the molar extinction coefficient of FITC-β-Ala-OH at 495 nm (ε_{495} = 76,300 M^{-1}·cm^{-1}). The stock solution of trypsin, chymotrypsin, and thrombin in the micromolar range was prepared in the buffer and stored in a freezer. The concentration of the trypsin solution was determined using the molar extinction coefficient of trypsin at 280 nm (ε_{280} = 36,280 M^{-1}·cm^{-1}).[33] The concentration of the

chymotrypsin solution was determined using the molar extinction coefficient of chymotrypsin at 280 nm (ε_{280} = 50,000 M^{-1}·cm^{-1}).[34] The concentration of the thrombin solution was determined using the molar extinction coefficient of thrombin at 280 nm (ε_{280} = 66,800 M^{-1} cm^{-1}).[35] The stock solution of Bowman–Birk inhibitor (BBI) in the micromolar range was prepared in distilled water and stored in a freezer. The concentration of BBI was estimated spectrophotometrically using the values of M_r = 7,975 Da and $A^{1\%}_{280}$ = 4.4.[36] The stock solutions were diluted with the buffer prior to the fluorescence measurements. The concentration of DMSO in the assay was less than 5%.

2.4.3.2. Investigation of self-quenching efficiency of 1, 2, and 3

The stock solutions of **1**, **2**, **3**, and FITC-β-Ala-OH were diluted with the buffer, and an equimolar solution of each of the FITC moieties (1 µM) was prepared. The fluorescence spectra of these solutions upon excitation at 485 nm were measured with a spectrofluorometer. The self-quenching efficiency was calculated by using the following equation:

$$\text{Self-Quenching efficiency (\%)} = \left(1 - \frac{F_{\text{substrate}}}{F_{\text{control}}} \right) \times 100 \qquad (1)$$

where $F_{\text{substrate}}$ is the fluorescence intensity of **1**, **2**, or **3** and F_{control} is the fluorescence intensity of FITC-β-Ala-OH.

48

2.4.3.3. Examination of influence of 4 and 5 on trypsin assays using 1

The stock solutions of **1**, **4**, and **5** were diluted with the buffer, and the final concentration of **1** was adjusted to 10 µM. The final concentration of **4** or **5** ranged from 2 µM to 10 µM. The stock solution of trypsin was also diluted with the buffer, and the final concentration of trypsin was adjusted to 1 nM. The hydrolysis of **1** mixed with the different concentrations of **4** or **5** was initiated by the addition of trypsin solution, and monitored fluorometrically by using a microplate reader with an excitation of 485 nm and an emission of 535 nm. According to these fluorescence recovery, the initial velocities were calculated and compared respectively.

2.4.3.4. Calculation of kinetic parameters of 1, 2, 3, and 6

The stock solutions of **1**, **2**, **3**, and **6** were diluted with the buffer, and the final concentration of these substrates ranged from 1 to 32 µM. The stock solution of trypsin was also diluted with the buffer, and the final concentration of trypsin was adjusted to 1 nM. Similarly, the stock solution of chymotrypsin was also diluted with the buffer, and the final concentration of chymotrypsin was adjusted to 10 nM. The stock solution of thrombin was also diluted with the buffer, and the final concentration of thrombin was adjusted to 296 nM (for **1**), 196 nM (for **2**), and 1 nM (for **3**). The hydrolysis of the different concentrations of **1**, **2**, and **3** was initiated by the addition of trypsin, chymotrypsin, or thrombin solution, and monitored fluorometrically by using a microplate reader with an excitation of 485 nm and an emission of 535 nm. For **6**, an

excitation of 370 nm and emission of 460 nm were adopted. The kinetic parameters of K_m, V_{max}, k_{cat}, and k_{cat}/K_m were calculated by fitting the Michaelis–Menten equation described below with the least-squares method.

$$v_0 = \frac{V_{max}[S]}{K_m + [S]} \tag{2}$$

$$k_{cat} = \frac{V_{max}}{[E]} \tag{3}$$

where v_0 is the initial velocity, [S] is the substrate concentration, K_m is the Michaelis constant, V_{max} is the maximal velocity, [E] is the protease concentration, and k_{cat} is the turnover number.

2.4.3.5. Determination of detection limit in trypsin and chymotrypsin assays

The final concentration of **1**, **2**, and **3** was adjusted to 10 μM. The final concentration of trypsin ranged from 10 pM to 1 nM, and the final concentration of chymotrypsin ranged from 250 pM to 10 nM. The fluorescence recovery of each substrate in the presence of different concentrations of trypsin or chymotrypsin was measured using a microplate reader. The detection limit for trypsin or chymotrypsin was calculated using the following formula:[37]

$$\text{Limit of detection (LOD)} = \frac{3s_{y/x}}{K} \tag{4}$$

where $s_{y/x}$ is the standard deviation of y-residuals and K is the slope of the linear plot of fluorescence intensity versus trypsin or chymotrypsin concentration.

2.4.3.6. Determination of IC$_{50}$ and K_i of BBI

The final concentration of **1** and **2** was adjusted to 10 μM, and the final concentration of trypsin was adjusted to 1 nM. The final concentration of BBI ranged from 0 to 40 nM. Hydrolysis reactions for the different concentrations of BBI were initiated by the addition of the trypsin solution, and monitored fluorometrically by using a microplate reader as mentioned above. The IC$_{50}$ for BBI was estimated by fitting the Hill equation described below with the least-squares method.[38]

$$\text{Inhibition efficiency (\%)} = E_{\text{bottom}} + \frac{E_{\text{top}} - E_{\text{bottom}}}{1 + \exp\{n(\ln \text{IC}_{50} - \ln[\text{I}])\}} \tag{5}$$

where E_{bottom} is the minimal inhibition efficiency (0%), E_{top} is the maximal inhibition efficiency (100%), n is the Hill constant, and [I] is the BBI concentration.

Subsequently, the K_i for BBI was estimated by fitting the Morrison equation described below with the least-squares method.[39]

$$\frac{v_i}{v_0} = 1 - \frac{([\text{E}] + [\text{I}] + K_i) - \sqrt{([\text{E}] + [\text{I}] + K_i)^2 - 4[\text{E}][\text{I}]}}{2[\text{E}]} \tag{6}$$

where v_i is the initial velocity in the presence of BBI, v_0 is the initial velocity in the absence of BBI, [E] is the trypsin concentration, [I] is the BBI concentration, and K_i is the dissociation constant.

2.5. Results and discussion

2.5.1. Investigation of self-quenching efficiency

Initially, we investigated the self-quenching efficiency of **1**, **2**, and **3**. A total of 0.5 μM of **1**, **2**, and **3** were prepared in 50 mM Tris-HCl buffer (pH 8.0) containing 150 mM NaCl, 1 mM $CaCl_2$, and 0.1 mg/mL BSA. Similarly, 1 μM of a FITC-β-Ala-OH solution was also prepared in the buffer as a control sample. All of the solutions contained 1 μM of the FITC moieties, a concentration that did not cause self-quenching in a preliminary experiment. The fluorescence spectra upon excitation at 485 nm of each sample prior to the addition of trypsin or chymotrypsin were measured using a spectrofluorometer (Fig. 19). Substrates **1**, **2**, and **3** exhibited lower fluorescence emission compared with FITC-β-Ala-OH. Hence, it was demonstrated that **1**, **2**, and **3** showed quenched fluorescence by self-quenching. Using the spectral data, the quenching efficiencies were calculated. The substrates displayed moderate quenching efficiency with 60.7% for **1**, 64.1% for **2**, and 63.8% for **3**.
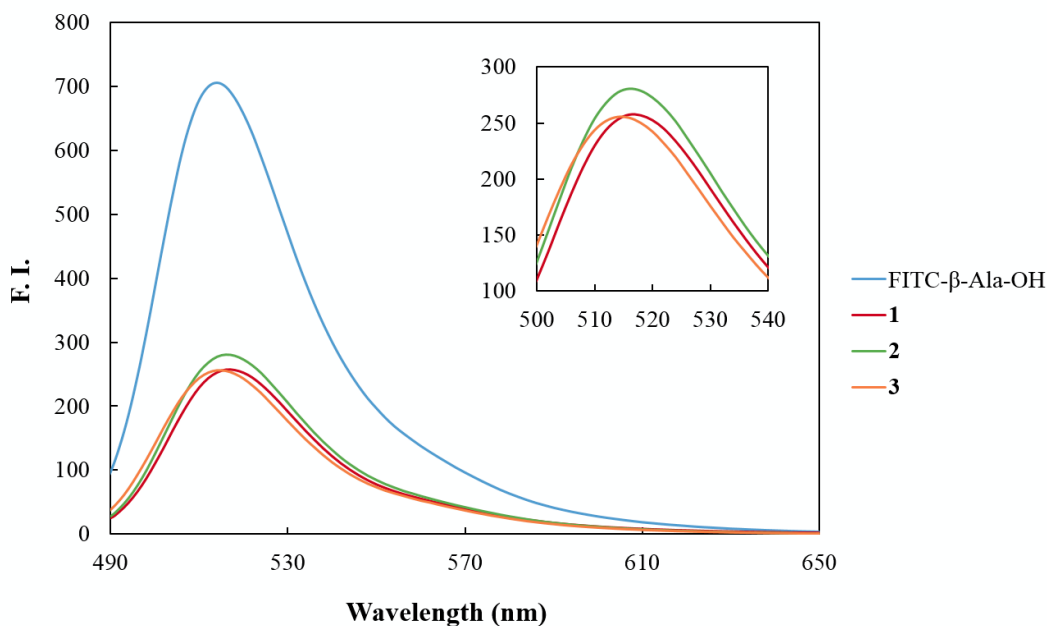
Fig. 19　Fluorescent spectra of **1**, **2**, **3** (0.5 µM), and FITC-β-Ala-OH (1 µM) in 50 mM Tris-HCl buffer (pH 8.0) containing 150 mM NaCl, 1 mM CaCl$_2$, and 0.1 mg/mL BSA at room temperature. Excitation wavelength was 485 nm.

2.5.2. Effect of cleavable substrate residues on kinetic assays

The substrates had two protease cleavage sites per molecule. For example, **1** contains two cleavage sites for trypsin. Cleaved substrates **4** and **5** still contain one cleavage site for trypsin (Scheme 3). Therefore, **4** and **5** might function as inhibitors. However, since the substrates were characterized by measuring the initial rates of turnover, any inhibition resulting from the production of **4** and **5** was minimized. As a control, to confirm that the products **4** and **5** did not significantly inhibit the turnover of their respective substrates, the initial velocity was calculated using 10 µM of **1** combined with 10% (based on the concentration of **1**) of **4** or **5** in the presence of 1 nM of trypsin. Under these conditions, the initial velocity decreased by only 3.2–3.5% compared with the rate of turnover of

substrate alone. It is likely that **4** and **5** are poor inhibitors for trypsin because of their increased hydrophilicity compared to the corresponding substrate caused by the release of one of the two hydrophobic fluorescent peptides, and thus, trypsin has reduced affinity for **4** and **5**. According to the above-mentioned results, analysis was carried out using standard Michaelis–Menten kinetic treatment.
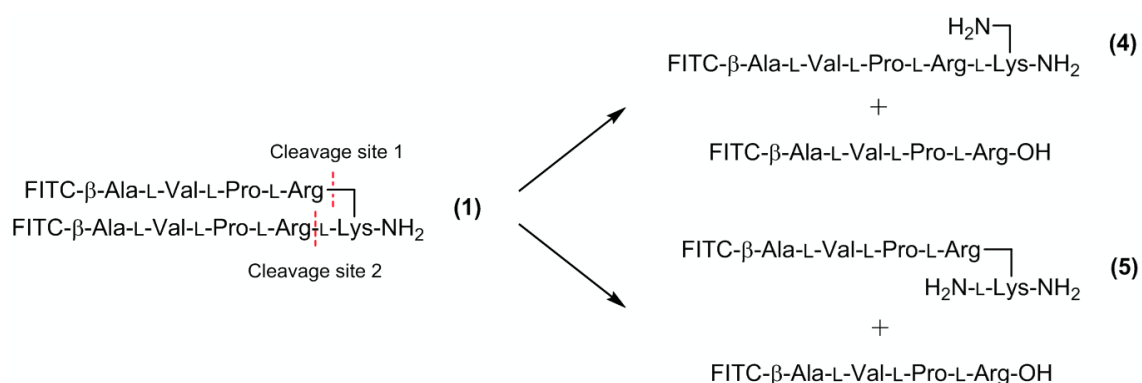
Scheme 3 Generation of hydrolysable residues **4** and **5**.

2.5.3. Kinetic assays of trypsin and chymotrypsin

Next, the increase in the fluorescence intensity of different concentrations of the substrates during tryptic or chymotryptic degradation was monitored. To each concentration of the substrates (1, 2, 4, 10, 16, 24, and 32 μM), 1 nM of trypsin or 10 nM of chymotrypsin was added, and the fluorescence recovery at 535 nm upon excitation at 485 nm was recorded using a fluorescence plate reader. Subsequently, the kinetic parameters for trypsin were calculated. According to the fluorescence recovery, the increases in the fluorescence intensities were converted to the corresponding initial velocities for the hydrolysis reactions. The kinetic parameters for trypsin or chymotrypsin

activity such as K_m, V_{max}, k_{cat}, and k_{cat}/K_m were estimated by fitting the data to the Michaelis–Menten equation using the least-squares method (Fig. 20).
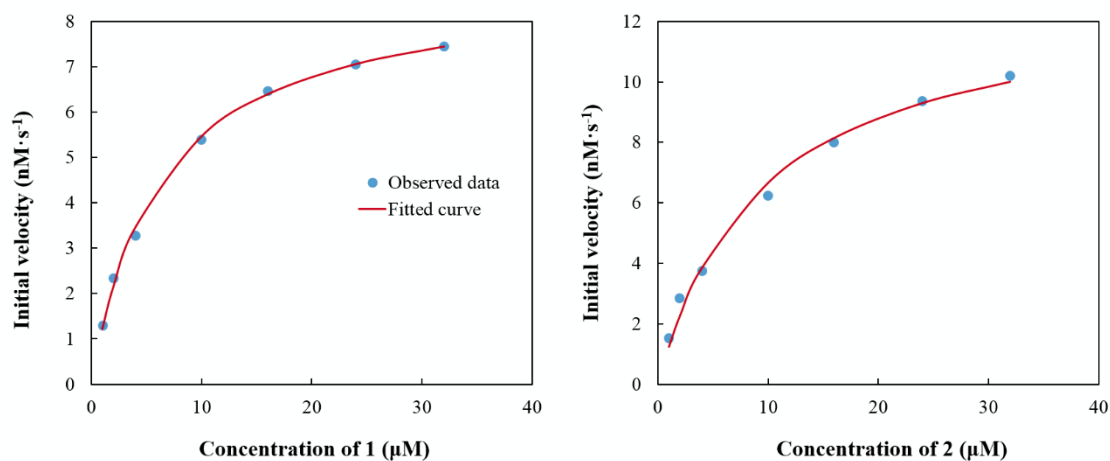

Fig. 20 Michaelis–Menten curve of **1** and **2** catalyzed by trypsin (1 nM) in 50 mM Tris-HCl buffer (pH 8.0) containing 150 mM NaCl, 1 mM $CaCl_2$, and 0.1 mg/mL BSA at room temperature with fluorometric method. Excitation/emission wavelengths were 485 nm/535 nm.

The K_m value of **2** was 1.5-fold higher than that of **1**, which meant that the affinity of **2** toward trypsin was slightly less than that of **1** (Table 1). The retention time of **2** from H analysis was shorter than that of **1**, indicating that the hydrophobicity of **2** was lower than that of **1**. As a result of the difference of the hydrophobic properties between **1** and **2**, it was expected that a difference of K_m values might be observed. The V_{max} and k_{cat} values of **2** were 1.5-fold higher than that of **1**, which indicated that **2** was easily liberated from trypsin because the extra glycine offered conformational and hydrophilic benefits for the release of the enzyme from the enzyme-substrate complex. The resulting k_{cat}/K_m values of **1** and **2** were almost equal. This indicated that extra glycine in **2** only minimally affected the interaction of **1** and **2** with trypsin.

Furthermore, kinetic analysis of ^{i}Boc-VPR-MCA (**6**), which is a commonly used fluorescent substrate, was determined for comparison purposes (Fig. 21).

^{i}Boc-VPR-MCA   **(6)**

Fig. 21   Standard fluorescent probe, ^{i}Boc-VPR-MCA (**6**).

After addition of trypsin into the substrate solutions, fluorescence recovery at 460 nm upon excitation at 370 nm was recorded using a fluorescence plate reader, and initial velocity was calculated (Fig. 22).

Fig. 22 Michaelis–Menten curve of **6** catalyzed by trypsin (1 nM) in 50 mM Tris-HCl buffer (pH 8.0) containing 150 mM NaCl, 1 mM CaCl$_2$, and 0.1 mg/mL BSA at room temperature with fluorometric method. Excitation/emission wavelengths were 370 nm/460 nm.

While the K_m value of **6** was lower than that of **1** and **2**, the V_{max} and k_{cat} values of **6** were lower than those of **2** (Table 1). These data indicated that the turnover number for **2** was larger than that for **6** although the affinity of trypsin toward **6** was stronger than its affinity toward **1** or **2**. The resulting k_{cat}/K_m values revealed that the activities of trypsin for **1** and **2** were almost comparable to the standard fluorescent substrate **6**.

Similarly, the kinetic parameters for chymotrypsin were also estimated by fitting the data to the Michaelis–Menten equation using **3** as a substrate (Fig. 23).
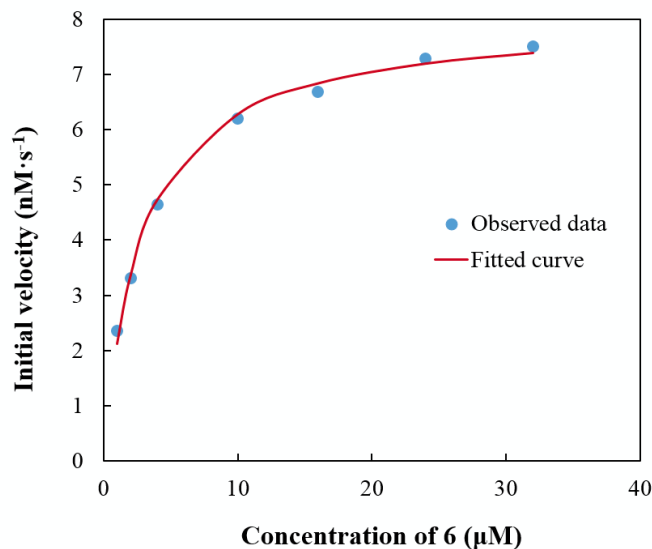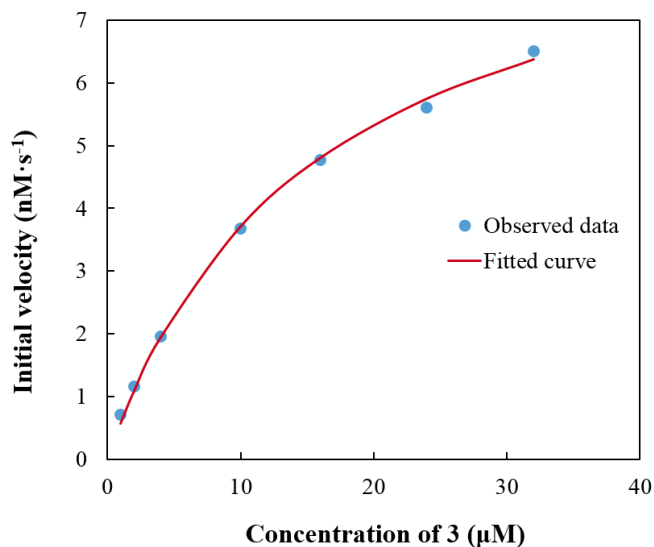
Fig. 23 Michaelis–Menten curve of **3** catalyzed by chymotrypsin (10 nM) in 50 mM Tris-HCl buffer (pH 8.0) containing 150 mM NaCl, 1 mM CaCl$_2$, and 0.1 mg/mL BSA at room temperature with fluorometric method. Excitation/emission wavelengths were 485 nm/535 nm.

The K_m, V_{max}, and k_{cat} values of **3** were 15.5 µM, 9.46 nM·s^{-1}, and 0.946 s^{-1} respectively, and the resulting k_{cat}/K_m was 6.1 x 10^{-2} µM^{-1}·s^{-1} (Table 1). This indicated that self-quenching-based substrates were applicable for not only trypsin but also chymotrypsin.

Table 1 Summary of the kinetic parameters of **1**, **2**, **3**, and **6** for trypsin or chymotrypsin.

Substrate	K_m (µM)	V_{max} (nM·s^{-1})	k_{cat} (s^{-1})	k_{cat}/K_m (µM^{-1}·s^{-1})
1	6.31	8.91	8.91	1.41
2	9.48	13.0	13.0	1.37
6	2.80	8.04	8.04	2.87
3	15.5	9.46	0.946	6.1 x 10^{-2}

2.5.4. Determination of detection limit of trypsin and chymotrypsin

To achieve a quantitative assay for trypsin using our substrates, the detection limit was examined. The concentration of the substrates was fixed at 10 µM, and different concentrations of trypsin (0.001 (only tested on **6**), 0.05, 0.1, 0.25, 0.5, 0.75, and 1 nM) were employed. According to the linear relationship observed between the relative fluorescence recovery and trypsin concentration, the detection limits for the assays were calculated (Fig. 24). A lower limit of 111 pM trypsin could catalyze the fluorescence recovery of substrates **1** and **2** compared with 30.9 pM trypsin for **6**. A lower limit of 711 pM chymotrypsin for the catalysis of **3** was also obtained.
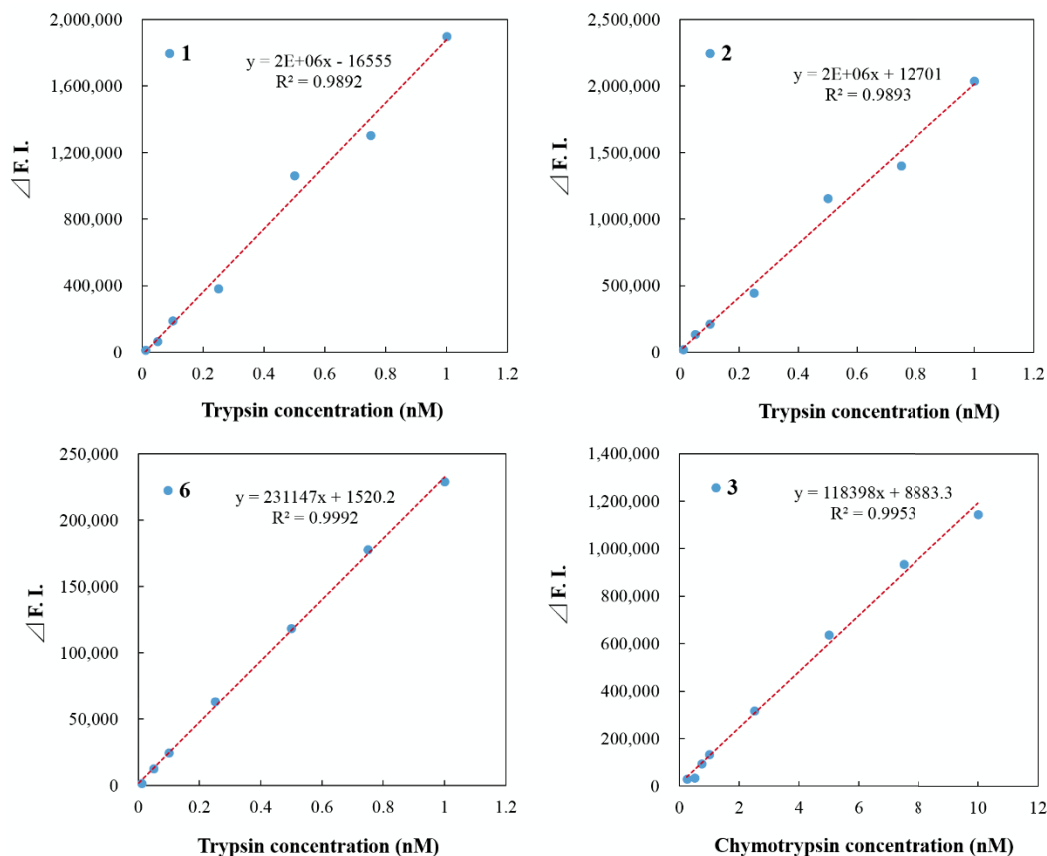
Fig. 24 The linear relationship between amounts of change of the fluorescence intensity of the substrates (10 μM) within a set time of 20 minutes. Excitation/emission wavelengths were 485 nm/535 nm for **1–3** and 370 nm/460 nm for **6**.

2.5.5. Evaluation of trypsin inhibitor

Next, we confirmed whether our substrates could be used for inhibitor evaluation. The inhibition of trypsin activity by the Bowman−Birk inhibitor (BBI), which is the most commonly used trypsin inhibitor, was investigated using our substrates. To 10 μM of **1**, **2**, and **6**, different concentrations of BBI (0, 2, 5, 10, 15, 20, 30, and 40 nM) were added, followed by addition of 1 nM of trypsin. During tryptic cleavage, fluorescence recovery at 535 nm upon excitation at 485 nm (for **1** and **2**) or 460 nm with excitation at 370 nm

(for **6**) was recorded by a fluorescence plate reader. As expected, the higher the concentration of BBI present in the reaction mixture, the slower the fluorescence recovery was (Fig. 25).

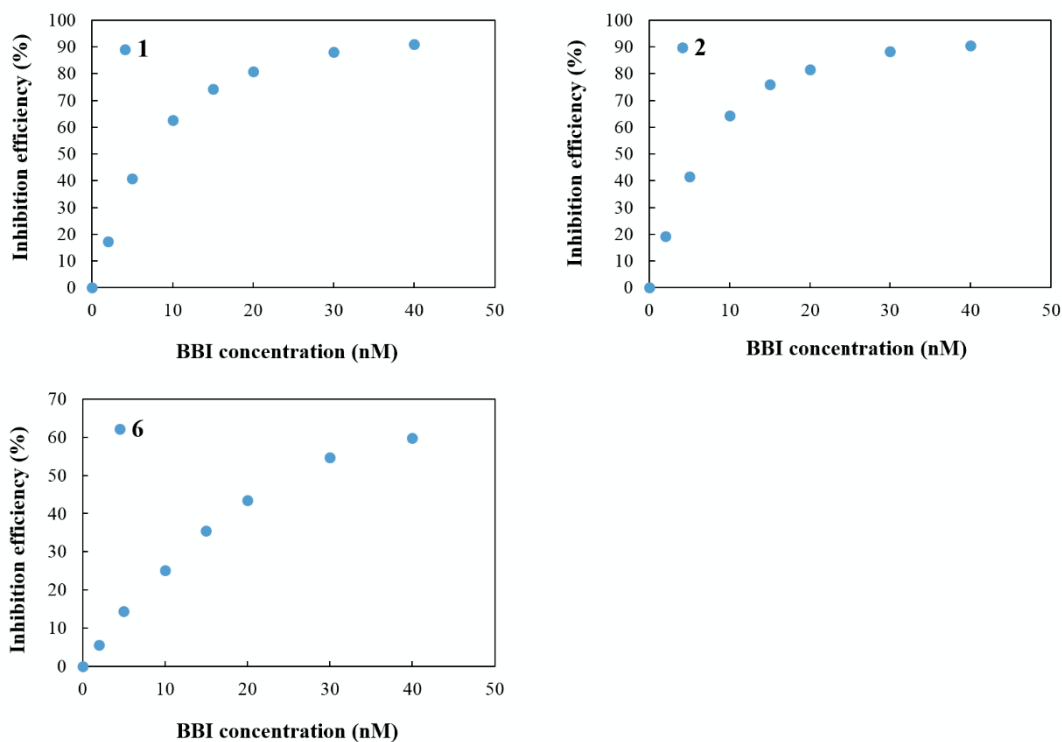**Fig. 25**   Plots of inhibition efficiencies of BBI toward trypsin (1 nM) with the substrates (10 μM).

After plotting the inhibition efficiencies versus the BBI concentrations, the IC_{50} values were calculated by fitting the data to the Hill equation (Fig. 26). The IC_{50} values for BBI using **1**, **2**, and **6** as substrates were estimated as 6.64, 6.34, and 26.3 nM respectively.

Fig. 26 Semilogarithmic plots and fitting curve with Hill equation of inhibition efficiencies of BBI toward trypsin (1 nM) with 10 µM of **1** (a), **2** (b), and **6** (c).

Because IC_{50} values depend on enzyme concentration,[40] the K_i values for BBI were calculated by using the Morrison equation to get a more accurate representation of the inhibition (Fig. 27). The K_i values determined from the Morrison equation were 5.96 nM (**1**), 5.59 nM (**2**), and 26.1 nM (**6**). The K_i of BBI has been reported to be between 10^{-7} and 10^{-9} M, and our values fall within this range.[41] Therefore, these self-quenching-based substrates can be used for evaluation of inhibitors of trypsin.
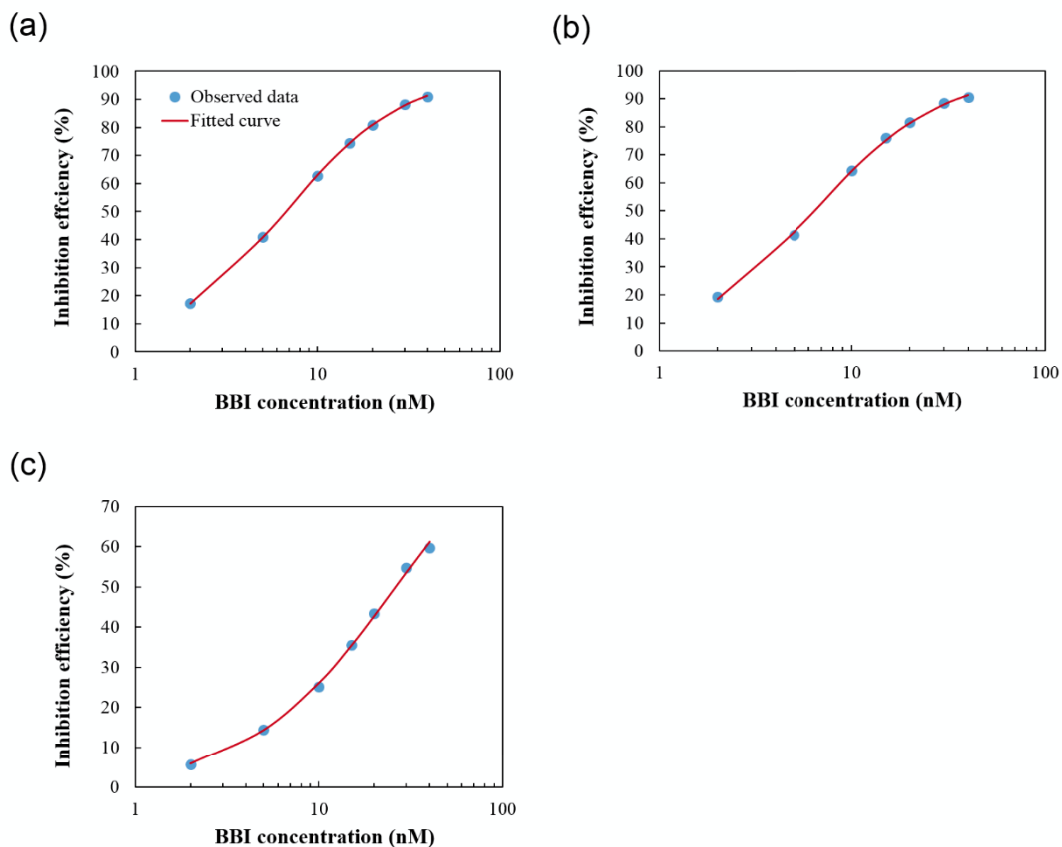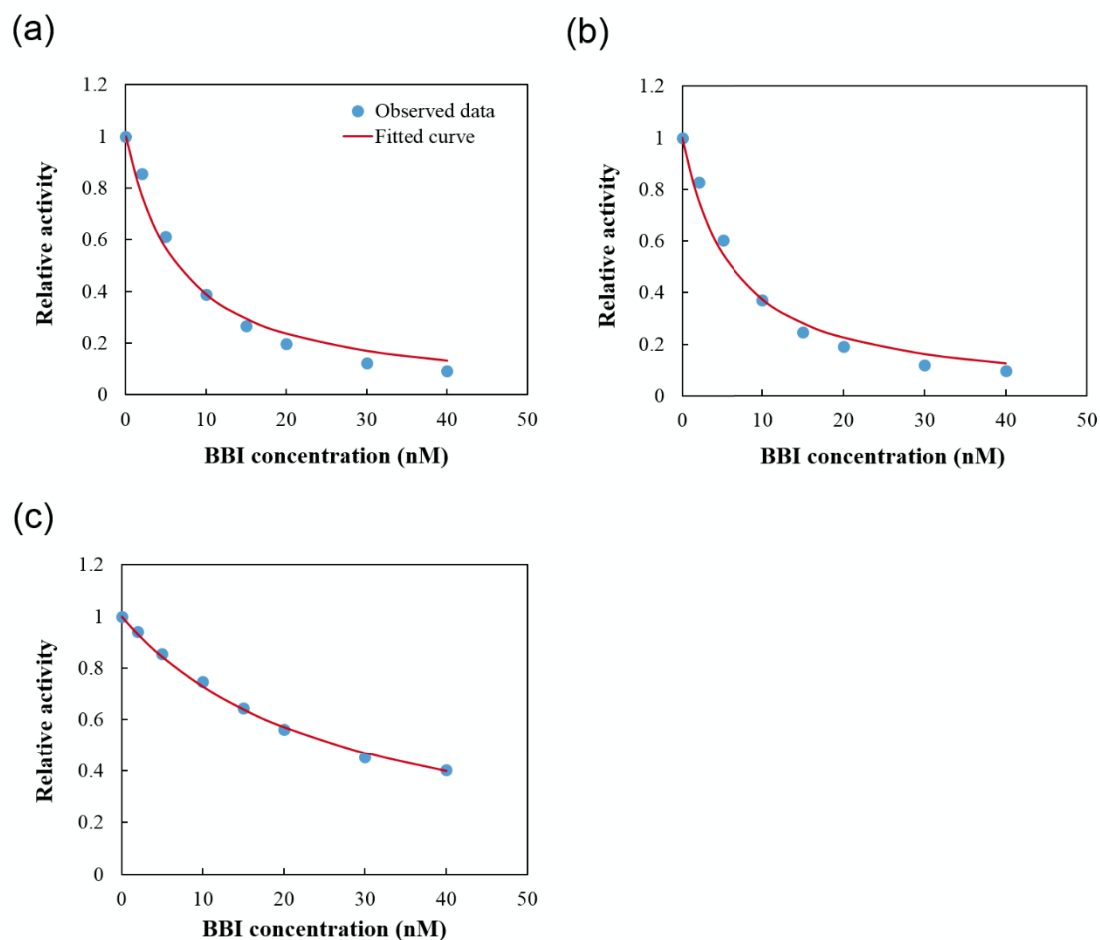
Fig. 27 Plots and fitting curve with Morrison equation of inhibition efficiencies of BBI toward trypsin (1 nM) with 10 µM of **1** (a), **2** (b), and **6** (c).

2.5.6. Kinetic assay of thrombin

Finally, the increase in the fluorescence intensity of different concentrations of the substrates during thrombin cleavage was monitored. To each concentration of the substrates (0.893, 1.79, 3.58, 8.94, 14.3, 21.5, and 28.6 µM for **1**, 0.945, 1.90, 3.79, 9.47, 15.2, 22.7, and 30.3 µM for **2**), 294 nM (for **1**) or 196 nM (for **2**) of thrombin was added, and the fluorescence recovery at 535 nm upon excitation at 485 nm was recorded using a fluorescence plate reader. According to the fluorescence recovery, the increases in the

fluorescence intensities were converted to the corresponding initial velocities for the hydrolysis reactions. The kinetic parameters for thrombin such as K_m, V_{max}, k_{cat}, and k_{cat}/K_m were estimated by fitting the data to the Michaelis–Menten equation using the least-squares method (Fig. 28).

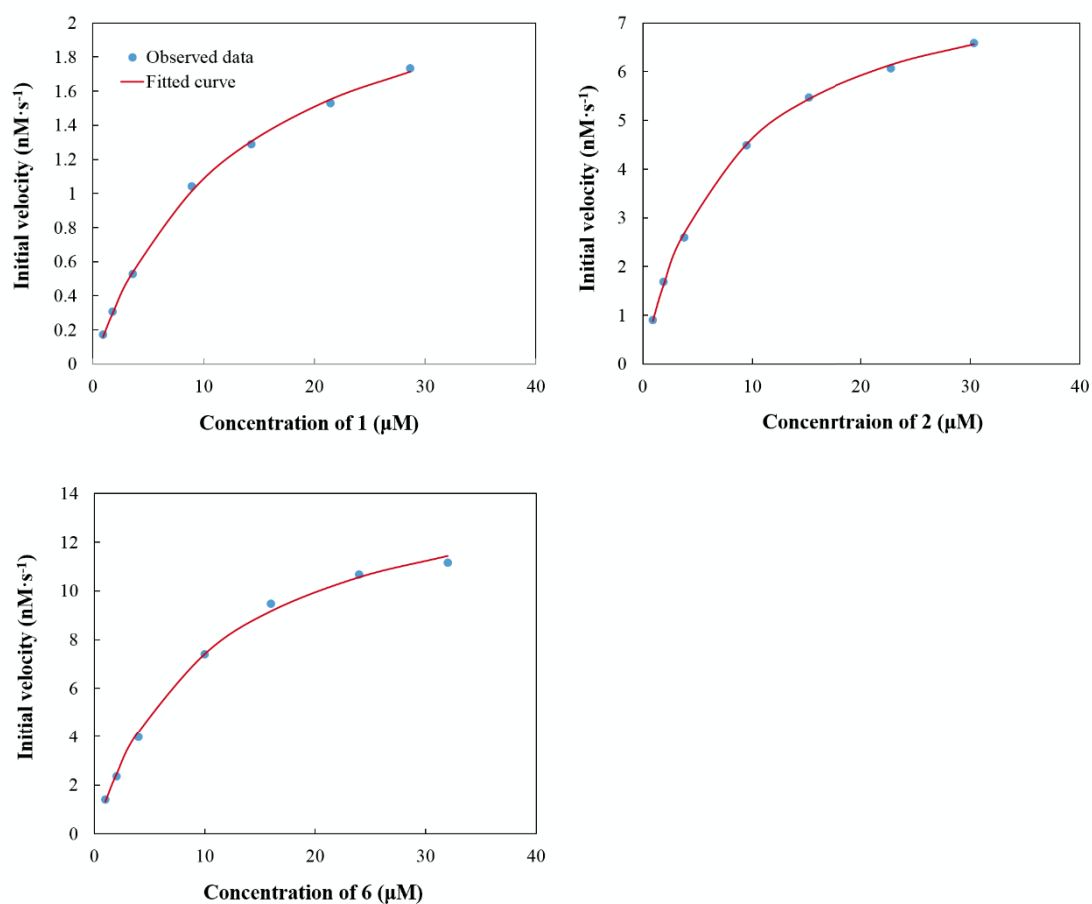**Fig. 28** Michaelis–Menten curve of **1**, **2**, and **3** catalyzed by thrombin in 50 mM Tris-HCl buffer (pH 8.0) containing 150 mM NaCl, 1 mM $CaCl_2$, and 0.1 mg/mL BSA at room temperature with fluorometric method. Excitation/emission wavelengths were 485 nm/535 nm for **1–3** and 370 nm/460 nm for **6**.

The K_m value of **1** was 1.6-fold higher than that of **2**, which meant that the affinity of **2** toward thrombin was better than that of **1** (Table 2). The k_{cat} value of **2** was 5-fold higher than that of **1**. The resulting k_{cat}/K_m value of **2** was 10-fold higher than that of **1**. Thrombin may prefer Val-Pro-Arg-Gly sequence which has an extra glycine at P1′ position to Val-Pro-Arg because natural substrate for α-thrombin from human such as factor XIII includes -Leu-Val-Pro-Arg-Gly- sequence.[42,43] The activity of thrombin for **2** was higher than its activity for **1** due to the reflection of the specificity of P1′ glycine in **2**.

Furthermore, kinetic analysis of **6** was determined for comparison purposes. To each concentration of the substrate (1, 2, 4, 10, 16, 24, and 32 µM), 1 nM of thrombin was added, and the fluorescence recovery at 460 nm upon excitation at 370 nm was recorded using a fluorescence plate reader. While the K_m value of **6** was similar to that of **1**, the k_{cat} value of **6** was dramatically higher than that of **1** and **2**. The resulting k_{cat}/K_m values revealed that the activities of thrombin for **1** and **2** were lower than its activity for standard fluorescent substrate **6**.

Table 2 Summary of the kinetic parameters of **1**, **2**, and **6** for thrombin.

Substrate	K_m (µM)	V_{max} (nM·s^{-1})	k_{cat} (s^{-1})	k_{cat}/K_m (µM^{-1}·s^{-1})
1	12.9	2.49	8.47×10^{-3}	6.54×10^{-4}
2	7.93	8.28	4.22×10^{-2}	5.32×10^{-3}
6	12.5	8.44	8.44	0.677

2.5.7. Molecular simulation

To investigate the cause of difference of kinetic parameters, the simplified molecular docking was performed. First, the difference of specificity toward thrombin between **1** and **6** were surveyed *in silico*. The three-dimensional structure of D-Phe-Pro-Arg chloromethylketone in active site of human α-thrombin (PDB entry: 1PPB) was manually modified to those of **1** or **6** by Molecular Operating Environment (MOE) software. The structural optimizations near the substrates were performed in MMFF94x force field. In the case of **6**, it appeared that **6** fitted substrate binding pocket of thrombin (Fig. 29). On the other hand, it would seem that **1** did not bind as tightly as **6** because **1** was sterically bulkier than **6**.
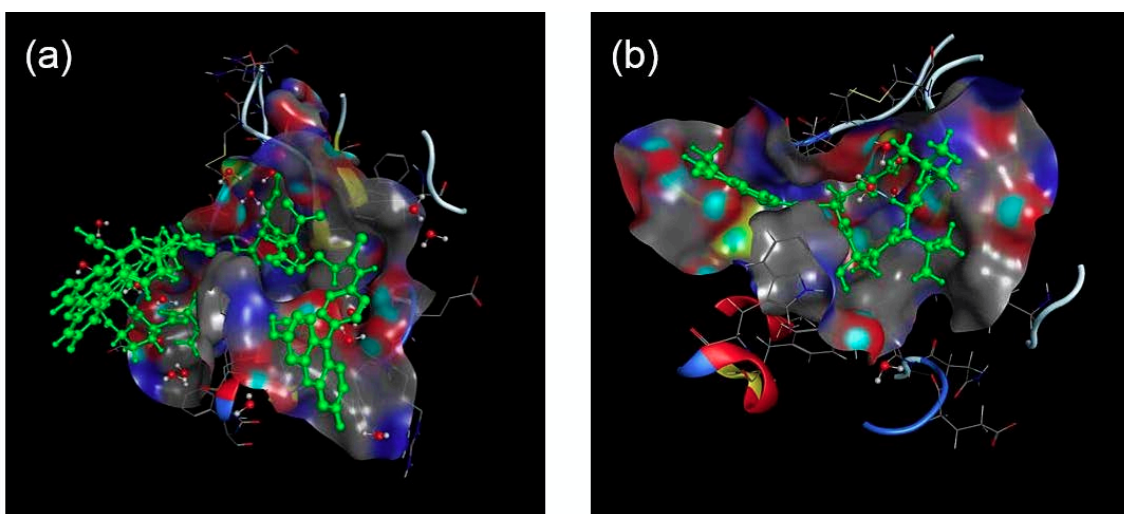
Fig. 29   Simulated binding model in the active site of thrombin. The substrates **1** (a) and **6** (b) were shown as green ball and stick model.

Next, the difference of specificity of self-quenching substrates between trypsin and thrombin were also assessed *in silico*. Comparing the catalytic site of trypsin (PDB entry: 1PTC) with thrombin (PDB entry: 1PPB) on MOE software, substrate binding pocket of thrombin looked more sterically hindered than that of trypsin (Fig. 30). These indicated that lower specificity of **1** and **2** for thrombin was ascribed to the bulkiness of self-quenching substrates and narrower entrance to active site of thrombin.

Fig. 30 Active sites in ligand-enzyme complex. The inhibitors of trypsin (a) and thrombin (b) were shown as green line model.

2.6. Conclusion

In summary, novel self-quenching-based substrates for the detection of trypsin, chymotrypsin, and thrombin activities were developed. These substrates can be conveniently synthesized by Fmoc SPPS. The results from the fluorescence spectra demonstrated that more than 60% of the fluorescence of the substrates was advantage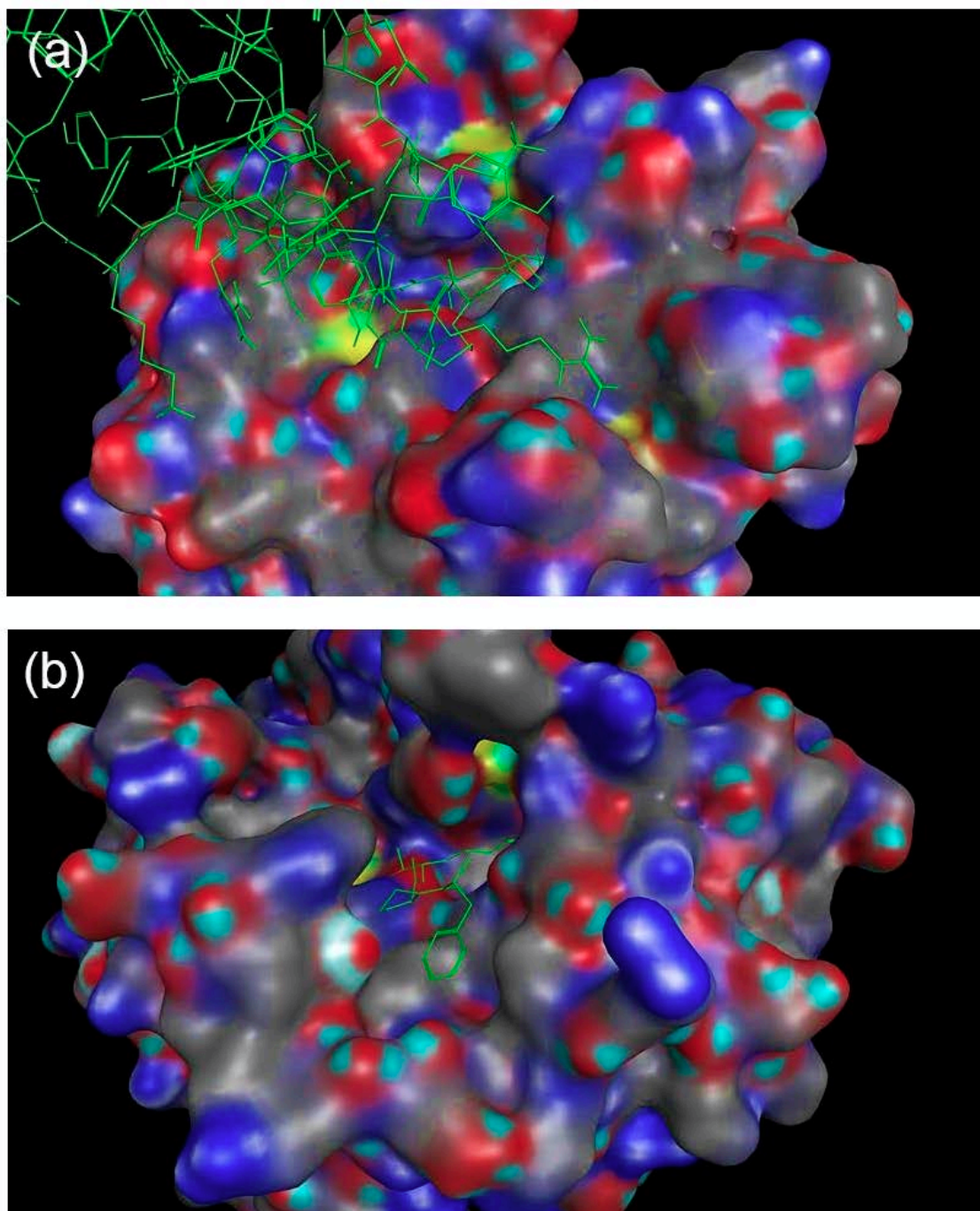ously quenched by intramolecular self-quenching and the diminished fluorescence was recovered by proteolytic cleavage. The activities of trypsin for **1** and **2** were almost comparable to that of **6**, the standard fluorescent probe. The substrates **1** and **2** enabled the detection of trypsin at concentrations as low as 111 pM. Inhibitor evaluation of BBI revealed that this assay could be applied to inhibitor screening and be used to determine not only IC_{50} but also K_i values. Moreover, kinetic assays for the detection of chymotrypsin activity using **3** indicated that our self-quenching-based substrates could be applicable for the detection of other disease-related protease activities and inhibitor screening. Although in thrombin assay by using **1** and **2**, P1′ amino acid could be reflected in the kinetic parameters, the activity of thrombin for **1** and **2** was lower than its activity for **6** due to the bulkiness of the self-quenching substrates and sterically hindered entrance to active site of thrombin according to the simple molecular docking with MOE software.

2.7. References

1. Packard, B. Z.; Toptygin, D. D.; Komoriya, A.; Brand, L. Profluorescent protease substrates: intramolecular dimers described by the exciton model. *Proc. Natl. Acad. Sci. USA* 1996, **93**(21), 11640−11645.

2. Ternon, M.; Díaz-Mochon, J. J.; Belsom, A.; Bradley, M. Dendrimers and combinatorial chemistry—tools for fluorescent enhancement in protease assays. *Tetrahedron* 2004, **60**(39), 8721−8728.

3. Galande, A. K.; Hilderbrand, S. A.; Weissleder, R.; Tung, C. Enzyme-targeted fluorescent imaging probes on a multiple antigenic peptide core. *J. Med. Chem.* 2006, **49**(15), 4715−4720.

4. Avlonitis, N.; Debunne, M.; Aslam, T.; McDonald, N.; Haslett, C.; Dhaliwal, K.; Bradley, M. Highly specific, multi-branched fluorescent reporters for analysis of human neutrophil elastase. *Org. Biomol. Chem.* 2013, **11**(26), 4414−4418.

5. Cera, E. D. Thrombin. *Mol. Aspects Med.* 2008, **29**(4), 203−254.

6. Crawley, J. T. B.; Zanardelli, S.; Chion, C. K. N. K.; Lane, D. A. The central role of thrombin in hemostasis. *J. Thromb. Haemost.* 2007, **5**(s1), 95−101.

7. Krishnaswamy, S.; Mann, K. G.; Nesheim, M. E. The prothrombinase-catalyzed activation of prothrombin proceeds through the intermediate meizothrombin in an ordered, sequential reaction. *J. Biol. Chem.* 1986, **261**(19), 8977−8984.

8. Walker, R. K.; Krishnaswamy, S. The activation of prothrombin by the prothrombinase complex: the contribution of the substrate-membrane interaction to catalysis. *J. Biol. Chem.* 1994, **269**(44), 27441−27450.

9. Krishnaswamy, S. Exosite-driven substrate specificity and function in coagulation. *J. Thromb. Haemost.* 2005, **3**(1), 54−67.

10. Weisel, J. W. Fibrin assembly: lateral aggregation and the role of the two pairs of fibrinopeptides. *Biophys. J.* 1986, **50**(6), 1079−1093.

11. Wolberg, A. S. Thrombin generation and fibrin clot structure. *Blood Rev.* 2007, **21**(3), 131−142.

12. Fenton, J. W.; Fasco, M. J.; Stackrow, A. B. Human thrombins: production, evaluation, and properties of α-thrombin *J. Biol. Chem.* 1977, **252**(11), 3587−3598.

13. Oliver, J. A.; Monroe, D. M.; Roberts, H. R.; Hoffman, M. Thrombin activates factor XI on activated platelets in the absence of factor XII. *Arterioscler. Thromb. Vasc. Biol.* 1999, **19**(1), 170−177.

14. Alquwaizani, M.; Buckley, L.; Adams, C.; Fanikos, J. Anticoagulants: a review of the pharmacology, dosing, and complications. *Curr. Emerg. Hosp. Med. Rep.* 2013, **1**(2), 83−97.

15. Borissoff, J. I.; Spronk, H. M. H.; Heeneman, S.; Cate, H. Is thrombin a key player in the 'coagulation-atherogenesis' maze? *Cardiovasc. Res.* 2009, **82**(3), 392−403.

16. Brummel-Ziedins, K. E.; Vossen, C. Y.; Butenas, S.; Mann, K. G.; Rosendaal, F. R. Thrombin generation profiles in deep venous thrombosis. *J. Thromb. Haemost.* 2005, **3**(11), 2497−2505.

17. Popović, M.; Smiljanić, K.; Dobutović, B.; Syrovets, T.; Simmet, T.; Isenović, E. R. Thrombin and vascular inflammation. *Mol. Cell. Biochem.* 2012, **359**(1-2), 301−313.

18. Davalos, D.; Baeten, K. M.; Whitney, M.A.; Mullins, E. S.; Friedman, B.; Olson, E. S.; Ryu, J. K.; Smirnoff, D. S.; Petersen, M. A.; Bedard, C.; Degen, J. L.; Tsien, R. Y.; Akassoglou, K. Early detection of thrombin activity in neuroinflammatory disease. *Ann. Neurol.* 2014, **75**(2), 303−308.

19. Deng, B.; Lin, Y.; Wang, C.; Li, F.; Wang, Z.; Zhang, H.; Li, X. F.; Le, X. C. Aptamer binding assays for proteins: the thrombin example—a review. *Anal. Chim. Acta* 2014, **837**, 1−15.

20. Kitamoto, Y.; Imamura, T.; Fukui, H.; Tomita, K. Role of thrombin in mesangial proliferative glomerulonephritis. *Kidney Int.* 1998, **54**(5), 1767−1768.

21. Kitamoto, Y.; Arizono, K.; Fukui, H.; Tomita, K.; Kitamura, H.; Taguma, Y.; Imamura, T. Urinary thrombin: a novel marker of glomerular inflammation for the diagnosis of crescentic glomerulonephritis (prospective observational study). *PLoS ONE* 2015, **10**(3), e0118704.

22. Hedstrom, L. Serine protease mechanism and specificity. *Chem. Rev.* 2002, **102**(12), 450−4524.

23. Cera, E. D. Serine proteases. *IUBMB Life* 2009, **61**(5), 510−515.

24. Hirota, M.; Ohmuraya, M.; Baba, H. The role of trypsin, trypsin inhibitor, and trypsin receptor in the onset and aggravation of pancreatitis. *J. Gastroenterol.* 2006, **41**(9), 832−836.

25. Pepeliaev, S.; Krahulec, J.; Černý, Z.; Jílková, J.; Tlustá, M.; Dostálová, J. High level expression of human enteropeptidase light chain in Pichia pastoris. *J. Biotechnol.* 2011, **156**(1), 67−75.

26. Artigas, J. M. G.; Garcia, M. E.; Faure, M. R. A.; Gimeno, A. M. B. Serum trypsin levels in acute pancreatic and non-pancreatic abdominal conditions. *Postgrad. Med. J.* 1981, **57**(666), 219−222.

27. Rinderknecht, H. Activation of pancreatic zymogens: normal activation, premature intrapancreatic activation, protective mechanisms against inappropriate activation. *Dig. Dis. Sci.* 1986, **31**(3), 314−321.

28. Lankisch, P. G.; Burchard-Reckert, S.; Lehnick, D. Underestimation of acute pancreatitis: patients with only a small increase in amylase/lipase levels can also have or develop severe acute pancreatitis. *Gut.* 1999, **44**(4), 542−544.

29. Byrne, M. F.; Mitchell, R. M.; Stiffler, H.; Jowell, P. S.; Branch, M. S.; Pappas, T. N.; Tyler, D.; Baillie, J. Extensive investigation of patients with mild elevations of serum amylase and/or lipase is 'low yield'. *Can. J. Gastroenterol.* 2002, **16**(12), 849−854.

30. Gaber, A.; Johansson, M.; Stenman, U. H.; Hotakainen, K.; Pontén, F.; Glimelius, B.; Bjartell, A.; Jirström, K.; Birgisson, H. High expression of tumour-associated trypsin inhibitor correlates with liver metastasis and poor prognosis in colorectal cancer. *Br. J. Cancer* 2009, **100**(10), 1540−1548.

31. Wu, L.; Yang, S. H.; Xiong, H.; Yang, J. Q.; Guo, J.; Yang, W. C.; Yang, G. F. Nonpeptide-based small-molecule probe for fluorogenic and chromogenic detection of chymotrypsin. *Anal. Chem.* 2017, **89**(6), 3687−3693.

32. Lefkowitz, R. B.; Schmid-Schönbein, G. W.; Heller, M. J. Whole blood assay for elastase, chymotrypsin, matrix metalloproteinase-2, and matrix metalloproteinase-9 activity. *Anal. Chem.* 2010, **82**(19), 8251−8258.

33. Azarkan, M.; Dibiani, R.; Goormaghtigh, E.; Raussens, V.; Baeyens-Volant, D. The papaya Kunitz-type trypsin inhibitor is a highly stable β-sheet glycoprotein. *Biochim. Biophys. Acta* 2006, **1764**(6), 1063−1072.

34. Kozlova, N. O.; Bruskovskaya, I. B.; Melik-Nubarov, N. S.; Yaroslavov, A. A.; Kabanov, V. A. Catalytic properties and conformation of hydrophobized α-chymotrypsin incorporated into a bilayer lipid membrane. *FEBS Lett.* 1999, **461**(3), 141−144.

35. Winquist, J.; Geschwindner, S.; Xue, Y.; Gustavsson, L.; Musil, D.; Deinum, J.; Danielson, U. H. Identification of structural-kinetic and structural-thermodynamic relationships for thrombin inhibitors. *Biochemistry* 2013, **52**(4), 613−626.

36. Frattali, V. Soybean inhibitors: III. Properties of a low molecular weight soybean proteinase inhibitor. *J. Biol. Chem.* 1969, **244**(2), 274−280.

37. Dwivedi, A. K.; Iyer, P. K. A fluorescence turn on trypsin assay based on aqueous polyfluorene. *J. Mater. Chem. B* 2013, **1**(32), 4005−4010.

38. O'Connor, M.; Lee, C.; Ellens, H.; Bentz, J. A novel application of *t*-statistics to objectively assess the quality of IC_{50} fits for P-glycoprotein and other transporters. *Pharma. Res. Per.* 2014, **3**(1), e00078.

39. Morrison, J. F. Kinetics of the reversible inhibition of enzyme-catalysed reactions by tight-binding inhibitors. *Biochim. Biophys. Acta* 1969, **185**(2), 269−286.

40. Cer, R. Z.; Mudunuri, U.; Stephens, R.; Lebeda, F. J. IC_{50}-to-K_i: a web-based tool for converting IC_{50} to K_i values for inhibitors of enzyme activity and ligand binding. *Nucleic Acids Res.* 2009, **37**, W441−W445.

41. Souza, L. C.; Camargo, R.; Demasi, M.; Santana, J. M.; Sá, C. M.; Freitas, S. M. Effects of an anticarcinogenic Bowman-Birk protease inhibitor on purified 20S proteasome and MCF-7 breast cancer cells. *PLoS One* 2014, **9**(1), e86600.

42. Gallwitz, M.; Enoksson, M.; Thorpe, M.; Hellman, L. The extended cleavage specificity of human thrombin. *PLoS ONE* 2012, **7**(2), e31756.

43. Chang, J. Y. Thrombin specificity: requirement for apolar amino acids adjacent to the thrombin cleavage site of polypeptide substrate. *Eur. J. Biochem.* 1985, **151**(2), 217−224.

Chapter 3

Novel bispyrenyl substrates for detection of thrombin and trypsin activities

3.1. Introduction

In prior chapter, we referred to the development of novel self-quenching-based substrates for protease assay. These substrates have the potential for easily synthesizable, inexpensive, and sensitive fluorescent probes for protease assay. However these substrates showed insufficient self-quenching efficiency (more than 60%), indicating low signal-to-noise (S/N) ratio. According to these findings, the fluorescence switch system of the self-quenching-based substrates which uses the change in single wavelength of the fluorophore was altered to a dual emission system. The system exploits shift between two characteristic wavelengths of the fluorophores. To establish the switch system of emission wavelength shift, we focused on pyrene as a fluorophore.

Pyrene has been exploited for the detection and imaging of protein and nucleic acid targets because pyrene has two unique fluorescence characteristics, which display an monomer fluorescence emission peaks (370−420 nm) and an excimer band (450−550 nm) when two pyrene molecules are spatially proximal (~10 Å) (Fig. 1).[1,2]
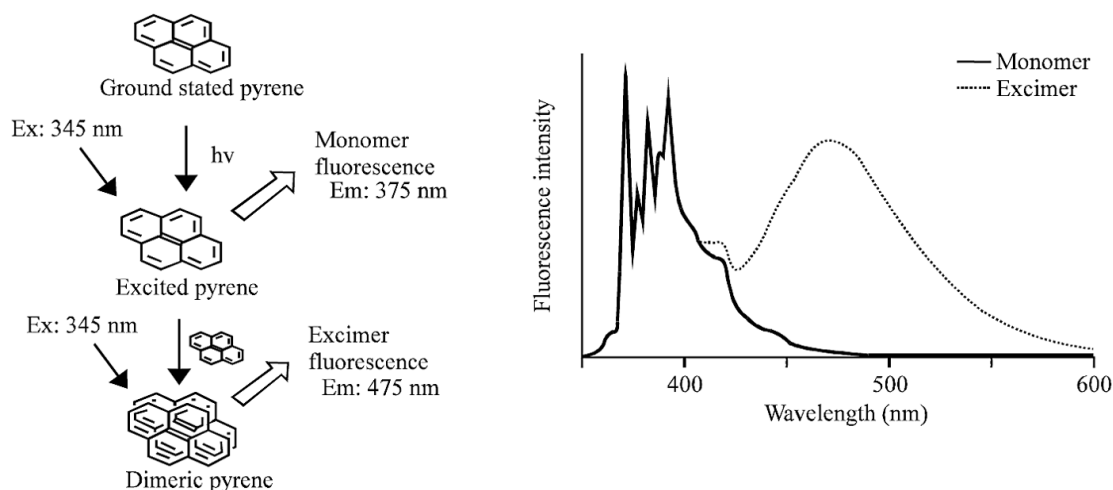
Fig. 1 Excimer formation by pyrene.[3]

Pyrene excimer emission, which can be easily observed by naked eyes, donates large Stokes shifts (~130 nm) and long fluorescence lifetimes (~40 ns).[4,5] However, the advantages of pyrene monomer/excimer signaling have been rarely exploited for the detection of protease activity.[6,7]

Recently, a few exactly controlled aggregation and dissociation systems of pyrenyl compounds have been used for protease assays. Xu *et al.* reported that electrostatic interaction of negatively charged *N*-[4-(1-pyrenyl)butanoyl]-L-tryptophan with positively charged melittin was taken advantage of for the detection of trypsin activity.[8] Tang *et al.* developed sodium 3-(pyren-1-yloxy)propane-1-sulfonate (PyOPS)-protamine complex for the detection of trypsin activity.[9] This complex emits excimer fluorescence due to the electrostatic interaction between anionic sulfonic acid of PyOPS and cationic Arg residues of protamine in which Arg residues accounts for approximately 67% of contents. Cleavage of the protamine by trypsin leads to diminished excimer emission, allowing the

detection of trypsin activity. In addition, Wang *et al.* designed a pyrene-functionalized peptidic inhibitor which contains two Pyrene-Lys-Trp-Lys attached via the *C*-terminus to a lysine amide as a branched unit.[10] This cationic peptide is allowed to bind to the negatively charged surface of β-tryptase, and this non-covalently binding changes monomer/excimer signal of pyrene moieties due to aggregation-induced emission (AIE). In those systems, assembly and disassembly of pyrenyl compound by intermolecular electrostatic interaction lead to the transition of pyrene monomer/excimer emission, which enables the detection of protease activity. However, the sensitivity of these sensing manner can be scarcely regulated since it depends on the responses of the formation and dissolution of the entire assembly of pyrene complexes.[11] Moreover, the kinetic assay is complicated in these system.

Instead of these intermolecular interaction systems, intramolecular excimer forming substrates were also developed. Ahn *et al.* developed two pyrene-labelled peptide substrates which contain two pyrene moieties incorporated into the *N*- and *C*-terminus of the substrate peptide for trypsin.[12]

Although several protease probes using pyrene have been reported as noted above, the applications of intramolecular pyrene monomer/excimer signaling to the detection of protease activity are still rare, and further investigations such as the determination of detection limit and inhibitor evaluation using these substrates were not reported.

3.2. Design

In this study, we designed and synthesized pyrene monomer/excimer-based peptide substrates for the detection of trypsin and thrombin activities. They are composed of two 1-pyrenebutyric acid (Pba) and one or two substrate peptides for trypsin and thrombin. Two types of substrates were designed: long-type substrates and short-type substrate. The long-type substrates **1**, **2**, **3**, and **4** are comprised of two corresponding Pba-linked substrate peptides on both edges of a core (Fig. 2). The short-type substrate **5** is comprised of one corresponding Pba-linked substrate peptide and Pba on each edge of the core respectively. These substrates include hexamethylenediamine as the core. Considering the effect of sterically hindered pyrene molecule, β-alanine was inserted between the Pba and valine residue in **1**, **3**, and **5**. Moreover, one extra amino acid, glycine was also inserted between the arginine residue and core in **1**, **2**, and **5** to demonstrate that the specificity of the P1′ amino acid residue can be reflected in the artificial substrate.

Pba-β-Ala-L-Val-L-Pro-L-Arg-Gly-HN-(CH$_2$)$_6$-NH-Gly-L-Arg-L-Pro-L-Val-β-Ala-Pba   **(1)**
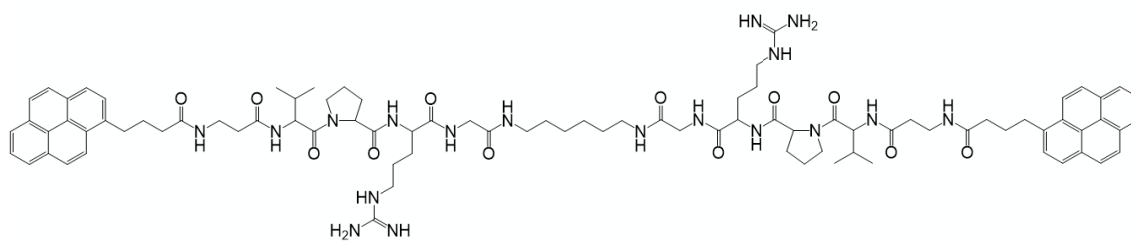
Pba-L-Val-L-Pro-L-Arg-Gly-HN-(CH$_2$)$_6$-NH-Gly-L-Arg-L-Pro-L-Val-Pba   **(2)**
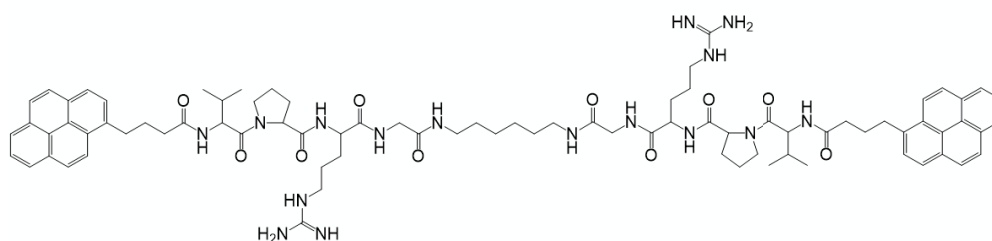
Pba-β-Ala-L-Val-L-Pro-L-Arg-HN-(CH$_2$)$_6$-NH-L-Arg-L-Pro-L-Val-β-Ala-Pba   **(3)**
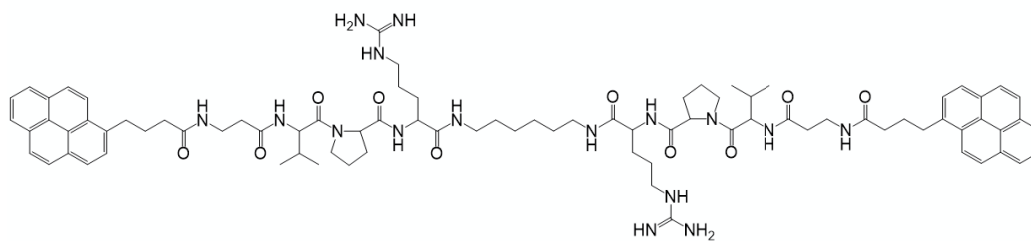
Pba-L-Val-L-Pro-L-Arg-HN-(CH$_2$)$_6$-NH-L-Arg-L-Pro-L-Val-Pba   **(4)**
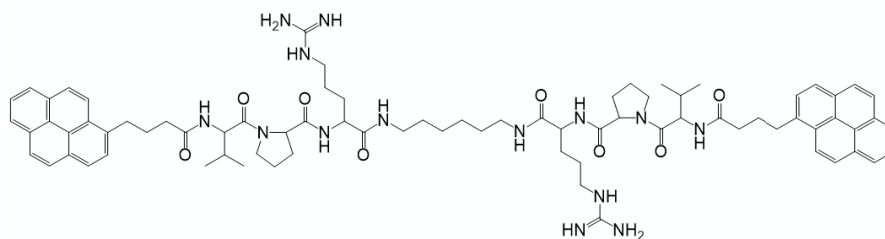
Fig. 2   Design of the long-type bispyrenyl substrates **1**, **2**, **3**, and **4**.

80

Pba-β-Ala-L-Val-L-Pro-L-Arg-Gly-HN-(CH$_2$)$_6$-NH-Pba   **(5)**
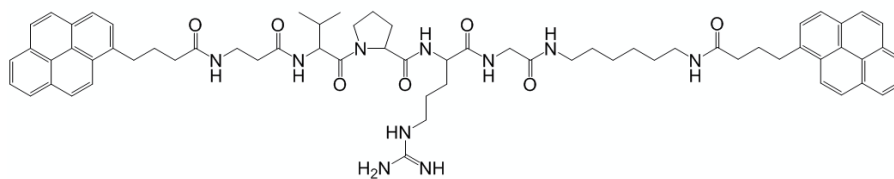
Fig. 3   Design of the short-type bispyrenyl substrate **5**.

Proximate two pyrene moieties form excited-state dimers in the substrates, and the substrates emit excimer fluorescence (Fig. 4). After proteolytic cleavage, these pyrene excimer formations dissociate, and the excimer fluorescence decreased as the monomer fluorescence increases. Hence, the change of excimer fluorescence enables to detect protease activity.
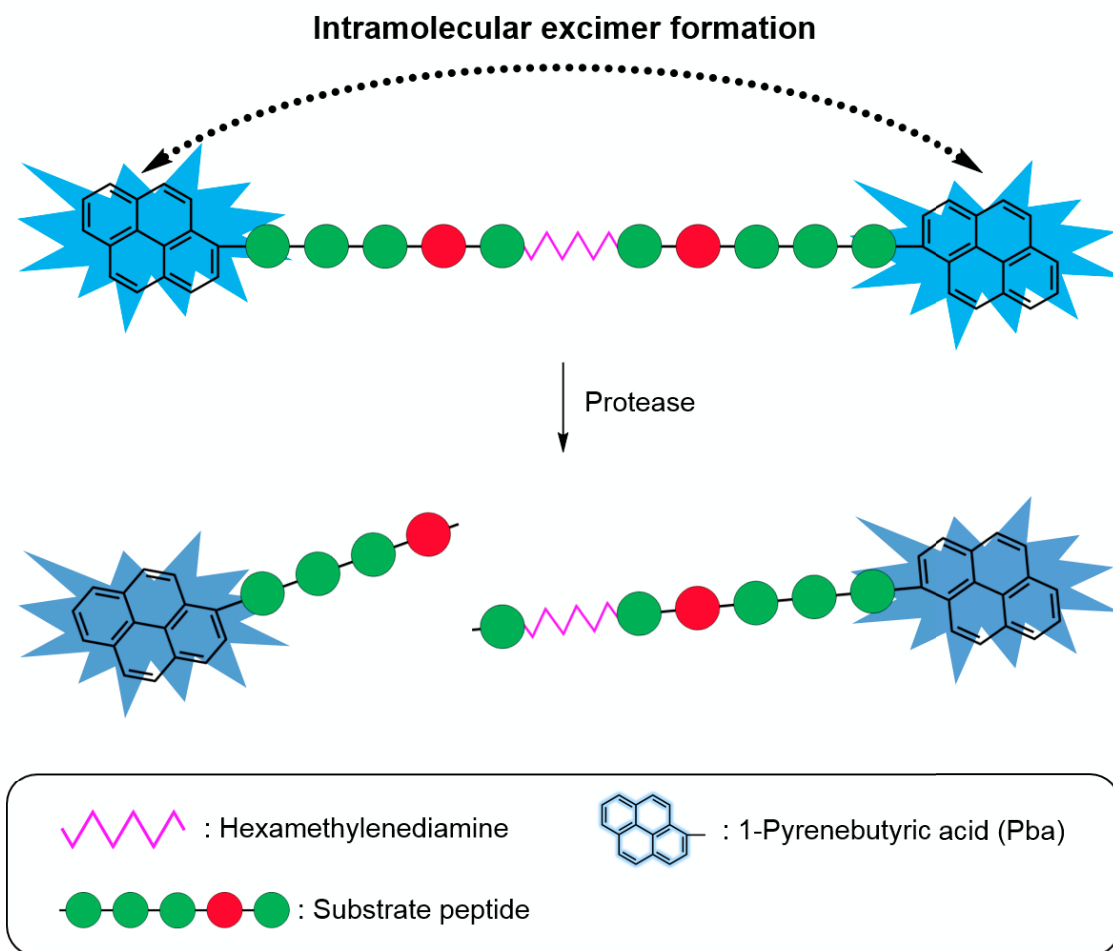
Fig. 4 Schematic representation of the detection system for **1**.

For the synthesis of long-type substrates, corresponding protected Pba-peptides which were synthesized by standard Fmoc solid-phase peptide synthesis (Fmoc SPPS) were coupled with both edges of hexamethylenediamine, followed by the deprotection of Pbf or Pmc groups. For the synthesis of short-type substrate, *N*-Boc-hexamethylenediamine was coupled with Pba. After the deprotection of Boc group from the previously obtained compound, Pba-β-Ala-L-Val-L-Pro-L-Arg(Pbf)-Gly-OH synthesized by Fmoc SPPS was then linked. Finally, Pbf group was deprotected.

3.3. Experimental section

3.3.1. Materials and instruments

All Fmoc-protected amino acids, Cl-Trt(2-Cl) resin, piperidine, *O*-(1H-benzotriazol-1-yl)-*N,N,N′,N′*-tetramethyluronium hexafluorophosphate (HBTU), 1-hydrolxy-1H-benzotriazole hydrate (HOBt·H$_2$O), *N,N*-diisopropylethylamine (DIEA), trifluoroethanol, 2,2,2-trifluoroacetic acid (TFA), and 4 M HCl/Dioxane were purchased from Watanabe Chemical Industries, Ltd. α-Trypsin from bovine pancreas, α-chymotrypsin from bovine pancreas, thrombin from human plasma, and Bowman-Birk inhibitor from *Glycine max* (soybean) were obtained from Sigma-Aldrich Co. LLC. All solvents and other reagents were ordered from Wako Pure Chemical Industries, Ltd. The assay buffer solution was 50 mM Tris-HCl buffer (pH 8.0) containing 150 mM NaCl, 1 mM CaCl$_2$, and 0.02% (w/v) PEG6000. Analytical high performance liquid chromatography (HPLC) was performed on a Hitachi L-7100 instrument equipped with a chromolith performance RP-18e column (4.6 x 100 mm; Merck). The mobile phases were 0.1% TFA in H$_2$O (solvent A) and 0.1% TFA in H$_2$O (solvent B) using a linear gradient of solvent B in solvent A (0–100% over 15 min) with a flow rate of 2.0 mL/min, and absorbance at 220 nm was used for the detection. Gel filtration chromatography was performed using Sephadex LH-20 eluting with DMF. Electrospray ionization time-of-flight mass spectrometer (ESI-TOF-MS) data were measured on a JEOL THE ACCUTOF LC-PLUS JMS-T100LP instrument. Fast atom bombardment (FAB)-MS spectra were measured on a JEOL JMS-SX 102A instrument. pH measurements were made with a D-71 LAQUA portable pH meter (Horiba). Absorbance was measured using a GE Healthcare Ultrospec 3300 pro

UV/Vis spectrometer or a JASCO V-550 UV/VIS spectrophotometer. Fluorescence spectra and enzyme reaction were measured on a JASCO FP-6600 spectrofluorometer. Deionized water was obtained from a Milli-Q Plus system (Millipore).

3.3.2. Synthesis

3.3.2.1. Solid-phase synthesis of different sequences of protected pyrenyl peptides

The first Fmoc-protected amino acid was loaded onto Cl-Trt(2-Cl) resin. Corresponding peptide chains were elongated using Fmoc/piperidine strategies. HBTU and HOBt·H$_2$O were used as activating agents. Subsequently, Pba was coupled to the elongated peptides in the presence of HBTU, HOBt·H$_2$O, and DIEA. The resin-supported peptides were cleaved from the resin in the cleavage cocktail (AcOH/DCM/Trifluoroethanol = 1:3:1). The peptides were precipitated by ether in an ice bath, and purified by gel filtration chromatography. The purified peptides were analyzed by HPLC and FAB-MS (data not shown).

3.3.2.2. Synthesis of 1

To Pba-β-Ala-L-Val-L-Pro-L-Arg(Pbf)-Gly-OH (0.306 g, 0.30 mmol, 2.5 equiv) in 10 mL of DMF, hexamethylenediamine (0.0016 mL, 0.12 mmol, 1.0 equiv), HBTU (0.114 g, 0.30 mmol, 2.5 equiv), HOBt·H$_2$O (0.046 g, 0.30 mmol, 2.5 equiv), and DIEA (0.053

mL, 0.30 mmol, 2.5 equiv) were added, and the reaction mixture was then stirred at room temperature overnight. Evaporated reaction mixture was dissolved in small amount of DMF, and purified by gel filtration chromatography. The purified compound (0.050 g, 0.025 mmol) was dissolved in 10 mL of the deprotection cocktail (TFA/Triisopropylsilane/H_2O = 95:2.5:2.5), and the reaction mixture was then stirred for 4 hours at room temperature. The peptide was precipitated by ether in an ice bath. The substrate **1** was obtained with 60% yield (0.040 g, 0.022 mmol), and analyzed by HPLC and HR-MS (ESI-TOF-MS).

m/z calcd. for [(M+H)$^+$] $C_{88}H_{117}N_{18}O_{12}$: 1617.90983; found: 1617.91845, Retention time: 7.54 min.

Fig. 5　HPLC profile of **1**. HPLC conditions: a linear gradient of solvent B in solvent A (0–100% over 15 min); Chromolith performance RP-18e column (4.6 x 100 mm; Merck); flow rate, 2 mL/min; solvent A: 0.1% TFA in H_2O; solvent B: 0.1% TFA in CH_3CN; detection at 220 nm.

Mass	Intensity	Calc. Mass	Mass Difference [mDa]	Mass Difference [ppm]	Possible Formula	Unsaturation Number
1617.91845	1172.48	1617.90983	8.62	5.33	$^{12}C_{88}{}^1H_{117}{}^{14}N_{18}{}^{16}O_{12}$	39.5
		1617.88630	32.15	19.87	$^{12}C_{89}{}^1H_{114}{}^{14}N_{18}{}^{23}Na_1{}^{16}O_{10}$	41.5
1618.92175	1335.55	1618.91766	4.10	2.53	$^{12}C_{88}{}^1H_{118}{}^{14}N_{18}{}^{16}O_{12}$	39.0
		1618.89412	27.63	17.07	$^{12}C_{89}{}^1H_{115}{}^{14}N_{18}{}^{23}Na_1{}^{16}O_{10}$	41.0

Fig. 6　MASS spectrum of **1**.

3.3.2.3. Synthesis of 2

To Pba-L-Val-L-Pro-L-Arg(Pbf)-Gly-OH (0.285 g, 0.30 mmol, 2.5 equiv) in 10 mL of DMF, hexamethylenediamine (0.016 mL, 0.12 mmol, 1.0 equiv), HBTU (0.114 g, 0.30 mmol, 2.5 equiv), HOBt·H_2O (0.046 g, 0.30 mmol, 2.5 equiv), and DIEA (0.053 mL, 0.30 mmol, 2.5 equiv) were added, and the reaction mixture was then stirred at room temperature overnight. Evaporated reaction mixture was dissolved in small amount of DMF, and purified by gel filtration chromatography. The purified compound (0.050 g, 0.025 mmol) was dissolved in 10 mL of the deprotection cocktail (TFA/Triisopropylsilane/H_2O = 95:2.5:2.5), and the reaction mixture was then stirred for 4 hours at room temperature. The peptide was precipitated by ether in an ice bath. The substrate **2** was obtained with 34% yield (0.037 g, 0.022 mmol), and analyzed by HPLC and HR-MS (ESI-TOF-MS).

m/z calcd. for [(M+H)$^+$] $C_{82}H_{107}N_{16}O_{10}$: 1475.83561; found: 1475.82969, Retention time: 7.80 min.
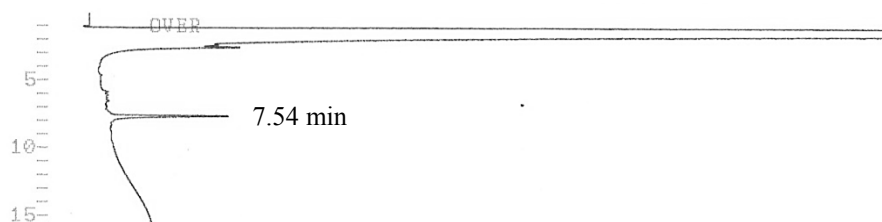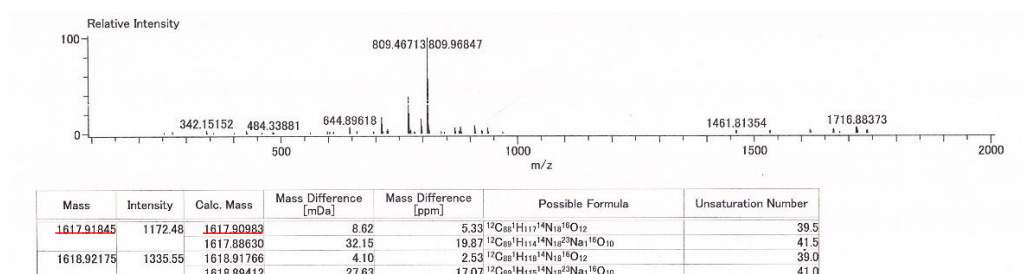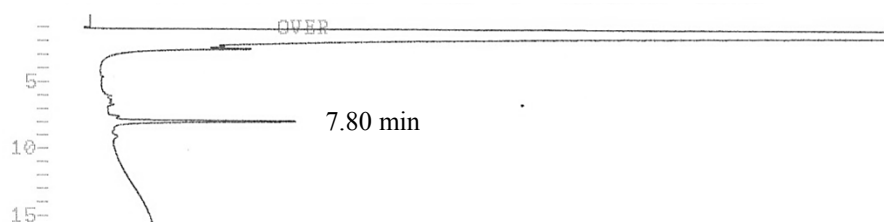

Fig. 7   HPLC profile of **2**. HPLC conditions: a linear gradient of solvent B in solvent A (0–100% over 15 min); Chromolith performance RP-18e column (4.6 x 100 mm; Merck); flow rate, 2 mL/min; solvent A: 0.1% TFA in H_2O; solvent B: 0.1% TFA in CH_3CN; detection at 220 nm.

Mass	Intensity	Calc. Mass	Mass Difference [mDa]	Mass Difference [ppm]	Possible Formula	Unsaturation Number
1475.82969	5660.88	1475.83561	−5.91	−4.01	$^{12}C_{92}{}^{1}H_{107}{}^{14}N_{16}{}^{16}O_{10}$	37.5
		1475.82303	6.66	4.52	$^{12}C_{86}{}^{1}H_{105}{}^{14}N_{17}{}^{16}O_{10}$	38.0
1476.83315	5745.60	1476.83085	2.30	1.56	$^{12}C_{86}{}^{1}H_{106}{}^{14}N_{17}{}^{16}O_{10}$	37.5
		1476.80732	25.83	17.49	$^{12}C_{82}{}^{1}H_{103}{}^{14}N_{17}{}^{23}Na_{1}{}^{18}O_{8}$	39.5

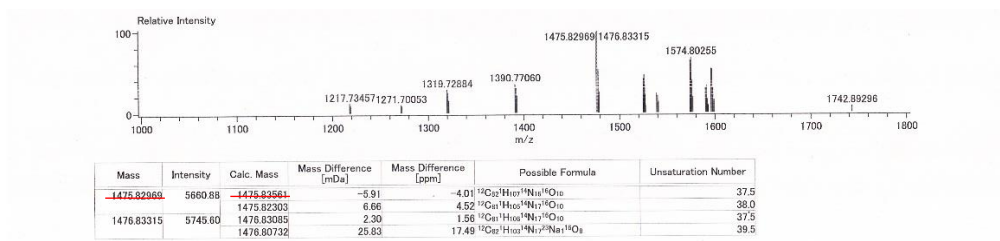**Fig. 8**   MASS spectrum of **2**.

3.3.2.4. Synthesis of 3

To Pba-β-Ala-L-Val-L-Pro-L-Arg(Pmc)-OH (0.372 g, 0.38 mmol, 2.5 equiv) in 10 mL of DMF, hexamethylenediamine (0.0019 mL, 0.15 mmol, 1.0 equiv), HBTU (0.144 g, 0.38 mmol, 2.5 equiv), HOBt·H_2O (0.058 g, 0.38 mmol, 2.5 equiv), and DIEA (0.066 mL, 0.38 mmol, 2.5 equiv) were added, and the reaction mixture was then stirred at room temperature overnight. Evaporated reaction mixture was dissolved in small amount of DMF, and purified by gel filtration chromatography. The purified compound (0.060 g, 0.029 mmol) was dissolved in 10 mL of the deprotection cocktail (TFA/Triisopropylsilane/H_2O = 95:2.5:2.5), and the reaction mixture was then stirred for 4 hours at room temperature. The peptide was precipitated by ether in an ice bath. The substrate **3** was obtained with 52% yield (0.040 g, 0.023 mmol), and analyzed by HPLC and HR-MS (ESI-TOF-MS).

m/z calcd. for [(M+H)$^{+}$] $C_{84}H_{111}N_{16}O_{10}$: 1503.86691; found: 1503.86824, Retention time: 7.26 min.
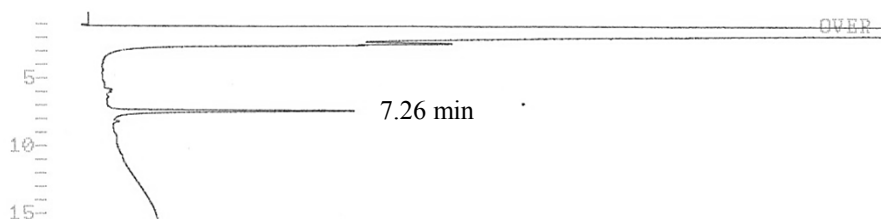
7.26 min

Fig. 9 HPLC profile of **3**. HPLC conditions: a linear gradient of solvent B in solvent A (0–100% over 15 min); Chromolith performance RP-18e column (4.6 x 100 mm; Merck); flow rate, 2 mL/min; solvent A: 0.1% TFA in H$_2$O; solvent B: 0.1% TFA in CH$_3$CN; detection at 220 nm.

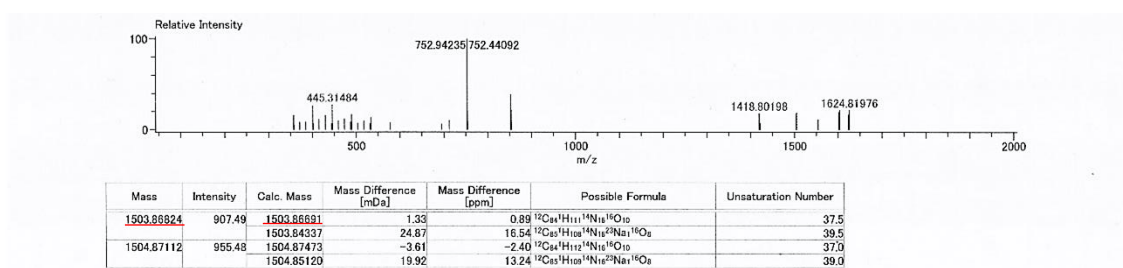| Mass	Intensity	Calc. Mass	Mass Difference [mDa]	Mass Difference [ppm]	Possible Formula	Unsaturation Number
1503.86824	907.49	1503.86691	1.33	0.89	$^{12}C_{84}{}^{1}H_{111}{}^{14}N_{18}{}^{16}O_{10}$	37.5
		1503.84337	24.87	16.54	$^{12}C_{85}{}^{1}H_{109}{}^{14}N_{16}{}^{23}Na_1{}^{16}O_8$	39.5
1504.87112	955.48	1504.87473	−3.61	−2.40	$^{12}C_{84}{}^{1}H_{112}{}^{14}N_{16}{}^{16}O_{10}$	37.0
		1504.85120	19.92	13.24	$^{12}C_{85}{}^{1}H_{109}{}^{14}N_{16}{}^{23}Na_1{}^{16}O_8$	39.0

Fig. 10 MASS spectrum of **3**.

3.3.2.5. Synthesis of 4

To Pba-L-Val-L-Pro-L-Arg(Pbf)-OH (0.268 g, 0.30 mmol, 2.5 equiv) in 10 mL of DMF, hexamethylenediamine (0.016 mL, 0.12 mmol, 1.0 equiv), HBTU (0.114 g, 0.30 mmol, 2.5 equiv), HOBt·H$_2$O (0.046 g, 0.30 mmol, 2.5 equiv), and DIEA (0.053 mL, 0.30 mmol, 2.5 equiv) were added, and the reaction mixture was then stirred at room temperature overnight. Evaporated reaction mixture was dissolved in small amount of DMF, and purified by gel filtration chromatography. The purified compound (0.050 g, 0.027 mmol) was dissolved in 10 mL of the deprotection cocktail (TFA/Triisopropylsilane/H$_2$O = 95:2.5:2.5), and the reaction mixture was then stirred for 4 hours at room temperature.

The peptide was precipitated by ether in an ice bath. The substrate **4** was obtained with 29% yield (0.037 g, 0.023 mmol), and analyzed by HPLC and HR-MS (ESI-TOF-MS). *m/z* calcd. for $[(M+H)^+]$ $C_{78}H_{101}N_{14}O_8$: 1361.79268; found: 1361.78771, Retention time: 7.96 min.
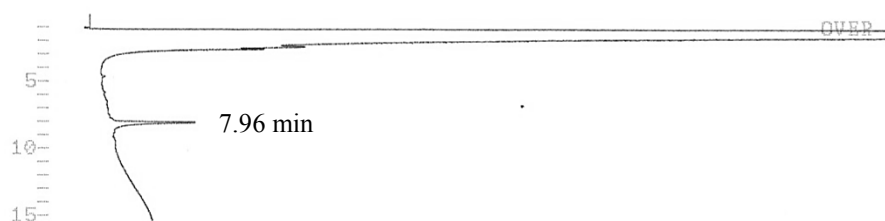

Fig. 11   HPLC profile of **4**. HPLC conditions: a linear gradient of solvent B in solvent A (0–100% over 15 min); Chromolith performance RP-18e column (4.6 x 100 mm; Merck); flow rate, 2 mL/min; solvent A: 0.1% TFA in H_2O; solvent B: 0.1% TFA in CH_3CN; detection at 220 nm.
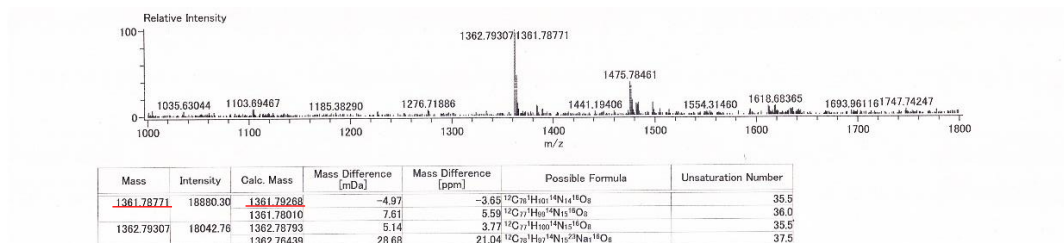

Fig. 12   MASS spectrum of **4**.

3.3.2.6. Synthesis of 5

3.3.2.6.1. Synthesis of Boc-HN-(CH$_2$)$_6$-NH-Pba

N-Boc-hexamethylenediamine hydrochloride (0.506 g, 2.0 mmol, 1.0 equiv) was dissolved in 10 mL of DMF using an ice bath to cool down, Pba (0.577 g, 2.0 mmol, 1.0 equiv), HBTU (0.910 g, 2.4 mmol, 1.2 equiv), HOBt·H$_2$O (0.368 g, 2.4 mmol, 1.2 equiv), DIEA (0.42 mL, 2.4 mmol, 1.2 equiv) were added to the solution. The reaction mixture was stirred at room temperature overnight. The mixture was concentrated, and the desired compound was crystallized by ether in an ice bath. The pure compound was obtained with 82% yield (0.820 g, 1.7 mmol), and analyzed by HPLC and ESI-TOF-MS (HPLC profile and MASS spectrum not shown).

m/z calcd. for [(M+Na)$^+$] C$_{31}$H$_{38}$N$_2$NaO$_3$: 509.28; found: 509.25, Retention time: 6.54 min.

3.3.2.6.2. Synthesis of H$_2$N-(CH$_2$)$_6$-NH-Pba·HCl

The suspension of Boc-HN-(CH$_2$)$_6$-NH-Pba (0.500 g, 1.0 mmol, 1.0 equiv) in 4 M HCl/Dioxane was incubated for 2 hours in an ice bath. The suspension was concentrated, and desired compound was crystallized by ether in an ice bath. The pure compound was obtained with over 100% yield (0.454 g, 1.1 mmol), and analyzed by HPLC (HPLC profile not shown).

Retention time: 5.01 min.

3.3.2.6.3. Synthesis of 5

H_2N-$(CH_2)_6$-NH-Pba·HCl (0.085 g, 0.20 mmol, 1.0 equiv) and Pba-β-Ala-L-Val-L-Pro-L-Arg(Pbf)-Gly-OH (0.163 g, 0.16 mmol, 0.8 equiv) were dissolved in 10 mL of DMF in an ice bath. HBTU (0.091 g, 0.24 mmol, 1.2 equiv), HOBt·H_2O (0.037 g, 0.24 mmol, 1.2 equiv), and DIEA (0.075 mL, 0.44 mmol, 2.2 equiv) were added to the solution, and the reaction mixture was then stirred at room temperature overnight. Evaporated reaction mixture was dissolved in small amount of DMF, and purified by gel filtration chromatography. The purified compound (0.020 g, 0.014 mmol) was dissolved in 10 mL of the deprotection cocktail (TFA/Triisopropylsilane/H_2O = 95:2.5:2.5), and the reaction mixture was then stirred for 4 hours at room temperature. The peptide was precipitated by ether in an ice bath. The substrate **5** was obtained with 22% yield (0.040 g, 0.022 mmol), and analyzed by HPLC and HR-MS (ESI-TOF-MS).

m/z calcd. for [(M+H)$^+$] $C_{67}H_{81}N_{10}O_7$: 1137.62897; found: 1137.62864, Retention time: 8.36 min.
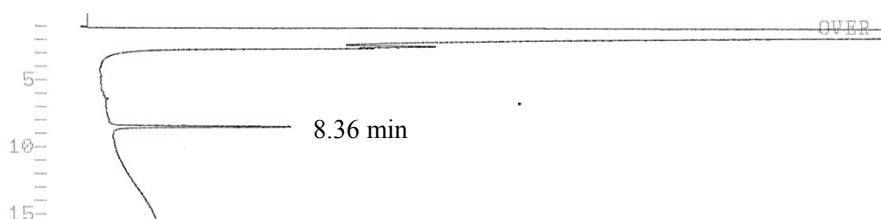

Fig. 13 HPLC profile of **5**. HPLC conditions: a linear gradient of solvent B in solvent A (0–100% over 15 min); Chromolith performance RP-18e column (4.6 x 100 mm; Merck); flow rate, 2 mL/min; solvent A: 0.1% TFA in H_2O; solvent B: 0.1% TFA in CH_3CN; detection at 220 nm.
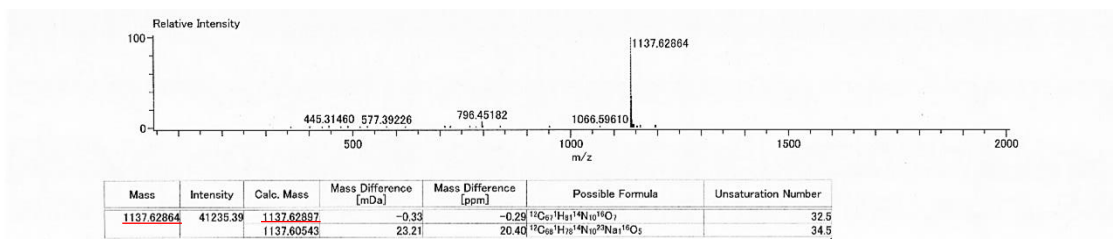
Fig. 14   MASS spectrum of **5**.

Mass	Intensity	Calc. Mass	Mass Difference [mDa]	Mass Difference [ppm]	Possible Formula	Unsaturation Number
1137.62864	41235.39	1137.62897	−0.33	−0.29	$^{12}C_{67}{}^{1}H_{81}{}^{14}N_{10}{}^{16}O_7$	32.5
		1137.60543	23.21	20.40	$^{13}C_{66}{}^{1}H_{76}{}^{14}N_{10}{}^{23}Na_1{}^{16}O_5$	34.5

3.3.3. Analysis

3.3.3.1. Preparation of stock solutions

The stock solutions of **1**, **2**, **3**, **4**, **5**, and Pba were prepared in dimethylsulfoxide (DMSO) and stored in a refrigerator. The concentration of the pyrene solutions was determined by the molar extinction coefficient of Pba in DMF at 344 nm (ε_{344} in DMF = 35,100 $M^{-1} \cdot cm^{-1}$). The stock solution of trypsin and thrombin in the micromolar range was prepared in the buffer and stored in a freezer. The concentration of the trypsin solution was determined using the molar extinction coefficient of trypsin at 280 nm (ε_{280} = 36,280 $M^{-1} \cdot cm^{-1}$).[13] The concentration of the thrombin solution was determined using the molar extinction coefficient of thrombin at 280 nm (ε_{280} = 66,800 $M^{-1} \cdot cm^{-1}$).[14] The stock solution of Bowman–Birk inhibitor (BBI) in the micromolar range was prepared in distilled water and stored in a freezer. The concentration of BBI was estimated spectrophotometrically using the values of M_r = 7,975 Da and $A^{1\%}{}_{280}$ = 4.4.[15]

3.3.3.2. Investigation of monomer and excimer emission

In the case of spectral survey, the stock solutions of **1**, **2**, **3**, **4**, **5**, and Pba were diluted with DMSO, and an equimolar solution of each of the pyrene moieties (4 µM) was prepared. The fluorescence spectra of these solutions upon excitation at 344 nm were measured with a spectrofluorometer.

As for the investigation of kinetic alteration, the stock solution of **1** was diluted with the buffer, and the final concentration of **1** was adjusted to 10 µM. The stock solution of trypsin was also diluted with the buffer, and the final concentration of trypsin was adjusted to 10 nM. The hydrolysis of **1** was initiated by the addition of trypsin solution, and monitored fluorometrically by using a spectrofluorometer with an excitation of 344 nm and an emission of 378 nm for monomer fluorescence or 480 nm for excimer fluorescence.

3.3.3.3. Selection of optimum substrate for trypsin

The stock solutions of **1**, **2**, **3**, **4**, and **5** were diluted with DMSO and the buffer, and the final concentration of these substrates ranged from 2 to 10 µM. The stock solution of trypsin was diluted with the buffer, and the final concentration of trypsin was adjusted to 0.4 nM (for **1**), 0.5 nM (for **2**), 30 nM (for **3**), 40 nM (for **4**), and 1.2 nM (for **5**) respectively. The hydrolysis of the different concentrations of **1**, **2**, **3**, **4**, and **5** was initiated by the addition of trypsin solution, and monitored fluorometrically by using a

spectrofluorometer with an excitation of 344 nm and an emission of 480 nm. The concentration of DMSO in the assay was approximately 20%. The kinetic parameters of K_m, V_{max}, k_{cat}, and k_{cat}/K_m were calculated by fitting the Lineweaver–Burk plot described below with the least-squares method.

$$\frac{1}{v_0} = \frac{K_m}{V_{max}}\frac{1}{[S]} + \frac{1}{V_{max}} \tag{1}$$

$$k_{cat} = \frac{V_{max}}{[E]} \tag{2}$$

where v_0 is the initial velocity, [S] is the substrate concentration, K_m is the Michaelis constant, V_{max} is the maximal velocity, [E] is the trypsin concentration, and k_{cat} is the turnover number.

3.3.3.4. Kinetic assay of trypsin using optimum substrate 1

The stock solution of **1** was diluted with the buffer, and the final concentration of **1** ranged from 2 to 10 µM. The stock solution of trypsin was also diluted with the buffer, and the final concentration of trypsin was adjusted to 40 pM. The hydrolysis of the different concentrations of **1** was initiated by the addition of trypsin solution, and monitored fluorometrically by using a spectrofluorometer with an excitation of 344 nm and an emission of 480 nm. The concentration of DMSO in the assay was less than 2%. The kinetic parameters of K_m, V_{max}, k_{cat}, and k_{cat}/K_m were calculated by fitting the Michaelis–Menten equation described below with the least-squares method.

$$v_0 = \frac{V_{max}[S]}{K_m + [S]} \tag{3}$$

where v_0 is the initial velocity, [S] is the substrate concentration, K_m is the Michaelis constant, V_{max} is the maximal velocity, [E] is the trypsin concentration, and k_{cat} is the turnover number.

3.3.3.5. Determination of detection limit of trypsin activity

The final concentration of **1** was adjusted to 10 μM. The final concentration of trypsin ranged from 7.5 to 150 pM. The fluorescence decrease of **1** at 480 nm in the presence of different concentrations of trypsin was measured using a spectrofluorometer. The detection limit for trypsin was calculated using the following formula:[16]

$$\text{Limit of detection (LOD)} = \frac{3s_{y/x}}{K} \tag{4}$$

where $s_{y/x}$ is the standard deviation of y-residuals and K is the slope of the linear plot of change of the excimer fluorescence intensity versus trypsin concentration.

3.3.3.6. Determination of IC$_{50}$ and K_i of BBI

The final concentration of **1** was adjusted to 10 μM, and the final concentration of trypsin was adjusted to 150 pM. The final concentration of BBI ranged from 0 to 20 nM. Hydrolysis reactions for the different concentrations of BBI were initiated by the addition of the trypsin solution, and monitored fluorometrically by using a spectrofluorometer as mentioned above. The IC$_{50}$ for BBI was estimated by fitting the Hill equation described below with the least-squares method.[17]

$$\text{Inhibition efficiency (\%)} = E_{\text{bottom}} + \frac{E_{\text{top}} - E_{\text{bottom}}}{1 + \exp\{n(\ln \text{IC}_{50} - \ln[\text{I}])\}} \tag{5}$$

where E_{bottom} is the minimal inhibition efficiency (0%), E_{top} is the maximal inhibition efficiency (100%), n is the Hill constant, and [I] is the BBI concentration.

Subsequently, the K_i for BBI was estimated by fitting the Morrison equation described below with the least-squares method.[18]

$$\frac{v_i}{v_0} = 1 - \frac{([\text{E}] + [\text{I}] + K_i) - \sqrt{([\text{E}] + [\text{I}] + K_i)^2 - 4[\text{E}][\text{I}]}}{2[\text{E}]} \tag{6}$$

where v_i is the initial velocity in the presence of BBI, v_0 is the initial velocity in the absence of BBI, [E] is the trypsin concentration, [I] is the BBI concentration, and K_i is the dissociation constant.

3.3.3.7. Detection of thrombin activity

The stock solution of **1** was diluted with the buffer, and the final concentration of **1** was adjusted to 10 μM. The stock solution of thrombin was also diluted with the buffer, and the final concentration of thrombin was adjusted to 88.5 nM. The hydrolysis of **1** was initiated by the addition of thrombin solution, and monitored fluorometrically by using a spectrofluorometer with an excitation of 344 nm and an emission of 480 nm.

3.4. Results and discussion

3.4.1. Investigation of monomer and excimer emission

Initially, we investigated that the intramolecular excimer emission of synthesized substrates was observed. A total of 2 µM of **1**–**5** were prepared in DMSO. Similarly, 4 µM of a Pba solution was also prepared in DMSO as a control sample. All of the solutions contained 4 µM of the pyrene moieties. The fluorescence spectra upon excitation at 344 nm of each sample prior to the addition of protease were measured using a spectrofluorometer. All substrates exhibited higher excimer fluorescence compared with Pba, which indicated that two pyrene moieties in the substrates were spatially proximate (Fig. 15). Substrates **5** showed the highest excimer fluorescence owing to its shortest peptide unit. The excimer fluorescence of **1** and **2**, which was almost equal, was slightly higher than that of **3**, and **4** had the lowest excimer emission. These indicated that inserted β-alanine in the substrates hardly affected the intramolecular excimer formation while extra glycine might lead to reduced excimer formation. However, excimer fluorescence intensities of **1**–**4** were not completely dependent on the length of peptide moiety.
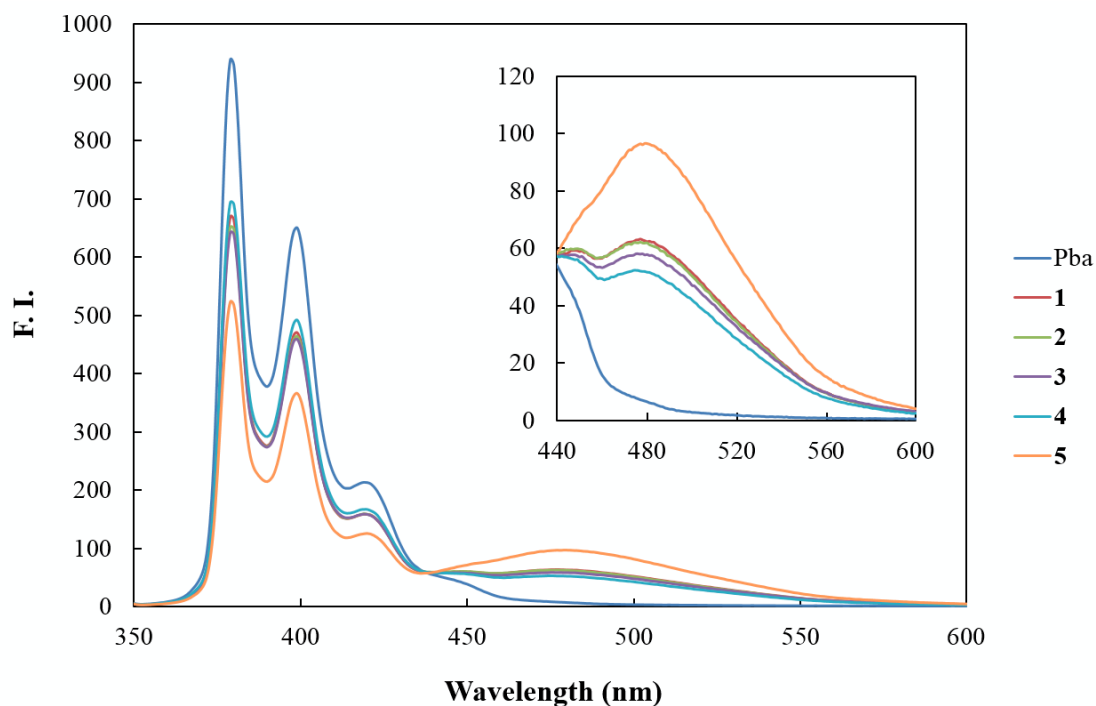
Fig. 15 Monomer and excimer emission of **1**, **2**, **3**, **4**, **5** (2 µM), and Pba (4 µM) in DMSO at room temperature. Excitation wavelength was 344 nm.

Then, the change of monomer and excimer emission during tryptic hydrolysis was traced. Final concentration of **1** was adjusted to 10 μM, and final concentration of trypsin was adjusted to 10 nM with the buffer. To a solution of **1** trypsin was added, and the monomer fluorescence intensity at 378 nm or the excimer fluorescence intensity at 480 nm upon excitation at 344 nm were recorded respectively. Tryptic cleavage led to the simultaneous changes that the monomer emission increased, and the excimer emission decreased (Fig. 16). These results were consistent with our expected design concept of the bispyrenyl substrates.
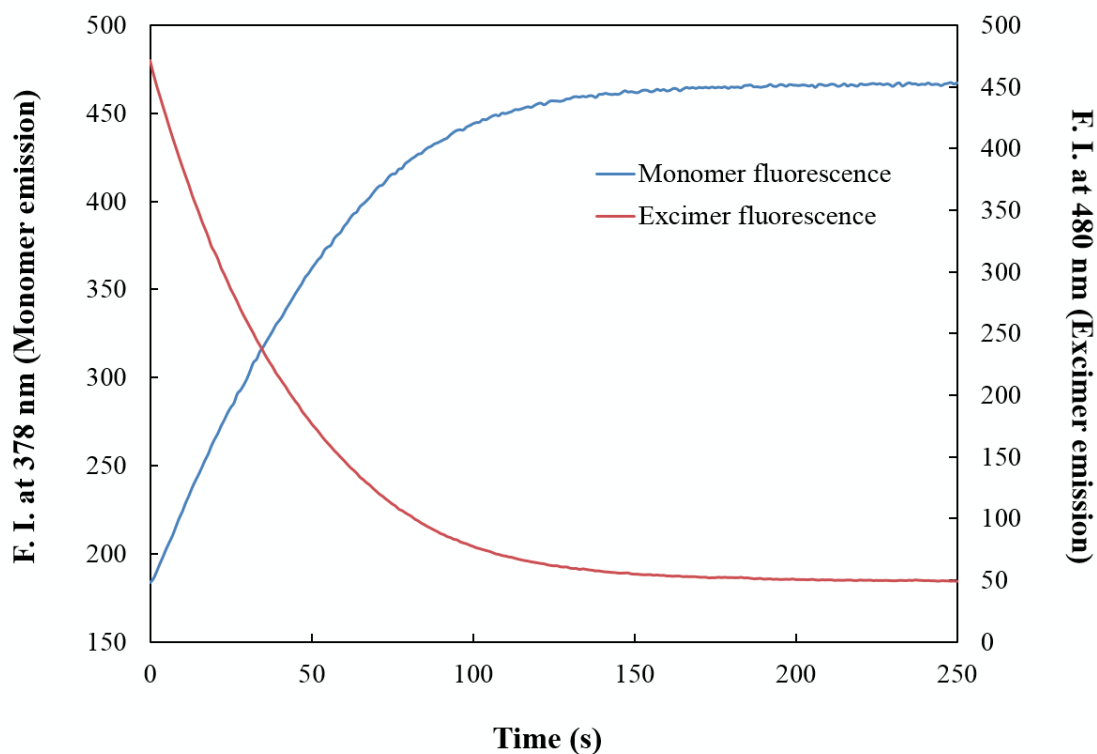
Fig. 16 Kinetic changes in monomer and excimer fluorescence of **1** (10 µM) during tryptic hydrolysis (10 nM) in 50 mM Tris-HCl buffer (pH 8.0) containing 150 mM NaCl, 1 mM CaCl$_2$, and 0.02% (w/v) PEG6000 at room temperature. Excitation wavelength was 344 nm.

3.4.2. Selection of optimum substrate according to kinetic assays of trypsin

Next, the decrease in the fluorescence intensity of different concentrations of the substrates during tryptic degradation was monitored. To each concentration of the substrates (2, 3, 4, 6, 8, and 10 µM), corresponding concentration of trypsin was added, and the excimer emission at 480 nm upon excitation at 344 nm was recorded. All of the final buffer solutions contained 20% (v/v) DMSO due to poor solubility of **4** and **5**. The final concentration of trypsin was adjusted to 400 pM (for **1**), 500 pM (for **2**), 30 nM (for

3), 40 nM (for **4**), or 1.2 nM (for **5**). Subsequently, the kinetic parameters for trypsin were

calculated. According to the change in excimer fluorescence, the decreases in the

fluorescence intensities were converted to the corresponding initial velocities for the

hydrolysis reactions. The kinetic parameters for trypsin activity such as Michaelis

constant (K_m), Maximum reaction rate (V_{max}), turnover number (k_{cat}), and specificity

constant (k_{cat}/K_m) were estimated by fitting the data to the Lineweaver–Burk plot using

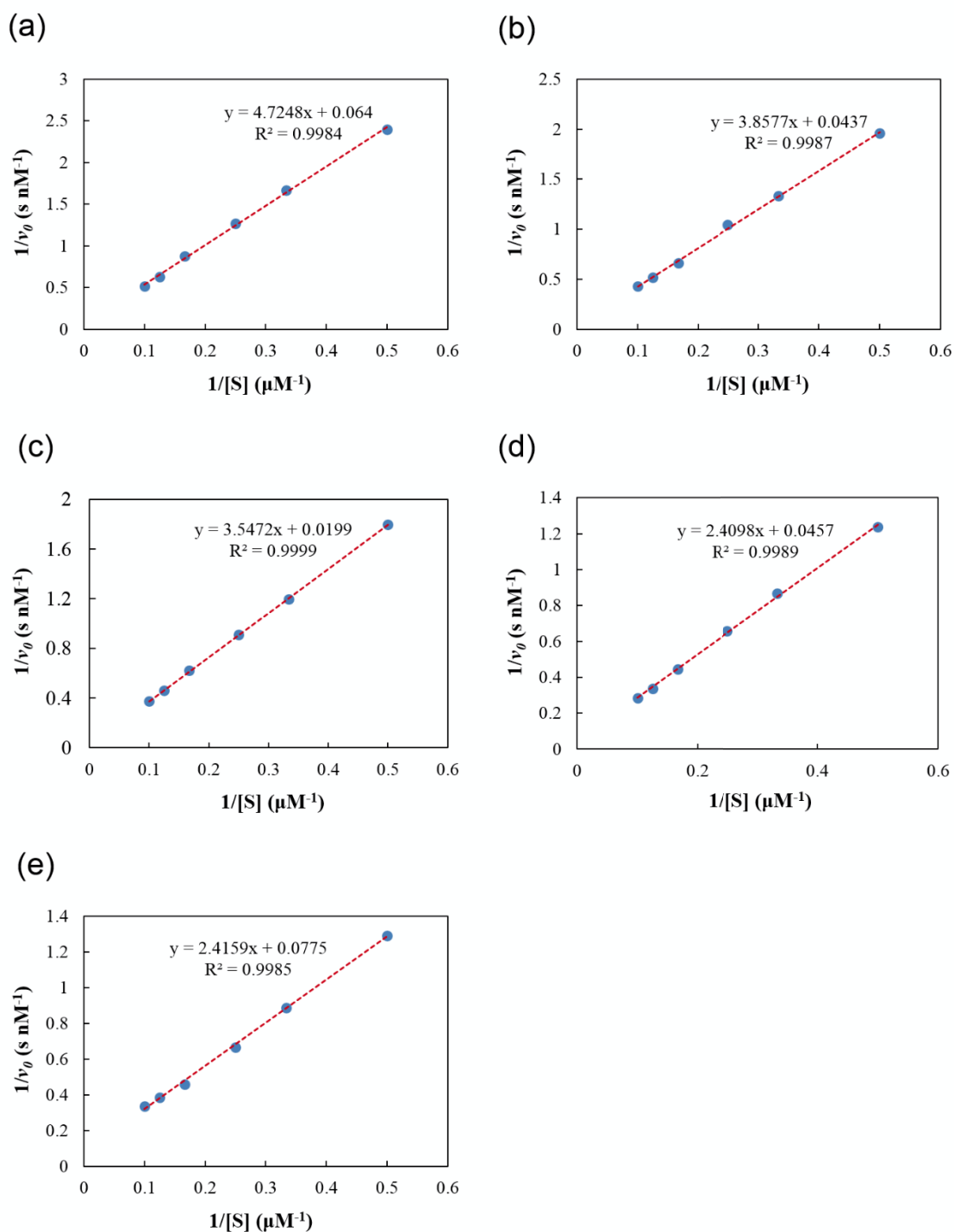the least-squares method (Fig. 17).

Fig. 17 Lineweaver–Burk plot of **1** (a), **2** (b), **3** (c), **4** (d), and **5** (e) catalyzed by trypsin in 20% DMSO in 50 mM Tris-HCl buffer (pH 8.0) containing 150 mM NaCl, 1 mM $CaCl_2$, and 0.02% (w/v) PEG6000 at room temperature with fluorometric method. Excitation/emission wavelengths were 344 nm/480 nm.

The K_m value of **5** was the lowest of that of the other substrates, which meant that the affinity of **5** toward trypsin was the highest (Table 1). This was because the retention time of **5** from HPLC analysis was the longest, indicating that the **5** had the highest hydrophobicity of the other substrates. As a result of the difference of the hydrophobic properties, it was expected that the difference of K_m values might be observed. Although the hydrophobicity of **3** was moderate, K_m value of **3** was dramatically high. As for **4**, modest K_m value was calculated, which was lower than that of **1** and **2**. In contrast, the k_{cat} value of **4** was the lowest of that of other substrates, which indicated that **4** was liberated from trypsin with difficulty. Substrates **1** and **2** exhibited higher k_{cat} values since the extra glycine provided conformational and hydrophilic benefits for the release of the enzyme from the enzyme-substrate complex. The k_{cat} value of **5** was considerably lower than that of **1** despite their same peptide sequences. One explanation was that **1** had two cleavage sites for trypsin compared with one site in **5**. The resulting k_{cat}/K_m values of **1** and **2** were almost equal, and 1.5-fold higher than that of **5**. This indicated that extra β-alanine minimally affected the interaction of **1** and **2** with trypsin, and the number of recognition sites influenced substrate specificity. On the other hand, the k_{cat}/K_m values of **3** and **4** were lower than that of the other substrates by far, which indicated that extra glycine had great influence on the specificity. Considering these results and solubility of the substrates, **1** was picked for the follow-up studies.

Table 1 Summary of the kinetic parameters of **1**, **2**, **3**, **4**, and **5** for trypsin in the presence of 20% DMSO.

Substrate	[E] (nM)	K_m (μM)	V_{max} (nM·s^{-1})	k_{cat} (s^{-1})	k_{cat}/K_m (μM^{-1}·s^{-1})
1	0.4	73.9	15.6	39.1	0.529
2	0.5	88.3	22.9	45.8	0.518
3	30	178	50.1	1.67	9.40×10^{-3}
4	40	52.7	21.9	0.546	1.04×10^{-2}
5	1.2	31.2	12.9	10.8	0.345

3.4.3. Kinetic assay of trypsin using selected substrate 1

The kinetic parameters of **1** for trypsin were verified under the condition of negligible amount of DMSO in the buffer. The final concentration of **1** was adjusted to 2, 3, 4, 6, 8, 10 μM with the buffer, and the final concentration of trypsin was adjusted to 40 pM with the buffer. DMSO included less than 2% in the reaction mixture. The kinetic parameters were estimated by fitting the data to the Michaelis–Menten equation using the least-squares method (Fig. 18).
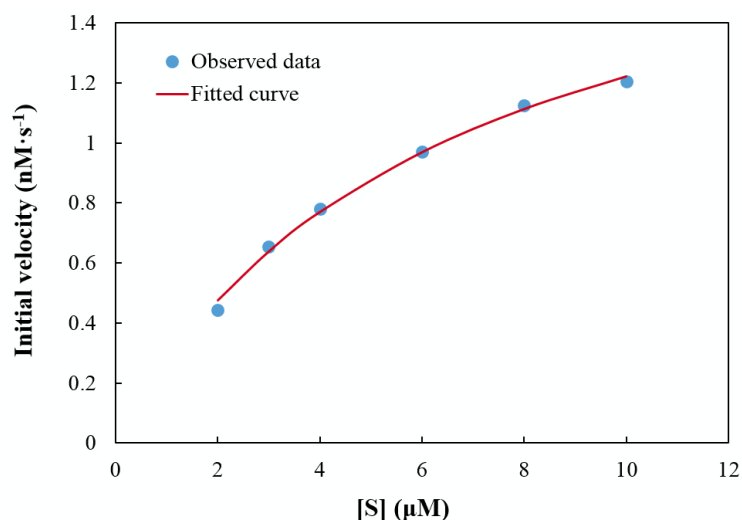
Fig. 18 Michaelis–Menten curve of **1** catalyzed by trypsin (40 pM) in 50 mM Tris-HCl buffer (pH 8.0) containing 150 mM NaCl, 1 mM CaCl$_2$, and 0.02% (w/v) PEG6000 at room temperature with fluorometric method. Excitation/emission wavelengths were 344 nm/480 nm.

On the basis of the above kinetics, K_m, V_{max}, k_{cat}, and k_{cat}/K_m values were determined to be 6.39 μM, 2.00 nM·s^{-1}, 50.0 s^{-1}, and 7.82 μM^{-1}·s^{-1} respectively. In previous chapter, it was stated that K_m, V_{max}, k_{cat}, and k_{cat}/K_m values of trypsin using standard fluorescent probe, ^{i}Boc-VPR-MCA (**6**), were determined to be 2.80 μM, 8.04 nM·s^{-1}, 8.04 s^{-1}, and 2.87 μM^{-1}·s^{-1} respectively. Comparison of these values clearly demonstrated that **1** was an appropriate substrate for measuring trypsin activity.

3.4.4. Determination of detection limit of trypsin

The limit of detection for trypsin using **1** was determined in order to accomplish a quantitative assay for trypsin. The concentration of the substrates was fixed at 10 μM, and different concentrations of trypsin (7.5, 10, 25, 50, 75, 100, 125, and 150 pM) were employed. According to the linear relationship observed between the relative excimer

reduction and trypsin concentration, the detection limit for trypsin was calculated (Fig. 19). A lower limit of 4.11 pM trypsin could catalyze the decrease of excimer fluorescence of **1** compared with 30.9 pM trypsin for conventional fluorescent probe **6** described in previous chapter. These results clearly demonstrated **1** was preferable for the detection of trypsin activity to standard fluorescent probe, Peptide-MCA.
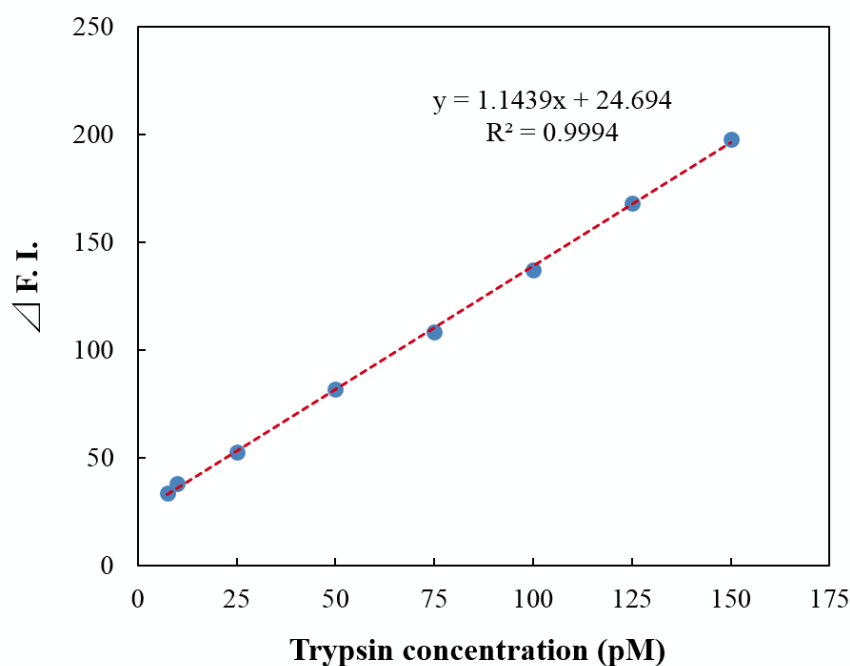

The plot shows data with trend line labeled:

$$y = 1.1439x + 24.694$$
$$R^2 = 0.9994$$

Fig. 19 The linear relationship between amounts of change of the fluorescence intensity of the substrates (10 µM) within a set time of 20 minutes. Excitation/emission wavelengths were 344 nm/480 nm.

3.4.5. Evaluation of trypsin inhibitor

Next, we confirmed whether **1** could be used for inhibitor evaluation. The inhibition of trypsin activity by the Bowman–Birk inhibitor (BBI) which is the most commonly used trypsin inhibitor was investigated using **1**. To 10 µM of **1**, different concentrations of BBI

(0, 1, 2, 3, 4, 5, 10, 15, and 20 nM) were added, followed by addition of 150 pM of trypsin. During tryptic cleavage, excimer emission at 480 nm upon excitation at 344 nm was recorded. As expected, the higher the concentration of BBI was present in the reaction mixture, the slower the fluorescence decrease was (Fig 20a). After plotting the inhibition efficiencies versus the BBI concentrations, the IC_{50} value was calculated by fitting the data to the Hill equation (Fig. 20b). The IC_{50} value for BBI using **1** as substrate was estimated as 8.73 nM.
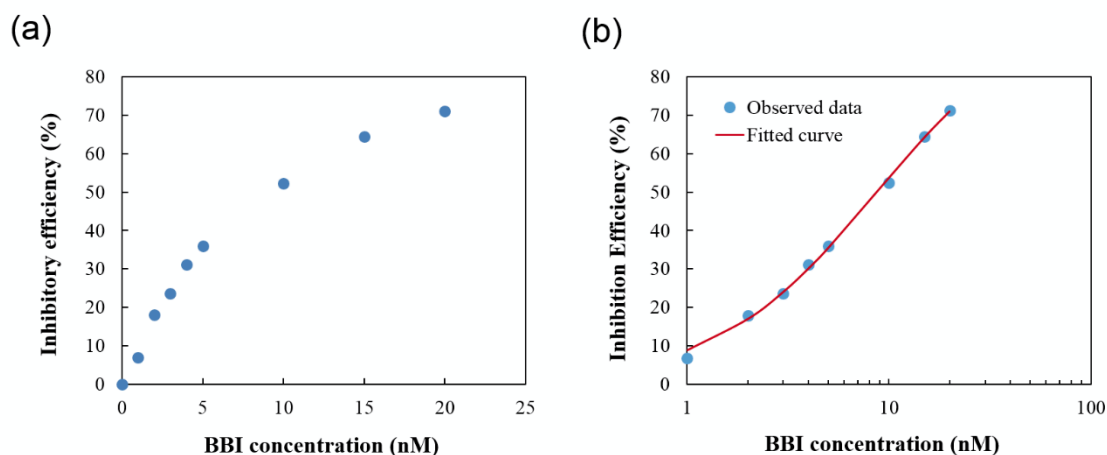

Fig. 20 Plots (a) and fitting curve with Hill equation (b) of inhibition efficiencies of BBI toward trypsin (150 pM) with 10 µM of **1**.

Because IC_{50} value depends on enzyme concentration,[19] the K_i value for BBI was calculated by using the Morrison equation to obtain a more accurate representation of the inhibition (Fig. 21). The K_i value determined from the Morrison equation was 9.36 nM. The K_i of BBI has been reported to be between 10^{-7} and 10^{-9} M,[20] and our value fall within this range. Therefore, **1** can be used for evaluation of inhibitors of trypsin.
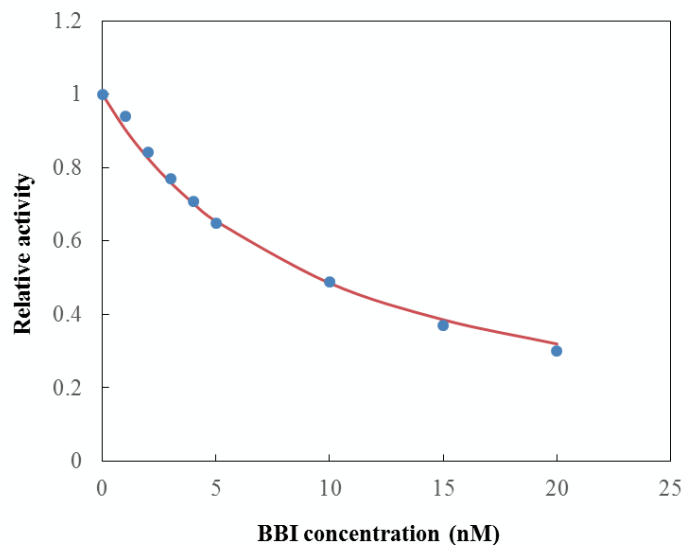
Fig. 21 Plots and fitting curve with Morrison equation of inhibition efficiencies of BBI toward trypsin (150 pM) with 10 µM of **1**.

3.4.6. Detection of thrombin activity

Finally, the decrease in the fluorescence intensity of **1** during thrombin cleavage was monitored. Final concentration of **1** was adjusted to 10 µM, and final concentration of thrombin was adjusted to 88.5 nM. To a solution of **1** thrombin was added, and the excimer emission at 480 nm upon excitation at 344 nm was recorded. The significant but relatively slow decrease in excimer fluorescence could be observed (Fig. 22). This slow cleavage of thrombin may be caused by the same reasons of self-quenching substrates that were the bulkiness of bispyrenyl substrates and narrower entrance to active site of thrombin as mentioned in previous chapter.
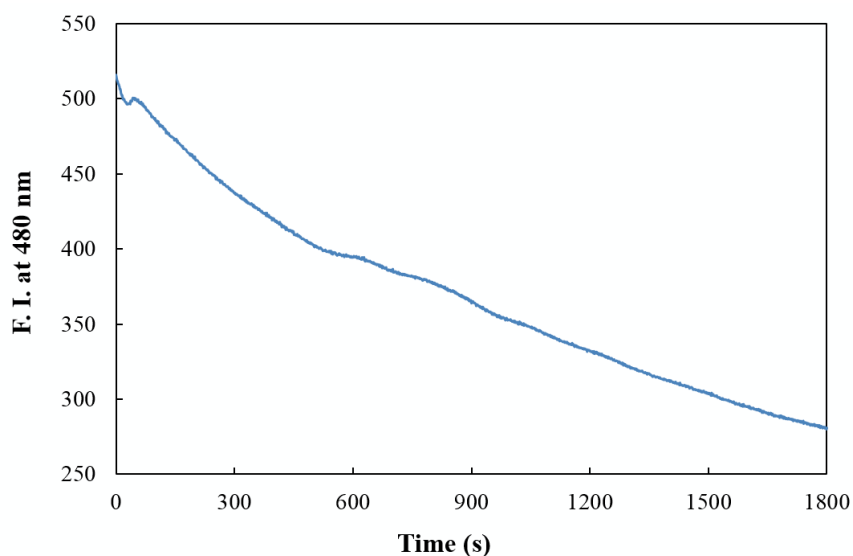
Fig. 22　Kinetic changes in excimer fluorescence of **1** (10 µM) during thrombin hydrolysis (88.5 pM) in 50 mM Tris-HCl buffer (pH 8.0) containing 150 mM NaCl, 1 mM CaCl$_2$, and 0.02% (w/v) PEG6000 at room temperature. Excitation wavelength was 344 nm.

3.5. Conclusion

In summary, novel pyrene monomer/excimer-based peptide substrate **1** for the detection of trypsin and thrombin activities was developed. The results from the fluorescence spectra demonstrated that the significant excimer fluorescence of **1–5** caused by intramolecular proximate pyrene moieties was observed, and this fluorescence was decreased by tryptic cleavage. The kinetic assays verified that the activity of trypsin for **1** was higher than that of **6**, the standard fluorescent probe. The substrates **1** enabled the detection of trypsin at concentrations as low as 4.11 pM which was considerably lower than 30.9 pM of **6**. Inhibitor evaluation of BBI revealed that this assay could be applied to inhibitor screening and be used to determine not only IC$_{50}$ but also K_i values. However,

thrombin activity could not be detected by **1** with adequate sensitivity due to the bulkiness of the substrates and sterically hindered entrance to active site of thrombin.

3.6. References

1. Bains, G.; Patel, A. B.; Narayanaswami, V. Pyrene: a probe to study protein conformation and conformational changes. *Molecules* 2011, **16**(9), 7909−7935.

2. Chen, J.; Liao, D.; Wang, Y.; Zhou, H.; Li, W.; Yu, C. Real-time fluorometric assay for acetylcholinesterase activity and inhibitor screening through the pyrene probe monomer-excimer transition. *Org. Lett.* 2013, **15**(9), 2132−2135.

3. Uddin, M. G.; Azam, A. T. M. Z. A novel oligo-DNA probe carrying non-nucleosidic silylated pyrene derivatives: synthesis and excimer forming ability. *Am. J. Biochem. Mol. Biol.* 2013, **3**(1), 175−181.

4. Tanhuanpää, K.; Virtanen, J.; Somerharju, P. Fluorescence imaging of pyrene-labeled lipids in living cells. *Biochim. Biophys. Acta* 2000, **1497**(3), 308−320.

5. Yang, C. J.; Jockusch, S.; Vicens, M.; Turro, N. J.; Tan, W. Light-switching excimer probes for rapid protein monitoring in complex biological fluids. *Proc. Natl. Acad. Sci. USA* 2005, **102**(48), 17278−17283.

6. Fischbach, M.; Resch-Genger, U.; Seitz, O. Protease probes that enable excimer signaling upon scission. *Angew. Chem. Int. Ed.* 2014, **53**(44), 11955−11959.

7. Wu, Y. X.; Zhang, X. B.; Li, J. B.; Zhang, C. C.; Liang, H.; Mao, G. J.; Zhou, L. Y. Tan, W.; Yu, R. Q. Bispyrene-fluorescein hybrid based FRET cassette: a convenient platform toward ratiometric time-resolved probe for bioanalytical applications. *Anal. Chem.* 2014, **86**(20), 10389−10396.

8. Xu, N.; Li, Y.; Li, H. W.; Wu, Y. A continuous fluorometric assay for trypsin based on melittin and the noncovalent-binding-induced pyrene excimer. *Chem. Lett.* 2013, **42**(12), 1528−1530.

9. Tang, B.; Yang, Y.; Wang, G.; Yao, Z.; Zhang, L.; Wu, H. C. A simple fluorescent probe based on a pyrene derivative for rapid detection of protamine and monitoring of trypsin activity. *Org. Biomol. Chem.* 2015, **13**(32), 8708−8712.

10. Wang, Q.; Shi, X.; Zhu, X.; Ehlers, M.; Wu, J.; Schmuck, C. A fluorescent light-up probe as an inhibitor of intracellular β-tryptase. *Chem. Commun.* 2014, **50**(46), 6120−6122.

11. Yao, Z.; Qiao, Y.; Liang, H.; Ge, W.; Zhang, L.; Cao, Z.; Wu, H. C. Approach based on polyelectrolyte-induced nanoassemblies for enhancing sensitivity of pyrenyl probes. *Anal. Chem.* 2016, **88**(21), 10605−10610.

12. Ahn, T.; Kim, J. S.; Choi, H. I.; Yun, C. H. Development of peptide substrates for trypsin based on monomer_excimer fluorescence of pyrene. *Anal. Biochem.* 2002, **306**(2), 247−251.

13. Azarkan, M.; Dibiani, R.; Goormaghtigh, E.; Raussens, V.; Baeyens-Volant, D. The papaya Kunitz-type trypsin inhibitor is a highly stable β-sheet glycoprotein. *Biochim. Biophys. Acta* 2006, **1764**(6), 1063−1072.

14. Winquist, J.; Geschwindner, S.; Xue, Y.; Gustavsson, L.; Musil, D.; Deinum, J.; Danielson, U. H. Identification of structural-kinetic and structural-thermodynamic relationships for thrombin inhibitors. *Biochemistry* 2013, **52**(4), 613−626.

15. Frattali, V. Soybean inhibitors: III. Properties of a low molecular weight soybean proteinase inhibitor. *J. Biol. Chem.* 1969, **244**(2), 274−280.

16. Dwivedi, A. K.; Iyer, P. K. A fluorescence turn on trypsin assay based on aqueous polyfluorene. *J. Mater. Chem. B* 2013, **1**(32), 4005−4010.

17. O'Connor, M.; Lee, C.; Ellens, H.; Bentz, J. A novel application of t-statistics to objectively assess the quality of IC_{50} fits for P-glycoprotein and other transporters. *Pharma. Res. Per.* 2014, **3**(1), e00078.

18. Morrison, J. F. Kinetics of the reversible inhibition of enzyme-catalysed reactions by tight-binding inhibitors. *Biochim. Biophys. Acta* 1969, **185**(2), 269−286.

19. Cer, R. Z.; Mudunuri, U.; Stephens, R.; Lebeda, F. J. IC_{50}-to-K_i: a web-based tool for converting IC_{50} to K_i values for inhibitors of enzyme activity and ligand binding. *Nucleic Acids Res.* 2009, **37**, W441−W445.

20. Souza, L. C.; Camargo, R.; Demasi, M.; Santana, J. M.; Sá, C. M.; Freitas, S. M. Effects of an anticarcinogenic Bowman-Birk protease inhibitor on purified 20S proteasome and MCF-7 breast cancer cells. *PLoS One* 2014, **9**(1), e86600.

Chapter 4

General conclusion

Proteases are some of the most vital physiological enzymes, and have been targeted for the development of simple and sensitive assays for disease diagnosis, therapy, and biological research. Therefore a variety of techniques for protease assays have been developed.

Immunological methods such as western blotting and ELISA are the sensitive techniques for the quantitation of the amount of target protease. However, progression and state of diseases are directly related to protease activity rather than protease amount, and measurement of protease activity is more significant in disease diagnosis, pathophysiological research, and drug discovery. In addition, immunological methods cannot be used for the evaluation of protease inhibitors. Inhibitor evaluation is essential in drug discovery. Besides, these assays are time consuming, and required expensive reagents and specific instruments.

Hence, many fluorescent peptide probes such as Peptide-MCA and FRET-based substrate have been developed, and are now commercially available. However, commercially available Peptide-MCA and FRET-based substrates are not versatile. In the case of an AMC-based assay, the specificity for the P1′ amino acid residue (counterpart of the S1′ subsite of the protease), which is important for substrate recognition and catalytic

efficiency, is not reflected in the artificial substrate. In a FRET-based assay, the combination of fluorophores and quenchers can be limiting, and expensive fluorophores or quenchers are often required. Furthermore, the synthesis of FRET-based substrates is usually complicated because at least one pair of orthogonal protecting groups is needed so that the two different dyes required for the FRET are coupled.

To overcome these problems in standard fluorescent probes for protease assays, two types of novel doubly labelled fluorescent peptide probes for the detection of protease activity using intramolecular interaction between identical fluorophores were developed.

Self-quenching-based substrates, which are consisted of two FITC-linked substrate peptides and lysine as a branched unit, were designed, and it is demonstrated that these substrates can be easily synthesized by only Fmoc SPPS technique. The substrates showed significant quenching by intramolecular self-quenching and the fluorescence recovery by proteolytic cleavage. The activities of trypsin for self-quenching substrates were almost comparable to that of the standard fluorescent probe, peptide-MCA. The substrates enabled the detection of trypsin at concentrations as low as 111 pM, and the inhibitor evaluation such as the calculation of IC_{50} and K_i values was also executed. The kinetic assay for thrombin was successfully carried out, and these results indicated that the activities of thrombin for the substrates were inferior to that of Peptide-MCA. Molecular simulation implied that this lower ability toward thrombin attributed in the bulkiness of these substrates and sterically hindered entrance to active site of thrombin.

Bispyrenyl substrates, which are consisted of two different lengths of Pba-linked substrate peptides and hexamethylenediamine as a core, were successfully designed and synthesized. The substrates showed significant excimer emission by intramolecular excimer formation of two pyrene moieties and this fluorescence decreased by tryptic cleavage. The activity of trypsin for the optimum substrate was higher than that of peptide-MCA. The substrate enabled the detection of trypsin activity at concentrations as low as 4.11 pM. This detection limit of the substrate was preferable for trypsin assay to Peptide-MCA, and was not inferior to those of the immunology-based methods. The evaluation of protease inhibitor was successfully performed. In spite of insufficient sensitivity for thrombin, the detection of disease-related thrombin activity according to the decrease of excimer emission of bispyrenyl substrate could be also executed.

The synthesis of both types of substrates is relatively easy due to incorporation of two identical fluorophores. As for the detection of trypsin activity, both types of substrates display comparable or higher sensitivity compared with Peptide-MCA. These substrates are favorable for exploration of optimum substrate sequence and screening potential inhibitor. To our knowledge, our study is the first to demonstrate that the fluorescent peptide probes exploiting intramolecular interaction between two identical fluorophores such as self-quenching or pyrene excimer formation can be applicable to substrate optimization and inhibitor screening. Though the sensitivity for thrombin is not satisfactory, these detection mechanisms can be adapted for other protease targets by simple change of the peptide sequence. Devoted improvement in the substrate design certainly allows usage of these substrates to expand into the detection of other disease-related protease activity. These intramolecular interaction-based substrates are expected

to be useful not only for biological and pathological investigations but also for clinical application such as *in vitro* diagnostic and point of care (POC).

Acknowledgement

Achievements

Publications

1. Novel fluorescent substrates for detection of trypsin activity and inhibitor screening by self-quenching

   <u>Daisuke Sato</u>, Tamaki Kato

   Bioorganic & Medicinal Chemistry Letters 2016, **26**(23), 5736–5740.

2. Detection of protease activity using intramolecular excimer forming bispyrene peptide substrates

   <u>Daisuke Sato</u>, Takuya Kondo, Tamaki Kato

   The Journal of Peptide Science 2017, 191–192.

3. Detection of protease activity by concentration quenching-based substrates

   <u>Daisuke Sato</u>, Wu Zhe, Tamaki Kato

   Proceedings of the 24th American Peptide Symposium 2015, 139–140.

4. Efficient near infrared fluorescence detection of elastase enzyme using peptide-bound unsymmetrical squaraine dye

   Maryala Sai Kiran, <u>Daisuke Sato</u>, Shyam Sudhir Pandey, Shuzi Hayase, Tamaki Kato

   Bioorganic & Medicinal Chemistry Letters 2017, **27**(17), 4024–4029.

5. Photophysical characterization and BSA interaction of the direct ring carboxy functionalized unsymmetrical NIR cyanine dyes

Maryala Sai Kiran, Daisuke Sato, Shyam Sudhir Pandey, Takeshi Ohta, Shuzi Hayase, Tamaki Kato

Dyes and Pigments 2017, **140**, 6–13.

Presentations at conferences

1. Poster presentation: Detection of protease activity by fluorescence alteration of pyrene using bispyrene peptide substrates

Daisuke Sato, Takuya Kondo, Tamaki Kato

25th American Peptide Symposium and 9th International Peptide Symposium, Whistler, Canada 2017

2. Poster presentation: Detection of protease activity using intramolecular excimer forming bispyrene peptide substrates

Daisuke Sato, Takuya Kondo, Tamaki Kato

34th European Peptide Symposium and 8th International Peptide Symposium, Leipzig, Germany 2016

3. Oral presentation: Detection of protease activity by concentration quenching using lysine-branched substrates

   Daisuke Sato, Tamaki Kato

   96th Chemical Society of Japan Annual Meeting, Kyoto, Japan 2016

4. Oral presentation: Detection of trypsin activity by concentration quenching-based substrates

   Daisuke Sato, Tamaki Kato

   India-Japan Expert Group Meeting on Biomolecular Electronics & Organic Nanotechnology for Environment Preservation 2015, Fukuoka, Japan 2015

5. Poster presentation: Detection of thrombin activity using concentration quenching-based substrates

   Daisuke Sato, Tamaki Kato

   7th International Peptide Symposium, Singapore 2015

6. Poster presentation: Detection of protease activity by concentration quenching-based substrates

   Daisuke Sato, Wu Zhe, Tamaki Kato

   24th American Peptide Symposium, Florida, USA 2015

7. Oral presentation: Novel concentration quenching-based substrates for protease

   Daisuke Sato, Wu Zhe, Tamaki Kato

   95th Chemical Society of Japan Annual Meeting, Chiba, Japan 2015